

MICROFACIES ANALYSIS OF UPPER DEVONIAN - LOWER
CARBONIFEROUS SHALLOW WATER CARBONATES OF THE YILANLI
FORMATION IN ZONGULDAK AREA, NORTH WESTERN, TURKEY

A THESIS SUBMITTED TO
THE GRADUATE SCHOOL OF NATURAL AND APPLIED SCIENCES
OF
MIDDLE EAST TECHNICAL UNIVERSITY

BY
NOUMAN AHMED

IN PARTIAL FULFILLMENT OF THE REQUIREMENTS
FOR
THE DEGREE OF MASTER OF SCIENCE
IN
GEOLOGICAL ENGINEERING

OCTOBER 2016

Approval of the thesis:

**MICROFACIES ANALYSIS OF UPPER DEVONIAN - LOWER
CARBONIFEROUS SHALLOW WATER CARBONATES OF THE YILANLI
FORMATION IN ZONGULDAK AREA, NORTH WESTERN, TURKEY**

submitted by **NOUMAN AHMED** in partial fulfillment of the requirements for the degree of **Master of Science in Geological Engineering Department, Middle East Technical University** by,

Prof. Dr. Gülbin Dural Ünver _____
Director, Graduate School of **Natural and Applied Sciences**

Prof. Dr. Erdin Bozkurt _____
Head of Department, **Geological Engineering**

Assoc. Prof. Dr. İsmail Ömer Yılmaz _____
Supervisor, **Geological Engineering Dept., METU**

Examining Committee Members:

Prof.Dr. Sevinç Özkan Altın _____
Geological Engineering Dept., METU

Assoc. Prof. Dr. İsmail Ömer Yılmaz _____
Geological Engineering Dept., METU

Prof. Dr. Uğur Kağan Tekin _____
Geological Engineering Dept., Hacettepe University

Assist. Prof. Dr. Erman Özsayın _____
Geological Engineering Dept., Hacettepe University

Assist. Prof. Dr. Fatma Toksoy Köksal _____
Geological Engineering Dept., METU

Date: 18-10-2016

I hereby declare that all information in this document has been obtained and presented in accordance with academic rules and ethical conduct. I also declare that, as required by these rules and conduct, I have fully cited and referenced all material and results that are not original to this work.

Name, Last name : NOUMAN AHMED

Signature :

ABSTRACT

MICROFACIES ANALYSIS OF UPPER DEVONIAN - LOWER CARBONIFEROUS SHALLOW WATER CARBONATES OF THE YILANLI FORMATION IN ZONGULDAK AREA, NORTH WESTERN, TURKEY

Ahmed, Nouman

M.S., Department of Geological Engineering

Supervisor: Assoc. Prof. Dr. İsmail Ömer Yılmaz

October 2016, 135 pages

The Yılanlı Formation of Upper Devonian to Lower Carboniferous succession of the Zonguldak region were measured from Gökgöl section near Zonguldak city, NW Turkey. The studied section dominantly consists of limestone of grey – dark grey color with thin to thick beds of black shale and claystone. A variety of lithofacies identified in the studied section including limestone, dolomite, shale, claystone and mudstone. Nine microfacies are identified as grainstone, packstone, wackstone, mudstone, bindstone, rudstone, shale, claystone and dolomite. Grainstone and packstone have abundant peloids, bioclast, intraclast and ooids. Wackstone and mudstone are characterized by bivalves, ostracods, lamination and breccia. The model for carbonate microfacies are generated by using texture, modal and spatial parameters in context of component analysis to interpret depositional environment. The depositional environment is interpreted as shallow marine sub-tidal to shallow lagoon environment of inner ramp type carbonate platform. The Yılanlı Formation is characterized by variety of fauna like ostracods, foraminifera, bivalves, gastropods, echinoderms, sponges, corals and green algae in the studied section.

Keywords: Upper Devonian-Lower Carboniferous, component analysis of carbonate microfacies, shallow water Inner ramp carbonate platform.

ÖZ

ÜST DEVONYEN – ALT KARBONİFER Sığ DENİZ KARBONATLARININ MİKROFASİYESLERİNİN İNCELENMESİ (YILANLI FORMASYONU, ZONGULDAK, KUZEYBATI ANADOLU)

Ahmed, Nouman
Yüksek Lisans, Jeoloji Mühendisliği Bölümü
Tez Yöneticisi: Doç. Dr. İsmail Ömer Yılmaz
Ekim 2016, 135 sayfa.

Zonguldak (Kuzeybatı Türkiye) yakınındaki Gököl kesitinden bir Üst Devonyen – Alt Karbonifer istifi olan Yılanlı Formasyonu ölçülmüştür. Çalışılan kesit başlıca inceden kalına tabakalanma gösteren siyah şeyl ve kilitaşları içeren gri – koyu gri renkli kireçtaşlarından oluşmaktadır. Çalışılan kesitte, kireçtaşı, dolomit, şeyl, kilitaş ve çamurtaşını içeren bir çeşitlilik saptanmıştır. Bu kesitte, tanetaşı, istiftaşı, çamurtaşı, killi şeyl, bağlamtaşı, kabataş, şeyl, kilitaş ve dolomit olarak belirlenen bir dizi litofasiyes belirlenmiştir. Tanetaşı ve istiftaşı olan birimlerde yoğun peloid, biyoklast, intraklast ve ooid bulunduğu saptanmıştır. Vaketaşı ve çamurtaşı birimleri bivalvlar, ostrakodlar, laminasyon ve breşlenme ile karakterize olmuştur. Karbonat mikrofasiyes modelleri, çökelim ortamını yorumlamak adına bileşenler analizi bağlamında, dokusal, şekilsel ve mekansal parametreler kullanılarak oluşturulmuştur. Çökelim ortamının iç karbonat yokuş platformunun sığ deniz alt-gelgit ortamı ile kısıtlı lagün ortamı arasında değişken olduğu belirlenmiştir. Yılanlı Formasyonda ostrakodlar, foraminiferler, bivalvlar, gastropodlar, ekinodermiler, süngerler, mercanlar ve yeşil algler içeren çok çeşitli bir faunanın varlığı gözlemlenmiştir.

Anahtar Kelimeler: Üst Devonyen – Alt Karbonifer, yüksek sıklıklı, karbonat mikrofasiyeslerinin bileşen analizi, sığ deniz iç karbonat yokuş platformu

To my beloved family....

ACKNOWLEDGMENTS

First of all I express my extreme gratitude to the Almighty for helping me through this significant academic endeavor of my life.

Secondly, I would like to express my sincere gratitude to Assoc. Prof. Dr. İsmail Ömer Yılmaz, my supervisor, for his patient and valuable guidance, enthusiastic encouragement, immense knowledge and valuable suggestions throughout this research work. I am thankful to all jury members.

A special thanks to my family. There is no words to express how grateful I am to my parents, Mr. Khalid Mehmood and my mother (Mrs. Khalid Mehmood) for all of the sacrifices that they have made on my behalf. Your prayers and advices for me were what sustained me thus far. A bundle of thanks to my brothers (Faheem Ahmed, Hassan Ali and Ahmed Ali) sisters and uncles Mr. Zafar Iqbal, Mr. Naeem Ahmed, whose unconditional love and support always encouraged me in every movement of my life.

I wish to thank my Pakistani and Turkish friends Bakht Zamir Afridi, Saeed Ahmad Khan, Adam Abdullah, Syed Tanvir Shah, Islam Aslam, Rafey Kazi, Abdul Qayum, Murat Ozkaptan, Mustafa Tuncer, Mustafa Kaplan, Nisan Sariaslan and Furkan Tolga Geleri for helping me get through the difficult times, and for all the emotional support, entertainment and care they provided.

TABLE OF CONTENTS

| | |
|--------------------------------|-------------|
| ABSTRACT | v |
| ÖZ | vi |
| ACKNOWLEDGEMENTS | viii |
| TABLE OF CONTENTS | ix |
| LIST OF TABLES | xiii |
| LIST OF FIGURES | xiv |
| LIST OF PLATES | xix |

CHAPTERS

| | |
|--|-----------|
| 1. INTRODUCTION | 1 |
| 1.1 Purpose and Scope..... | 1 |
| 1.2 Geographic Setting..... | 1 |
| 1.3 Methods of study..... | 2 |
| 1.4 Previous Studies..... | 6 |
| 1.5 Regional Geological Setting | 7 |
| 2. LITHOSTRATIGRAPHY | 12 |
| 2.1 Lithostratigraphy of Zonguldak Region..... | 11 |
| 2.2 Lithostratigraphy of the measured section..... | 16 |

| | |
|---|-----------|
| 3. MICROFACIES ANALYSIS..... | 29 |
| 3.1 Sedimentological Studies..... | 29 |
| 3.2 Results of point counting and measurements..... | 29 |
| 3.3 Microfacies of Gökgöl Tunnel Section | 35 |
| 3.3.1 MYF-I Grainstone Microfacies..... | 43 |
| 3.3.1.1 S-MYF I Peloidal Grainstone – Pel-Intra- oosparite..... | 43 |
| 3.3.1.2. Interpretation..... | 44 |
| 3.3.2 MYF-II Packstone Microfacies..... | 45 |
| 3.3.2.1. S-MYF I Bioclastic Packstone – Bio- pelmicrite..... | 45 |
| 3.3.2.2. S-MYF II Intraclastic Packstone – Intra-Oo- biomicrite..... | 45 |
| 3.3.2.3. S-MYF III Peloidal Packstone – Pel-Intra- biomicrite..... | 46 |
| 3.3.2.4. S-MYF IV Bivalve Packstone – Biomicrite..... | 46 |
| 3.3.2.5. Interpretation..... | 46 |
| 3.3.3 MYF-III Wackstone Microfacies..... | 47 |
| 3.3.3.1 S-MYF I Peloidal Wackstone – Pel- intramicrite..... | 47 |
| 3.3.3.2 S-MYF II Bioclastic Wackstone – Bio- intramicrite..... | 48 |
| 3.3.3.3 S-MYF III Intraclastic Wackstone – Intra- pelmicrite..... | 48 |

| | | |
|---------|---|----|
| 3.3.3.4 | Interpretation..... | 49 |
| 3.3.4 | MYF IV Mudstone Microfacies..... | 49 |
| 3.3.4.1 | S-MYF I Burrowed Lime Mudstone..... | 49 |
| 3.3.4.2 | S-MYF II Brecciated Mudstone..... | 50 |
| 3.3.4.3 | Interpretation..... | 50 |
| 3.3.5 | MYF V Bindstone Microfacies..... | 51 |
| 3.3.5.1 | Interpretation..... | 51 |
| 3.3.6 | MYF VI Rudstone Microfacies- | 52 |
| 3.3.6.1 | Interpretation..... | 53 |
| 3.3.7 | MYF VII Shale Microfacies..... | 55 |
| 3.3.7.1 | S-MYF I Clayey Shale..... | 55 |
| 3.3.7.2 | S-MYF II Silty Shale | 55 |
| 3.3.7.3 | S-MYF III Black Shale | 55 |
| 3.3.7.4 | Interpretation..... | 56 |
| 3.3.8 | MYF VIII Claystone Microfacies | 56 |
| 3.3.8.1 | S-MYF Claystone..... | 56 |
| 3.3.8.2 | S-MYF II Silty claystone..... | 56 |
| 3.3.8.3 | Interpretation..... | 57 |
| 3.3.9 | MYF-IX Dolomite Microfacies..... | 57 |
| 3.3.9.1 | Classification of Dolomite..... | 57 |
| 3.3.9.2 | Interpretation..... | 59 |
| 3.4 | Sedimentary structure in stratigraphic section..... | 59 |

| | | |
|-----------|--|------------|
| 3.4.1 | Bedding and Lamination..... | 59 |
| 3.4.2 | Bioturbation..... | 59 |
| 3.4.3 | Diagnostic Fossils..... | 59 |
| 3.5 | Component analysis of microfacies and interpretation of depositional conditions | 63 |
| 3.5.1 | Interpretation of depositional conditions of the measured succession | 64 |
| 4. | DEPOSITIONAL ENVIRONMENT..... | 79 |
| 5. | DEVONIAN–CARBONIFEROUS SUCCESSIONS..... | 83 |
| 5.1 | Introduction..... | 83 |
| 5.2 | Devonian – Carboniferous | 83 |
| 6. | DISCUSSION AND RECOMMENDATIONS | 89 |
| 7 | CONCLUSIONS..... | 91 |
| | REFERENCES..... | 93 |
| | APPENDIX | 111 |

LIST OF TABLES

| | |
|---|----|
| Table 2.1: Identification of samples with their color from the Gököl Section..... | 20 |
| Table 3.1: Petrographic and point counted data of the Gököl samples (data illustrated in graphic curve as Figure 3.1)..... | 31 |
| Table 3 2: Percentage data of the quantitative analysis using point count data for the measured Gököl section (data illustrated in graphic curves as well as in ternary diagrams)..... | 32 |
| Table 3 3: Grain size measurement of some samples of the Gököl section..... | 33 |
| Table 3.4: Microfacies and sub-microfacies of the Yılanlı Formation..... | 35 |
| Table 3.5: Folk (1965) classification for fine-grain sedimentary rock on the basis of texture..... | 54 |
| Table 3.6: Classifications of the Gököl section based on texture, grain and composition | 69 |
| Table 5.1. The Devonian – Carboniferous correlation of Zonguldak region with different parts of the world..... | 86 |
| Table 6.1. Source rock chart for hydrocarbon potential (McCarthy K. et al., 2011)..... | 90 |

LIST OF FIGURES

| | |
|--|----|
| Figure 1.1: Geographic location of the studied section in the Zonguldak region, NW Turkey (Red rectangle)..... | 4 |
| Figure 1.2: Satellite image showing the studied Section in the Zonguldak region, NW Turkey (Yellow arrow represents north direction of the Google map). | 5 |
| Figure 1.3: Close view of the satellite image red arrow showing the studied section in the Zonguldak region, NW Turkey..... | 5 |
| Figure 1.4: Dark Grey patches represent Paleozoic outcrops in the Zonguldak Terrane (simplified from Bozkaya et al., 2012)..... | 9 |
| Figure 1.5: The tectonic units of the Turkey, and Istanbul-Zonguldak terranes (simplified from Göncüoğlu et al., 1997; the red rectangle represents study area)..... | 10 |
| | |
| Figure 2.1: Geological map of the Istanbul – Zonguldak zone of the Western Pontides (simplified from Yilmaz et al., 1997)..... | 13 |
| Figure 2.2: Generalized columnar section of the Zonguldak region. (not to scale, modified from Bozkaya et al., 2012; Tüysüz et al., 2002)..... | 14 |
| Figure 2.3: The field photograph showing carbonate sequence of the Yılanlı Formation on the road side..... | 15 |
| Figure 2.4: General view of the bottom of thin to thick beds of carbonate of the Yılanlı Formation..... | 15 |
| Figure 2.5: Paleozoic formations of the Western Pontides (Black line represents the Yılanlı Formation equivalent to Fa2d –V1, Görür et al., 1997. Red rectangle represents studied sequence)..... | 18 |
| Figure 2.6: The field photograph displays the bottom of the studied section. Thick bedded limestone with thin shale (a), limestone (b) and mudstone (c) alternations..... | 19 |

| | |
|--|----|
| Figure 2.7: Shale interbedded with limestone in lower part of measured section..... | 21 |
| Figure 2.8: A photograph displaying parallel lamination on outcrop of mudstone. | 22 |
| Figure 2.9: A photograph showing corals in thick bedded limestone approximately in the middle of the section (GT25)..... | 22 |
| Figure 2.10: A photograph illustrating bivalve in the middle of the measured section of limestone..... | 23 |
| Figure 2.11: The lithologic log of the Yılanlı Formation at Gökgöl section (0-44 m)..... | 24 |
| Figure 2.11: The lithologic log of the Yılanlı Formation at Gökgöl section (44-86 m)..... | 25 |
| Figure 2.12: A field view of thick bedded limestone at the top of the studied section..... | 26 |
| Figure 2.13: A close view of thick bedded limestone and intercalation of shale represents different sample numbers..... | 26 |
| Figure 2.14: A photographs showing intraclast in rudstone microfacies of thick bedded limestone..... | 27 |
| | |
| Figure 3.1: Graphic illustration of point counting data of the Gökgöl section | 30 |
| Figure 3.2: Passega diagram. The area included by the black straight line is the pattern based on median (Coarse grain: C, median: M 2.9 phi value)..... | 34 |
| Figure 3.3: Graphic representation of percentage of different allochem, lime matrix and cement of the Gökgöl section (peloids (P), ooids (O), bioclast (Bl), bivalve (Bi), forams (Fm), echinoderms (Ec), intraclast (In), cement (C) and matrix (M)..... | 34 |
| | |
| Figure 3.4: Classification of carbonate rocks proposed by Kendall (2005) after Dunham (1962) | 37 |

| | |
|---|----|
| Figure 3.5: Textural classification of carbonate rocks by Folk and improved by Kendall (2005) after Folk (1959)..... | 37 |
| Figure 3.6: Classification of carbonate rocks based on crystal texture Strohmenger and Wirsing (1991) after Folk (1959)..... | 38 |
| Figure 3.7: Textural classification of carbonate rocks by Folk and improved by Kendall (2005) after Folk (1959)..... | 39 |
| Figure 3.8: Limestone classification on the basis of composition (Flügel and Haditsch, 1975; Oates 1998)..... | 39 |
| Figure 3.9: List of standard microfacies types of Wilson Model going from the basinal SMF Type 1 to sub-aerial SMF 26 (Wilson, 1975)..... | 40 |
| Figure 3.10: List of ramp microfacies types and depositional profile of the Wilson Model in different parts of a carbonate ramp (Wilson, 1975)..... | 41 |
| Figure 3.11: The comparison charts for visual percentage estimation for limestone's (Baccelle and Bosellini, 1965). The charts represents A - silt-sized and fine-sand sized particles, e.g. peloids, small intraclasts, or microfossils; B - coarse angular and subangular particles, e.g. intraclasts and angular skeletal grains; C - equal-sized ooids; D - differently sized ooids or peloids; E - oriented shells, e.g. bivalves; F - associations of various grains, here predominantly bioclasts, a few coated grains and peloids. G and H display the same percentage of skeletal grains with a black and with a white background. Low and high values: Most charts start with images at 10%; only the charts for the groups A and B show images below 10%. The largest percentage value shown is 50 or 60%. I and J: Few and abundant peloids contrasted; K and L: Few and abundant bioclasts.(modified from (Baccelle and Bosellini, 1965)..... | 42 |
| Figure 3.12: Classification of claystone on relative proportions of grains size, showing claystone sample (modified from Picard's 1971)..... | 54 |
| Figure 3.13: Classification of dolomite fabrics by Sibley and Gregg (1987)..... | 58 |
| Figure 3.14: Photograph illustrates lamination in the upper section of studied section..... | 60 |

| | |
|--|----|
| Figure 3.15: Photograph illustrates parallel lamination and calcite vein in the middle of the section..... | 60 |
| Figure 3.16: Photograph showing dark color lamination in the upper part of the section..... | 61 |
| Figure 3.17: Microphotograph illustrating bioturbation area with white dotted line (PPL, 4 X GT/S 64)..... | 61 |
| Figure 3.18: Microphotograph showing foraminifers (F) (PPL, 20 X GT/S 2)... | 62 |
| Figure 3.19: Microphotograph showing gastropods shell (PPL, 4 X GT/S 64)... | 62 |
| Figure 3.20: Photomicrograph illustrating ostracods (Os), stylolite with organic matter and chlorite (Cl) (PPL, GT/S 21)..... | 63 |
| Figure 3.21: Ternary diagrams of compositional modal from the basal part of the Yılanlı Formation used to interpret depositional model of microfacies and high frequency dynamic environmental changes (0-20m represent sample number from GT1-GT42).The ternary diagram, A. represent allochem, micrite and sparite, B. shows peloid, micrite and mollusca, C. displays mollusca, echinoderms and shallow benthic foraminifers..... | 66 |
| Figure 3.22: Ternary diagrams of compositional modal from the middle part of the Yılanlı Formation used to interpret depositional model of microfacies and high frequency dynamic environmental changes (20-60m represent sample number from GT43-GT54).The ternary diagram, A. represent allochem, micrite and sparite, B. shows peloid, micrite and mollusca, C. displays mollusca, echinoderms and shallow benthic foraminifers..... | 67 |
| Figure 3.23: Ternary diagrams of compositional modal from the upper part of the Yılanlı Formation used to interpret depositional model of microfacies and high frequency dynamic environmental changes (60-86 m represent sample number from GT55-GT68).The ternary diagram, A. represent allochem, micrite and sparite, B. shows peloid, micrite and mollusca, C. displays mollusca, echinoderms and shallow benthic foraminifers..... | 68 |
| Figure 3.24: The measured stratigraphic section of the Yılanlı Formation at Gököl section. (0-11) m. | 71 |
| Figure 3.24: The measured stratigraphic section of the Yılanlı Formation at Gököl section. (11-22 m.) | 72 |

| | |
|---|----|
| Figure 3.24: The measured stratigraphic section of the Yılanlı Formation at Gökgöl section. (22-33 m). | 73 |
| Figure 3.24: The measured stratigraphic section of the Yılanlı Formation at Gökgöl section. (33-44 m). | 74 |
| Figure 3.24: The measured stratigraphic section of the Yılanlı Formation at Gökgöl section. (44-55 m). | 75 |
| Figure 3.24: The measured stratigraphic section of the Yılanlı Formation at Gökgöl section. (55-66 m). | 76 |
| Figure 3.24: The measured stratigraphic section of the Yılanlı Formation at Gökgöl section. (66-77 m). | 77 |
| Figure 3.24: The measured stratigraphic section of the Yılanlı Formation at Gökgöl section. (77-86 m). | 78 |
| | |
| Figure 4.1: A general display of depositional environment. B Marine depositional environment (Kennett, 1982).) | 80 |
| Figure 4.2: Schematic block diagram displaying depositional model of the Yılanlı Formation, Zonguldak, NW Turkey (modified from Flügel, 2004). | 82 |
| | |
| Figure 5.1: A major Devonian event and sea level change, black rhombs represent Global event (Johnson et al., 1985) | 87 |
| Figure 5.2: Paleogeographic reconstruction of Gondwana, Baltica and Peri-Gondwanan European Terrane; A. Silurian. B. Devonian (Scotese et al., 1990) | 88 |
| Figure 5.3: Paleogeographic reconstruction map. A. Early Devonian. B. Early Carboniferous T represent location of Turkey (Scotese et al., 1990) | 88 |

LIST OF PLATES

Plate 1: 111

Figure A and B: Photomicrograph of peloidal grainstone sub-microfacies showing micritized ooids (MO), intraclast (Ir), peloid (P), bioclasts (B), grapestone (GP), vein (V) and sparry calcite matrix (M) (PPL, GT/S 22).

Figure C and D: Photomicrograph of peloidal grainstone sub-microfacies displaying micritized laminated ooids (O), intraclast (Ir), peloid (P), bioclasts (B) and calcisphere (Cs) (XPPL & PPL, GT/S 30).

Figure E and F: Photomicrograph of peloidal grainstone sub-microfacies displaying peloid (P), aggregate grain (Ag), micritized laminated ooids (O), foraminifera (Fr), intraclast (Ir), bioclasts (B), ostracods (Os), calcisphere (Cs) and stylolite (St) (PPL, GT/S 42).

Plate 2: 113

Figure A: Photomicrograph, of bioclastic packstone sub-microfacies showing partially sparite ostracods (Os), pyrite (Pr), bivalves (Bi), calcisphere (Cs) microcrystalline vein (V) and micrite matrix (M) (PPL, GT /S 4).

Figure B and C: Photomicrograph of bioclastic packstone sub-microfacies showing ostracods (Os), echinoderm (E), burrows (Br), charophyta (Cr), Pyrite (Pr), calcisphere (Cs) bivalves (Bi), calcite vein (V) and stylolite (S) (PPL, GT /S 21).

Figure D: Photomicrograph represent bioclastic packstone sub-microfacies showing foraminifers (Fm), echinoderm (E) and bivalves (Bi) (PPL, GT/S 50).

Figure E: Photomicrograph of bioclastic packstone sub-microfacies illustrating organic matter (OM), bivalves (Bi) and calcite vein (V). (PPL, GT/S 50).

Figure F: Photomicrograph of bioclastic packstone sub-microfacies showing aggregate grain (Ag), peloids (P) and bioturbation (Bt) (PPL, GT/S 64).

Plate 3:

115

Figure A: Photomicrograph of intraclastic packstone showing intraclast (Ir), corals (Co), ostracods (Os), ooids (O), bivalves (Bi), peloids (P), and organic matter (OM) (PPL, GT /S 7).

Figure B: Photomicrograph of intraclastic packstone showing peloids (P), ooids (O), intraclast (Ir) and (PPL, GT /S 5).

Figure C: Photomicrograph of peloidal packstone sub-microfacies showing Peloids (P), Ooids (O), ostracods (Os) and bivalves (Bi) (PPL, GT/S 10).

Figure D: Photomicrograph of peloidal packstone showing peloids (P) bivalves (Bi), intraclast (Ir) and stylolite (St) (PPL, GT/S 25).

Figure E: Photomicrograph of peloidal packstone sub-microfacies showing bioclasts (Bl) pyrite (Pr) and calcite vein (V) (PPL, GT/S 32).

Figure F: Photomicrograph of bivalve packstone sub-microfacies showing bivalves (pelecypods, Pe), dolomite crystal (D) and pyrite (Pr) (PPL, GT/S 46).

Plate 4:

117

Figure A: Photomicrograph of peloidal wackestone showing bioclast (Bl), peloids (P), pyrite (Pr) and calcite vein (V) (PPL, GT /S 44).

Figure B: Photomicrograph of peloidal wackestone showing peloids (P) and intraclast (Ir) (PPL, GT /S 65).

Figure C: Photomicrograph of bioclastic wackestone showing bivalve (Bi), ostracods (Os), organic matter (OM), stylolite (St), intraclast (Ir), and bioturbation (Bt) (PPL, GT/S 28).

Figure D: Photomicrograph of bioclastic wackestone sub-microfacies showing forams (Fm) and bivalves (Bi), (PPL, GT/S 60).

Figure E: Photomicrograph of bioclastic wackestone sub-microfacies showing gastropods is displaced due to microstructure fault (G), bivalve (Bi) and calcite vein (V) (PPL, GT/S 61).

Figure F: Photomicrograph of bioclastic wackestone showing Bivalve (Bi) calcisphere (Cs) and pyrite (Pr) (PPL, GT/S 63).

Plate 5:

119

Figure A: Photomicrograph of wackstone showing intraclast (Ir), bivalve (Bi), peloids (P), intraclast (Ir) and calcite vein (V) (PPL, GT /S 11).

Figure B and C: Photomicrograph of brecciated lime mudstone displaying stylolaminated, rhombohedral crystal of dolomite (D), intraclast (Ir) and stylolite (St) (PPL, GT /S 20).

Figure D: Photomicrograph of wackstone displaying tempestite and bivalves (Bi), (PPL, GT/S 24).

Figure E: Photomicrograph of wackstone represents bivalve (Bi) pyrite (Pr) and calcite vein (V) (PPL, GT/S 61).

Figure F: Photomicrograph of wackstone represents bivalve (Bi) calcisphere (Cs) and pyrite (Pr) (PPL, GT/S 57).

Plate 6:

121

Figure A and B: Photomicrograph of bindstone displaying fine layer between peloidal layer .consist of intraclast (Ir), ooids (O), peloids (P), stylolite (St) and calcite vein (V) (PPL, GT /S 23).

Figure C and D: Photomicrograph of bindstone microfacies showing dolomitization of fossil fragment and lime mud matrix, peloids (P), gastropods (G), bivalves (Bi), organic matter (OM) and calcite vein (V) (PPL, GT/S 41).

Figure E: Photomicrograph, of stromatolite bindstone microfacies showing algae (Al) organic matter (OM) and calcite vein (V) (PPL, GT/S 47).

Figure F: Photomicrograph of displaying skeletal stromatolite bindstone having agglutinated fabric. algae, calcisphere (Cs), organic matter (OM) and vein (V) (PPL, GT/S 48).

Plate 7:

123

Figure A and B: Photomicrograph illustrating rudstone microfacies showing dark grey intraclast (Ir), bioclast (B) and calcite cement (C), ostracods (Os) (A, PPL, and B XPPL GT/S 54).

Figure C: Photomicrograph displays rudstone microfacies showing micritic intraclast (Ir), peloid (P) and pyrite (Pr) (PPL GT/S 9).

Figure D: Photomicrograph displaying rudstone microfacies showing intraclast (Ir), peloid (P) and micritic ooids (MO) and aggregate grain (Ag) (PPL GT/S 54).

Figure E: Photomicrograph of rudstone microfacies showing A. peloids (P), intraclast (Ir), pyrite (Pr) and calcite cement (C). (PPL, GT/S 6)

Figure F: Photomicrograph of rudstone showing laminated ooid (O), ostracods (Os), embedded in sparite cement (Sp) (PPL, GT/S 68).

Plate 8: 125

Figure A and B: Photomicrograph shows rudstone displaying intraclast (Ir), bivalves (Bi), peloids (P), aggregate grain (Ag) and bioclast (Bl) (PPL, GT/S 14).

Figure C: Photomicrograph of rudstone microfacies showing calcisphere (Cs) Intraclast (Ir) (PPL, GT/S 26).

Figure D: Photomicrograph of peloidal packstone showing bioclast (Bl), intraclast (Ir) and pyrite (Pr) (PPL, GT/S 25).

Plate 9: Figure A, B and C: Photomicrograph of grey to black color clayey shale showing unidentified fossil fragment (Fl), bivalve (Bi), hematite (H) calcite vein (V) and organic matter (OM) (GT/S 13). 127

Plate 10: 129

Figure A and B: Photomicrograph, represent dark grey to black color silty shale showing parallel lamination (L), bivalve (Bi) and organic matter (OM) (GT/S 43).

Figure C and D: Photomicrograph of dark grey to black color black shale showing intraclast, calcite vein, fracture and organic matter (OM) (Figure A, XPPL; B. PPL, GT/S 56).

Plate 11: 131

Figure A and B: Photomicrograph of grey to black color claystone showing unidentified fossil fragment (Fl), hematite (H) micro fracture (Mf) and organic matter (OM) (Figure 1. 20X, PPL, Figure 2. 4X, GT/S 3).

Figure C: Photomicrograph representing hematite (H) and silicification (4X, PPL, GT/S 58).

Figure D: Thin section photograph of grey to black color claystone showing hematite (H) and silicification (S) (XPPL, GT/S 58).

Figure E: Photomicrograph of grey to black color claystone showing relict of feldspar (F) (XPPL, 10 X, GT/S 3).

Plate 12: 132

Figure A, B and C: Photomicrograph represents black color silty claystone displaying bivalves (Bi), burrows (Br), calcite vein (V), sparite (Sv) and organic matter (OM). (PPL, 4X, GT/S 45).

Plate 13: 134

Figure A and B: Microphotograph of microcrystalline dolomite fabrics consist of pyrite cubic crystal and calcite vein (A: PPL, 4X, B: PPL, 20 X, GT/S 35).

Figure C: Microphotograph of dolomite texture showing xenotopic and pyrite cubic crystal (PPL, 40 X GT/S 35).

CHAPTER 1

INTRODUCTION

1.1. PURPOSE AND SCOPE

The Devonian-Carboniferous period is significant time interval in the geological time scale because of different geological events occurred such as mass extinction, Variscan orogenesis. Therefore, these periods have been studied in depth all over the world for sedimentology, paleogeography, paleoclimatology, stratigraphic correlation, global tectonics and anoxic events. Several studies on the Devonian-Carboniferous sedimentology and anoxic events have been carried out by different scientists (i.e. Allen and Rajetzky, 1992; Göncüoğlu et al., 1997; Caplan et al., 1999; Menning et al., 2006; Yalçın and Yilmaz, 2010).

The aim of this study is to determine the depositional changes and sedimentological properties of the Yılanlı Formation of Upper Devonian-Lower Carboniferous of the Zonguldak region, Northwest Turkey. This study can be helpful for petroleum explorations and may be used to establish the correlation with other stratigraphic successions of different terranes like Moesian Terrane, Istanbul Terrane and Balkan Terrane (Garetskiy, 1970; Görür et al., 1997; Dachev et al., 1998).

No detailed sedimentological studies have been carried out so far in the Gökgöl tunnel section of the Yılanlı Formation. The present study covers the detail lithological description, facies, components analysis and sedimentological interpretation of 86 meter interval of the Yılanlı Formation (Upper Devonian - Lower Carboniferous) at the Gökgöl section.

1.2. GEOGRAPHIC SETTING

The study area is situated near Gökgöl tunnel in the Zonguldak region, Black Sea region, NW Turkey (Figures 1.1, 1.2 and 1.3). The studied section was measured about 268 km northwest of Ankara. The studied section of the Gökgöl tunnel (GT) is easily accessible from Zonguldak city. The studied section was sampled from the exposed outcrops near Gökgöl tunnel on the Çaycuma highway near Asma, Zonguldak city. The geographic coordinates of the measured stratigraphic section are latitude $41^{\circ}26'16.10''\text{N}$ and longitude $31^{\circ}50'11.30''\text{E}$ approximately.

1.3. METHODS OF STUDY

This study consists of field and laboratory works. The field study has been carried out in the exposed outcrops near the Gökgöl tunnel on the Çaycuma highway near Asma town, Zonguldak.

In the field, the stratigraphic section was measured from bottom to top of the formation by using centimeter tape. During the study 8,600 cm thick sedimentary sequence of the Yılanlı Formation was measured. Sixty eight oriented and disoriented samples were collected through the section. The sampling interval between the collected samples ranged from 2 cm to 1200 cm. The measured stratigraphic log was drawn along with description of observed sedimentary structures and identified fossils. The rock colors have been assigned to strata using dry color chart by visual estimation, according to international color codes of the geological rock color chart of Geological Society of America (GSA, 2009).

For microscopic studies, thin sections of all the samples were prepared and studied under the polarized microscopes. Detailed microfacies study was carried out in the laboratory. The quantitative analysis was carried out by point counting method using James Swift apparatus that is mounted to microscopic stage. This point counting data was used in order to obtain percentage and numbers of the components. 600-1100 points were counted per thin section. The point counting data and visual estimation observation of different components of the microfacies are used to generate a graph and ternary diagrams to interpret the depositional environment and component variation within the microfacies at different interval and through the measured section.

The microfacies analyses are carried out to determine the texture and composition of the sample using visual estimation chart (Baccelle and Bosellini, 1965), to classify different microfacies. Facies under the polarized microscope are used to determine the ratio between matrix and components within the individual lithofacies and the variations of matrix and terrigenous material along the measured section. The microphotographs of the thin sections were taken by Olympus SC30 camera in the Crustal Research Laboratory, Geological Engineering Department, Middle East Technical University. The graphic sedimentary log was prepared by the Sedlog software Sedlog 3.1. This software is developed by a Dimitrios Zervas (SedLog developer) at Royal Holloways. This is a multifunction software for creating a graphic sediment log that is used by geologist. This software provides an intuitive graphical user interface that make it very easy for anyone to use with minimum time and effort (<http://www.sedlog.com/>). These microscopic details were used for interpretation of sedimentology and depositional environments.



Figure 1.1: Geographic location of the studied section in the Zonguldak region, NW Turkey (Red rectangle).



Figure 1.2: Satellite image showing the studied location in the Zonguldak region, NW Turkey (Yellow arrow represents north direction of the Google map).



Figure 1.3: Close view of the satellite image red arrow showing the studied section in the Zonguldak region, NW Turkey.

1.4. PREVIOUS STUDIES

The study area is geographically located in the vicinity of the Zonguldak region (Okay, 1989) of north western Black Sea region. Zonguldak Terrane comprises four regions; Çamdağ, Zonguldak, Amasra and Safranbolu (Göncüoğlu and Kozur, 1998, a, b). Many studies have been carried out in the Pontides due to presence of natural resource such as petroleum and coal resources since 1890.

In Pontides, coal basins were studied by Stasinopoulos (1898), Pohl (1903), Yeğin (1912), Arni (1938, 1940 a, b, c, d, 1941), Eğemen and Pekmezçiler (1945), Arslan (1978), Bulut et al. (1982, 1992), Nekir et al. (1996), Yavuz et al. (2000). Zonguldak basin have a major bituminous coal deposit of Turkey. There are many coal seams in the area. Tonsteins and smectites are reported by Burger et al., (2000) from Zonguldak Terrane.

Studies on coal bed methane (CBM) were carried out (Yalçın 1991, 1997; Yalçın et al., 1994; Mann et al., 1995; Gürdal and Yalçın, 1995, 2000; Gürdal, 1998; Karayığit et al., 1998).

The petroleum and gas potential (Carboniferous) in the region was examined by Erdoğan (1963), Wedding (1968, 1969) and Taşman (1981).

The general geology of the Pontides region was studied by Lucius (1926), Ziglstra (1950), Fratschiner (1952), Tokay (1954), Pince (1982), Deveciler (1986), and Nejdi (1994a,b). Paleozoic of the Zonguldak Terrane is different from the Istanbul Terrane (Göncüoğlu and Kozur, 1998). The authors discussed the stratigraphy of the Zonguldak Terrane. Lower Paleozoic rocks of the Istanbul Terrane are similar to Zonguldak Terrane (Chen et al., 2002). Middle Devonian to Lower Carboniferous stratigraphic sequence consists of carbonates of the shelf type deposition that is overlain by non-marine coal bearing units. Yılmaz (2002) described sedimentology, cyclostratigraphy and sequence stratigraphy of pelagic and carbonate platform of the Zonguldak Terrane, NW Turkey. Upward shallowing pattern is observed in all the measured stratigraphic sections. Ünlüce (2013) studied the K-bentonite of the Yılanlı Formation of shallow marine carbonate platform of the Zonguldak region. Denayer

(2014) carried out studies on shallow marine limestone of the Yılanlı Formation and identified different species of corals and brachiopods.

Paleogeography and paleoclimatology of the Zonguldak Terrane was discussed and correlated with Istanbul Terrane, Moesian Terrane and Balkan Terrane (Göncüoğlu et al., 1997; Yanev, S. and Cassinis, G. 1998; Yanev, 2000).

REGIONAL GEOLOGICAL SETTING

The tectonic setting of Turkey represents a complex regional geological setting that is formed by the continental and oceanic crust, and show lateral tectonic setting with Alpine Orogeny (Şengör and Yılmaz, 1981; Göncüoğlu et al., 1997). The Pontides have almost the complete record of evolution of the Tethys. Pontides are divided into three regions (Figures 1.4 and 1.5): Western Pontides, Central Pontides and Eastern Pontides (Tüysüz, 1993). The Western Pontides comprise following tectonic units: The Istranca Massif, the Istanbul – Zonguldak zone, the Armutlu-Almacik zone and the Sakarya continent. The Istanbul – Zonguldak zone tectonically overlies on Rhodope – Pontide fragment and the northern most part of the Western Pontides. Istanbul and Zonguldak terranes were considered as a single unit (Görür et al., 1997). However, Göncüoğlu and Kozur (1998, 1999) suggested that Zonguldak Terrane is distinct to Istanbul Terrane. In Istanbul–Zonguldak terranes, the lower Paleozoic sedimentary sequence is similar on the basis of lithology and depositional features. In Istanbul–Zonguldak, the basement rocks consist of a high grade metamorphic crystalline assemblage. This assemblage consists of metagabbro, dolerite dykes, granite, gneiss and schist. The crystalline basement is overlain by a thick, lower Paleozoic sedimentary sequence. The sedimentary strata of Ordovician comprises Kurtköy and Aydos Formation (red conglomerate, mudstone and sandstone). The Aydos Formation sequence in Zonguldak Terrane is similar to Istanbul Terrane (Dean et al., 1997; Göncüoğlu, 1997). The Aydos Formation is overlain by thick limestone of Upper Ordovician. In the Zonguldak region the Upper Silurian is missing (Dean et al., 1993), while in the Istanbul region there is a transitional unit of Silurian and Devonian (Ketin, 1983). The Fındıklı Formation is overlain by the Ferizli Formation which consists of siltstone, shale and cross bedded sandstone. The upper contact of the Ferizli Formation is conformable with the Yılanlı Formation of Middle Devonian to

Lower Carboniferous. The general lithology of the Yılanlı Formation is dark grey, grey, beige colored nodular limestone interbedded with shale, marl, dolomite, chert, shale and clay. The Yılanlı Formation is conformably overlain by the Madendere Formation of turbidite. The Alacağazı Formation (Namurian), the Kozlu Formation, the Karadon Formation and the Kızıllı Formation (Kerey, 1984; Görür et al., 1997; Yiğitbaş et al., 1999) of Pennsylvanian of marine to continental rock units that consist shale bearing coal seams with sandstone bed and conglomerate of dark grey to black color and at the upper part of Kızıllı strata a red unfossiliferous bed are present. The Zonguldak Formation of Namurian to Westphalian consists of fluvial deltaic sediments comprising coal seams in Zonguldak Terrane (Akyol et al., 1974). The patchy outcrops of Mesozoic sediments unconformably overlie on the Paleozoic strata. The Çakraz Formation consists of river and flood plain deposits of Triassic having unconformable contact with underlying the Zonguldak Formation and overlain by the Himmetpaşa Formation of the Middle Jurassic of turbiditic clasts with coal beds at the base of the Formation. The İnaltı Formation has disconformable contact with the Himmetpaşa Formation and comprises homogeneous carbonate platform of Late Jurassic. Two sedimentary basins were formed during Cretaceous time period; the Zonguldak and the Ulus Basin (Tüysüz, 1999). The Ulus Formation consists of marine deposit resting unconformably on the İnaltı Formation. Görür (1997) described the Ulus sediment as syn-rift deposits of Western Black Sea Basin of Early Cretaceous. The Ulus Formation has four members: Mezeci clastics, İnpiri limestones, Türbeyanı marls and Ulus flysch. The upper contact of the Ulus Formation is unconformable with the Dereköy Formation of Turonian that comprises magmatic rocks with alternation of shallow and deep carbonate and clastics. This formation was reported as syn – rift deposit (Tüysüz, 1999). The Upper Santonian pelagic limestone of the Unaz Formation shows variable contact (unconformable and transitional) with underlying Dereköy Formation or syn-rift deposit due to horst and graben of the area. The Cambu Formation consists of a thick volcano sedimentary sequence of Campanian have a conformable contact with Dereköy Formation (Tüysüz and Sunal, 2002). The Akveren Formation of late Cretaceous (Maastrichtian) have conformable contact with the Cambu Formation which consists of calciturbidite and pelagic mudstone. This formation represents the end of arc magmatism. The Cenozoic of the Istanbul-Zonguldak terranes comprises the Atbaşı Formation and the Kusuri Formation. The

Atbaşı Formation consists of pelagic mudstone and marl of the Paleocene. The Kusuri Formation of Eocene displays regressive developments and consists of marl, turbiditic sandstone and shale (Akyol et al., 1974; Tüysüz, 1997; Ketin and Gümüş, 1963).



Figure 1.4: Dark grey patches represent Paleozoic outcrops in the Zonguldak Terrane (simplified from Bozkaya et al., 2012).

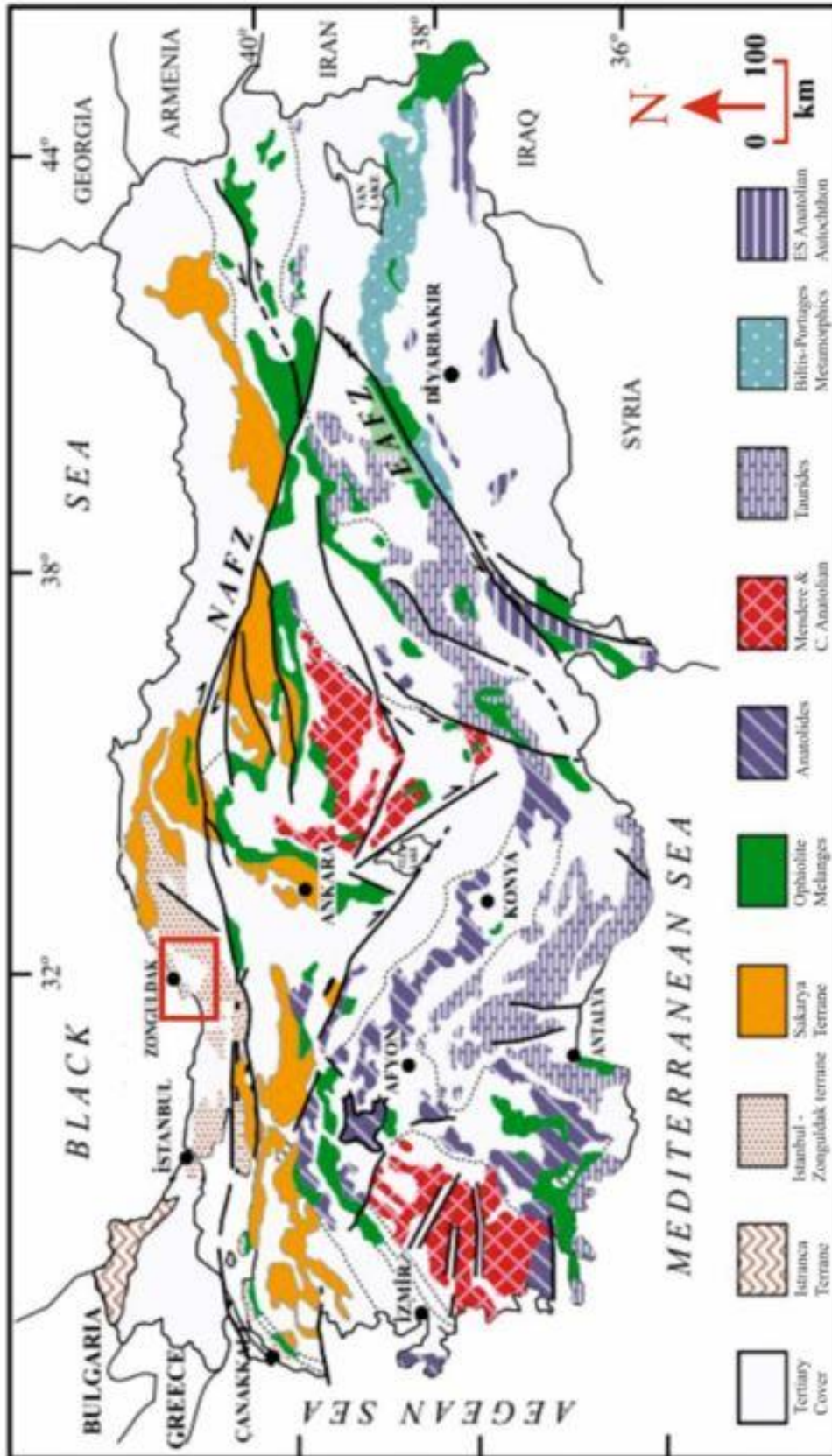


Figure 1.5: The tectonic units of the Turkey, and Istanbul-Zonguldak terranes (simplified from Göncüoğlu et al., 1997; the red rectangle represents the study area).

CHAPTER 2

LITHOSTRATIGRAPHY

2.1. LITHOSTRATIGRAPHY OF ZONGULDAK REGION

The general stratigraphy of the Zonguldak Terrane ranges from Precambrian to Carboniferous. The main exposed rocks are sedimentary that ranges from Ordovician to Carboniferous in the studied area. Lithological characters of various rock units were noted briefly, however, the exposed section of the Yılanlı Formation near Gökgöl tunnel, Asma village was studied in detail (Figures 2.1, 2.2, 2.3 and 2.4).

The basement of the Zonguldak Terrane is exposed in the Karadere area that comprises a metamorphic crystalline series of continental crust-originated gneisses; an oceanic set of gabbros, basalts and ultramafics of Cadomian (Chen et al., 2002; Göncüoğlu et al., 2014). The upper contact of Cadomian basement is unconformable with Lower Ordovician Bakacak member of Kurtköy Formation (Özgül, 2011) that consists of siltstone and mudstone (Göncüoğlu et al., 2014). The Kurtköy Formation consists of red, pinkish and grey colored arkosic conglomerate, sandstone, shale and mudstone unit (Dean et al., 1993). The Aydos Formation conformably overlies the Kurtköy Formation that consists of a thick – massive bedded light grey to white colored quartzite and quartz-arenite, have a gradational contact with the Karadere Formation that comprises thick beds of quartz sandstone in lower part of the Karadere Formation. The general lithology of the Karadere Formation is characterized by grey – dark grey mudstone followed by thin bedded shale having pyrite black-dark grey color (Dean et al., 1997, 2000). The Ketencikdere Formation has two members that are limestone and siltstone members. Limestone member consists of medium to thick bedded mudstone interbedded with black limestone while the siltstone member consists of a succession of poorly bedded dark grey to greyish green silty mudstone or siltstone that lies on the top of limestone bed. The upper strata of the Silurian were eroded. The Fındıklı Formation comprises graptolite bearing grey shale interbedded with mudstone of

greenish grey – grey colored with intercalations of thin beds of limestone. Graptolite was reported from the Fındıklı Formation dominantly consists of black siliceous argillites and lydites (Göncüoğlu et al., 2011). The Bıçkılı Formation unconformably overlies the Fındıklı Formation and consists of red color cross bedded sandstone and mudstone of Middle Devonian. The general lithology of the Ferizli Formation is characterized by shale, siltstone and limestone of grey to black color. The Yılanlı Formation of Late Middle Devonian - Lower Carboniferous includes shallow marine sequence that consists of limestone interbedded with shale and dolomite. According to Harput et al, (1999), the Yılanlı Formation in the Zonguldak Terrane has an average value of TOC is 0.63% which may have a potential for hydrocarbon generation. The Yılanlı Formation is conformably overlain by Lower to Upper Carboniferous strata that includes shallow marine to marine and continental deposits of the Madendere Formation, the Alacağazı Formation, the Kozlu Formation, the Karadon Formation, the Kızıllı Formation and the Zonguldak Formation. The Paleozoic sediments are unconformably overlain by a patchy outcrops of Mesozoic sediments that consists of continental deposits of Triassic followed by a homogeneous carbonate platform deposits. The Ulus Formation unconformably overlying the İnaltı Formation consists of marine sediments as syn-rift deposits of Western Black Sea basin of Early Cretaceous (Görür et al., 1997). The Ulus Formation is unconformably overlain by the alternations of volcanic rocks and shallow, deep marine carbonate and clastics of the Dereköy Formation have unconformable and transitional contact with the Unaz Formation that is followed by volcano sedimentary sequence, calciturbidites and pelagic mudstone of the Cambu and the Akveren Formations. The lower contact of the Akveren Formation is transitional – unconformable with the Cambu Formation while upper contact is conformable with the Atbaşı Formation. The Cenozoic of the Zonguldak Terrane consists of the Atbaşı Formation and the Kusuri Formation that represents the carbonates, pelagic mudstone and marl of Paleocene and marl, turbiditic sandstone and shale of Eocene respectively, were deposited in E-W trending narrow basin (Figure 2.1).

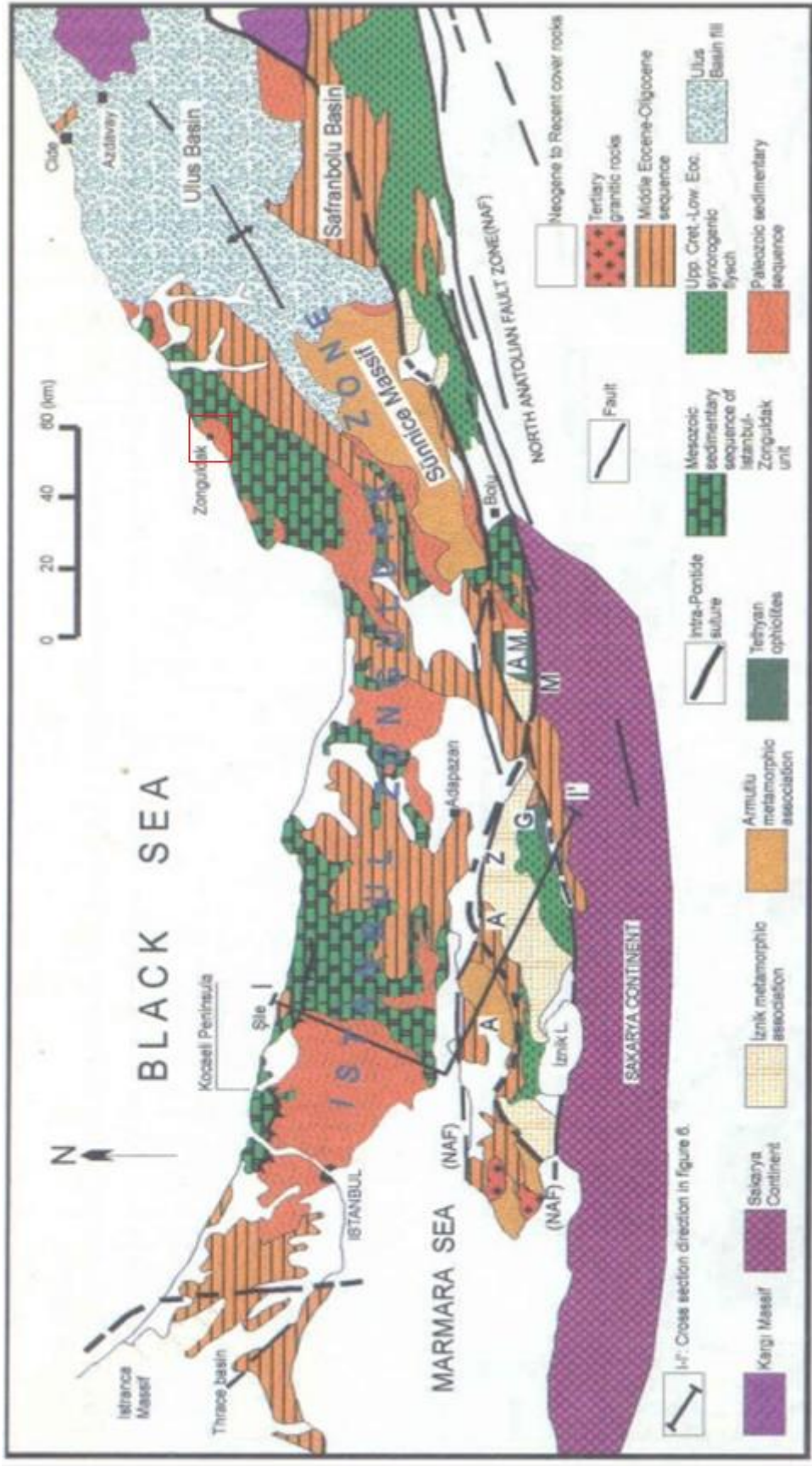


Figure 2.1: Geological map of the Istanbul - Zonguldak zone of the Western Pontides (simplified from Yilmaz et al., 1997).

| AGE | FORMATION | LITHOLOGY | EXPLANATION |
|---------------|----------------------|--|---|
| EOCENE | KUSURI | | Turbiditic sandstone - shale alternation. |
| PALEOCENE | ATBAŞI | | Carbonate Mudstone |
| CRETACEOUS | Mastrichtian | AKVEREN | Limestone, Clayey Limestone, Calcirudite, marl, Olistostome, Conglomerate. Confirmity / Unconfirmity |
| | Campanian | CAMBU | Andesite, Basalt, Agglomerate, Tuff, Volcanoclastics |
| | Up Station Campanian | UNAZ | Clayey Limestone, Marl. Post break - up unconfirmity |
| | Turonian Coniacian | DEREKÖY | Andesite, Basalt and Pyroclastics, Fault scarp deposits with limestone block Conglomerate, sandstone, micritic limestone, Tuff, lava Unconfirmity |
| | Lower | ULUS | Turbiditic sandstone - shale alternation blocks of Inaın Formation Marl with Ammonite, Conglomerate, sandstone, limestone, Mudstone. Unconfirmity |
| | JURASSIC | Malm | INALTI |
| Dogger | | HİMMETPAŞA | sandstone, shale, coal, Turbiditic sandstone - shale alternation Conglomerate, quartz sandstone and coal Unconfirmity |
| | | | |
| TRIASSIC | | ÇAKRABOZ | Marl and lacustrine limestone. |
| | | ÇAKRAZ | Red sandstone and Conglomerate. Unconfirmity |
| CARBONIFEROUS | | ZONGULDAK | Conglomerate, sandstone, shale and coal. |
| | | KIZILLI / KARADON KÖYÜ MADENDERE / ALACAGAZI | Violet - brown sandstone, green shale alternation with minor nodular limestone. |
| | | YILANLI | Grey nodular limestone with black chert. Grey- beige limestone interbedded with shale, dolomite and lime mudstone. Grey, medium, thick - bedded limestone and dolomite with yellowish - green volcanoclastic tephra. (K- bentonite layers) |
| DEVONIAN | | FERİZLİ | Beige grey shale, red - brown oolitic limestone, chamosite, black siltstone and nodular Limestone. |
| | | BIÇKI | Red, cross bedded sand - mudstone with conglomerate beds, yellowish brown sandstone and siltstone. Unconfirmity |
| | | | |
| SILURIAN | | FINDIKLI | Black shale with dark grey brown limestone and dolomitic Limestone interlayers. |
| | | KETENÇIKDERE | Black shale with light grey quartz - rich siltstone and rare Limestone interlayers. |
| ORDOVİCIAN | | KARADERE | Black - greenish grey, Well - cleaved shale, minor black siltstone. |
| | | AYDOS | White - buff, silica cemented, cross-bedded Quartz arenites with siltstone interlayer and conglomerate lenses. |
| | | KURTKÖY | Red violet sandstone and mudstone with conglomerate lenses. |
| | | SÖĞÜKSU - BAKACAK | Greenish grey sandstone- siltstone with grey shale mudstone interlayers. Unconfirmity |
| PRECAMBRIAN | YEDİGÖLLER | Gneiss, Amphibolite with apite pegmatite and microdiorite veins. | |

Figure 2.2: Generalized columnar section of the Zonguldak region (not to scale, modified from Bozkaya et al., 2012; Tüysüz et al., 2002).



Figure 2.3: The field photograph showing carbonate sequence of the Yılanlı Formation on the road side.



Figure 2.4: General view of the bottom of thin to thick beds of carbonate of the Yılanlı Formation.

2.2. LITHOSTRATIGRAPHY OF THE SECTION

The stratigraphic section measured at SE of Asma town at Gökgöl tunnel that lies in the upper part of the upper Middle Devonian - Lower Carboniferous of the Yılanlı Formation. This formation is characterized by cherty limestone, shale interbedded with limestone, dolomite and claystone with K-bentonite layers.

The Yılanlı Formation has two members, the Alabalık Member (Kipman, 1974) and the Manastır Member (Gedik and Önalın, 2001). The Alabalık Member comprises of the lower part of the Yılanlı Formation that mainly consists of dark grey lime mud rock succession followed by presence of small coral build-ups abundantly in the middle part of the member. The intercalations of limestone increase in thickness as move upward grading into the main body of the Yılanlı Formation. The presence of rugose and tabulate corals indicates a middle Eifelian age for this member (Kaya and Birenheide, 1988). The Manastır member is characterized by the alternation of nodular limestone, shale, siltstone and dolomite of beige, grey, greenish – yellowish, thin to medium bedded consists of abundance of macrofossils mainly corals, brachiopods, bivalves and yields the Eifelian age (Kaya and Birenheide, 1988). The general lithology of the Yılanlı Formation is characterized by grey to dark grey, beige, greenish colored limestone, lime mudstone, dolomitic limestone, dolomite, marl and chert of medium to thick bedded alternate with thin beds of clay, black shale, calcareous shale, carbonaceous shale and K-bentonite (Türkmenođlu et al., 2015). The Yılanlı Formation has a thickness of approximately 800 meter (Türkmenođlu et al., 2015). The upper contact of the Yılanlı Formation is transitional with the Alacađazı Formation (Yalçın and Yılmaz, 2010). In Çamdađ area, the Yılanlı Formation unconformably overlain by Permo – Triassic sediments of the Çakraz Formation or overlain by younger sediments (Kaya et al., 1988; Gedik et al., 2005; Yalçın and Yılmaz, 2010). The boundary between Devonian and Carboniferous is located in the lower part of the Yılanlı Formation (Okuyucu et al., 2005). In the Western Pontides, the Yılanlı Formation is exposed throughout.

The Yılanlı Formation was deposited in a shallow marine to shelf / carbonate platform of a typical marine environment in between Middle Devonian to Early Carboniferous time intervals (Aydın et al., 1987; Derman, 1997; Yalçın and Yılmaz, 2010; Bozkaya et al., 2012, 2016). On the basis of fossils, age of the Yılanlı Formation represents Eifelian – Visean (Middle Devonian to Lower Carboniferous) (Dil, 1976; Kaya and Birenheide, 1988). The Yılanlı Formation is partially equivalent to lithics of (Kaya, 1973). Kozyatağı limestone and time equivalent of Büyükada Formation in İstanbul region and Devonian (Dinantian) limestone of (Görür et al., 1997) (Figure 2.5).

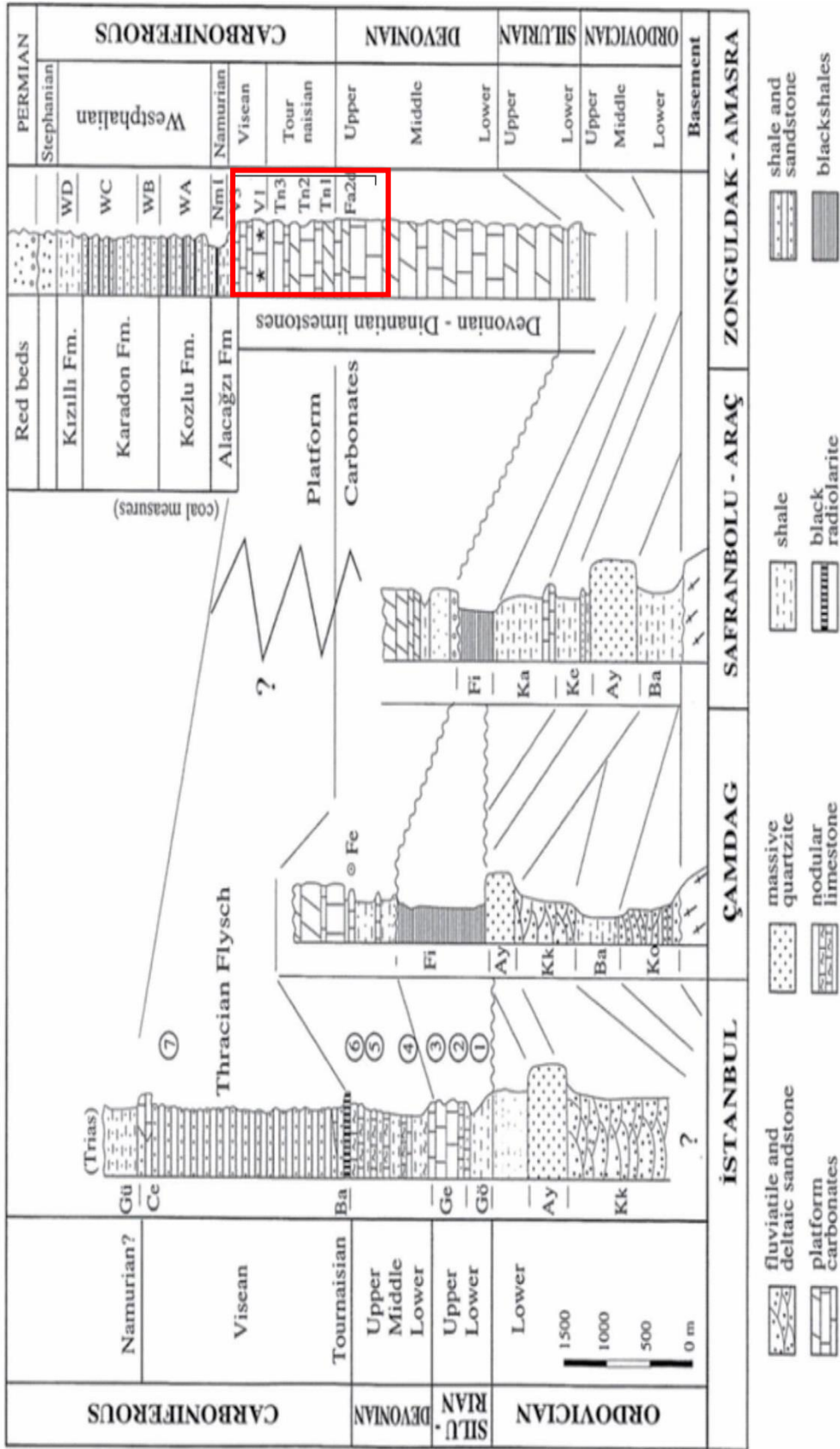


Figure 2.5: Paleozoic formations of the Western Pontides (Black line represents the Yılanlı Formation equivalent to Fa2d –V1, Görür et al., 1997. Red rectangle represents studied sequence.).

In the present study, different lithologic units of the Yılanlı Formation are studied (Table 2.1). The measured stratigraphic section starts from thin bed of dark grey to black color rich in organic matter of shale. Shale beds are alternating with grey, light grey, dark grey, beige to black colored limestone have intercalations of mudstone (Figures 2.6, 2.7 and 2.8). Some fossils like corals, bivalve, gastropods and stromatolite in this part of the formation are documented (Figures 2.9 and 2.10).



Figure 2.6: The field photograph displaying the bottom of the studied section. Thick bedded limestone with thin shale (a), limestone (b) and mudstone (c) alternations.

Table 2.1: Identification of samples with their color from the Gököl Section.

| Gököl Section Samples color name and their color code | | | | |
|---|--------|---|---|--|
| No. | Sample | Rock and their outcrop color | Color Name (Munsell Color Book) (GSA, 2009) | Geological Color Chart Code (Munsell Color Book) (GSA, 2009) |
| 1. | GT01 | Dark Grey Black color Clayey Shale | Greyish Black | N2 |
| 2. | GT02 | Grey color Bioclastic Packstone | Medium Grey | N5 |
| 3. | GT03 | Grey color Laminated Claystone | Medium Grey | N5 |
| 4. | GT04 | Dark Grey Black Bioclastic Packstone | Greyish Black | N2 |
| 5. | GT05 | Grey Beige color Intraclastic Packstone | Yellowish Grey | 5Y 8/1 |
| 6. | GT06 | Grey color Rudstone | Medium Grey | N5 |
| 7. | GT07 | Dark Grey Intraclastic Packstone | Dark Grey | N3 |
| 8. | GT08 | Dark Grey color burrowed lime Mudstone | Dark Grey | N3 |
| 9. | GT09 | Dark Grey - Beige color Rudstone | Dark Grey | N3 |
| 10. | GT10 | Dark Grey Beige color Peloidal Packstone | Pinkish Grey | 5YR 8/1 |
| 11. | GT11 | Dark Grey -Dark Beige color Bioclastic Wackestone | Dark Grey | N3 |
| 12. | GT12 | Light Grey-Beige color Peloidal Grainstone | Pinkish Grey | 5YR 8/1 |
| 13. | GT13 | Dark Black Clayey Shale | Black | N1 |
| 14. | GT14 | Dark Grey color Rudstone | Dark Grey | N3 |
| 15. | GT15 | Dark Grey color Burrowed Lime Mudstone | Dark Grey | N3 |
| 16. | GT16 | Yellow light brown color Burrowed Lime Mudstone | Dusky Red | 5R 3/4 |
| 17. | GT17 | Black color Muddy organic rich Shale | Black | N1 |
| 18. | GT18 | Beige color Bioclastic Wackestone | Yellowish Grey | 5Y 8/1 |
| 19. | GT19 | Grey Color Intraclastic Packstone | Medium Grey | N5 |
| 20. | GT20 | Beige color Brecciated Mudstone | Yellowish Grey | 5Y 8/1 |
| 21. | GT21 | Dark Grey Black Bioclastic Packstone | Greyish Black | N2 |
| 22. | GT22 | Dark Grey color Peloidal Grainstone | Dark Grey | N3 |
| 23. | GT23 | Black color Bindstone | Black | N1 |
| 24. | GT24 | Dark Grey color Bioclastic Wackestone | Dark Grey | N3 |
| 25. | GT25 | Dark Grey Beige color Peloidal Packstone | Pinkish Grey | 5YR 8/1 |
| 26. | GT26 | Black color Rudstone | Black | N1 |
| 27. | GT27 | Light Grey Beige color Bioclastic Wackestone | Yellowish Grey | 5Y 8/1 |
| 28. | GT28 | Light Grey Beige color Bioclastic Wackestone | Yellowish Grey | 5Y 8/1 |
| 29. | GT29 | Black color burrowed lime Mudstone | Black | N1 |
| 30. | GT30 | Light Grey Beige color Peloidal Grainstone | Yellowish Grey | 5Y 8/1 |
| 31. | GT31 | Grey Color Peloidal Packstone Yellow color claystone at bottom | Medium Grey Moderate Yellow | N5 5Y 7/6 |
| 32. | GT32 | Light Grey Beige color Peloidal Packstone | Yellowish Grey | 5Y 8/1 |
| 33. | GT33 | Light Grey Beige color Bioclastic Wackestone | Yellowish Grey | 5Y 8/1 |
| 34. | GT34 | Grey Black color Clayey Shale | Greyish Black | N2 |
| 35. | GT35 | Grey Beige color Sparite Dolomite | Pinkish Grey | 5YR 8/1 |
| 36. | GT36 | Grey Black color Shale | Greyish Black | N2 |
| 37. | GT37 | Grey Beige color Bioclastic Wackestone | Pinkish Grey | 5YR 8/1 |
| 38. | GT38 | Yellow color claystone | Moderate Yellow | 5Y 7/6 |
| 39. | GT39 | Light Grey color Rudstone | Light Grey | N7 |
| 40. | GT40 | Black color shale | Black | N2 |
| 41. | GT41 | Grey Color Bindstone | Medium Grey | N5 |
| 42. | GT42 | Dark Grey color Peloidal Grainstone | Dark Grey | N3 |
| 43. | GT43 | Black Silty shale having Mudstone | Greyish Black | N2 |
| 44. | GT44 | Dark Grey Black color Peloidal Wackestone | Greyish Black | N2 |
| 45. | GT45 | Black color Silty claystone | Greyish Black | N2 |
| 46. | GT46 | Dark Grey color Bivalve Packstone | Dark Grey | N3 |
| 47. | GT47 | Dark Grey Black Bindstone (stromatolite) | Black | N1 |
| 48. | GT48 | Dark Grey Black Bindstone (stromatolite) | Greyish Black | N2 |
| 49. | GT49 | Beige creamy color Bioclastic Wackestone | Pale yellowish Orange | 10YR 8/6 |
| 50. | GT50 | Grey color Bioclastic Packstone | Medium Grey | N5 |
| 51. | GT51 | Grey Creamy color Bioclastic Packstone | Pale Green to grey | G 7/2 |
| 52. | GT52 | Green color Bioclastic Packstone | Brilliant Green | 5G 6/6 |
| 53. | GT53 | Grey color Peloidal Packstone | Medium Grey | N5 |

Table 2.1: Continued

| | | | | |
|-----|------|---|---------------------|---------|
| 54. | GT54 | Dark Grey color Rudstone | Dark Grey | N3 |
| 55. | GT55 | Grey Color Bioclastic Packstone | Medium Grey | N5 |
| 56. | GT56 | Dark Grey color Black Shale | Dark Grey | N3 |
| 57. | GT57 | Grey color Intraclastic Wackestone | Medium Grey | N5 |
| 58. | GT58 | Grey color Claystone | Medium Grey | N5 |
| 59. | GT59 | Greyish Green color Intraclastic Wackestone | Light Greenish Grey | 5GY 6/1 |
| 60. | GT60 | Beige color Bioclastic Wackestone | Yellowish Grey | 5Y 8/1 |
| 61. | GT61 | Grey color Bioclastic Wackestone | Medium Grey | N5 |
| 62. | GT62 | Black color Peloidal Grainstone | Black | N1 |
| 63. | GT63 | Grey color Bioclastic Wackestone | Medium Grey | N5 |
| 64. | GT64 | Grey –Beige color Bioclastic calci Packstone | Yellowish Grey | 5Y 8/1 |
| 65. | GT65 | Dark grey color Peloidal Wackestone | Dark Grey | N3 |
| 66. | GT66 | Dark grey – Beige color Intraclastic Wackestone | Pinkish Grey | 5YR 8/1 |
| 67. | GT67 | Dark grey Black color Clayey Shale | Greyish Black | N2 |
| 68. | GT68 | Dark grey color Rudstone | Dark Grey | N3 |



Figure 2.7: Shale interbedded with limestone in lower part of measured section.



Figure 2.8: A photograph displaying parallel lamination on outcrop of mudstone.



Figure 2.9: A photograph showing corals in thick bedded limestone approximately in the middle of the section (GT25).



Figure 2.10: A photograph illustrating bivalve in the middle of the measured section of limestone.

From bottom to top of the sequence a stratigraphic log was prepared (Figure 2.11). During the field different lithologies were recorded and some microfossils, intraclast and parallel laminations were observed (Figures 2.12, 2.13 and 2.14).

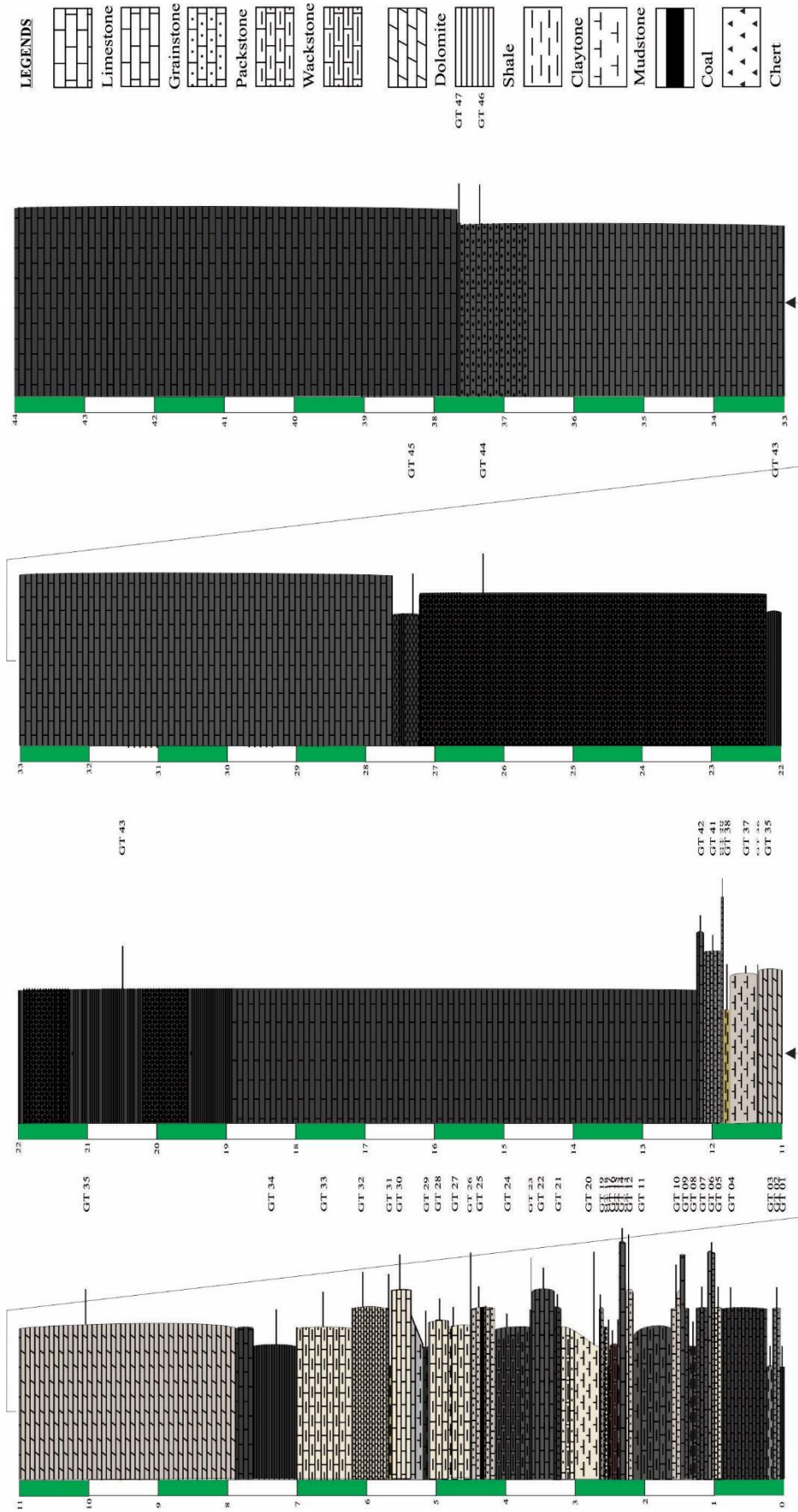


Figure 2.11: The lithologic log of the Yılanlı Formation at Gökçöl section (0-44 m).

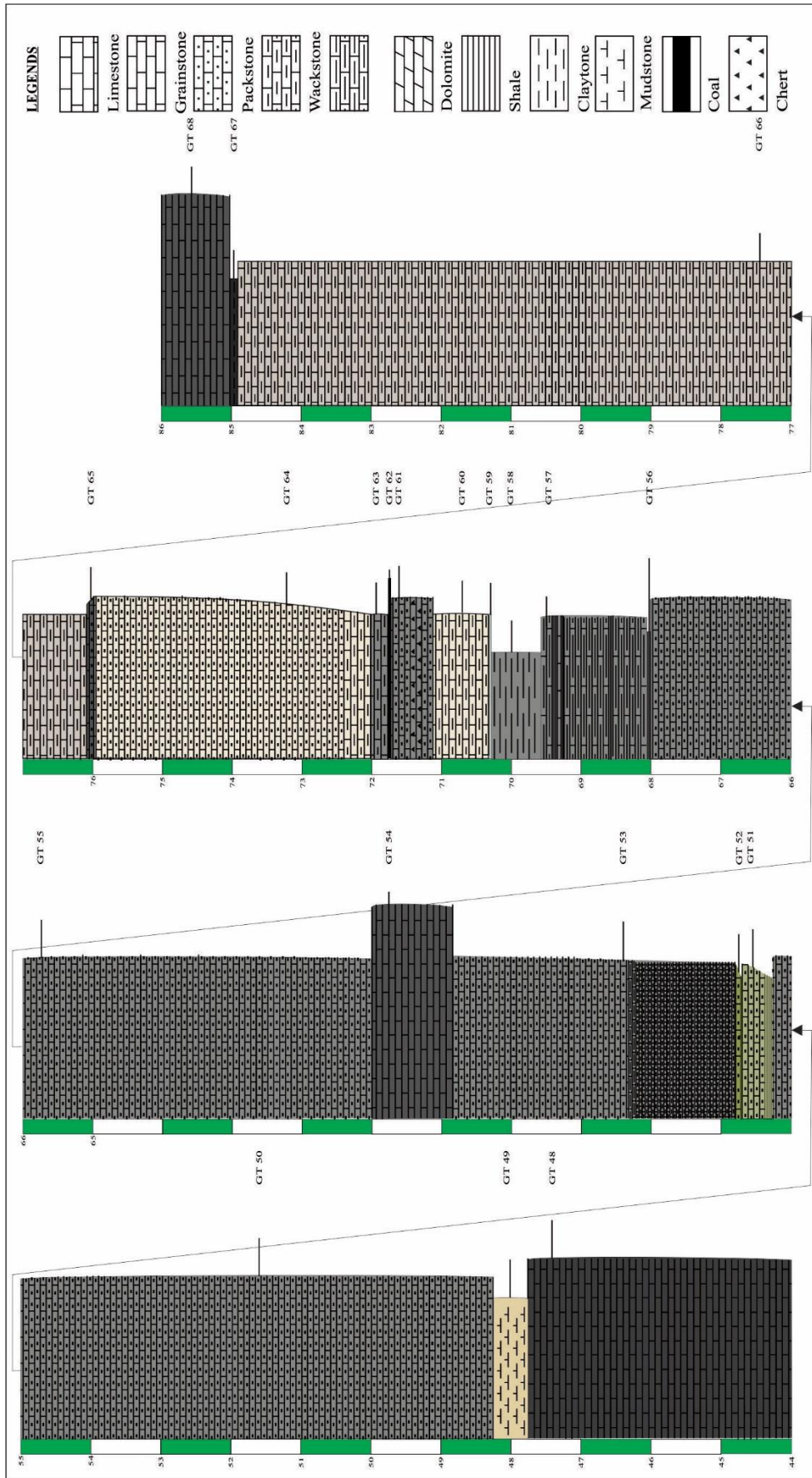


Figure 2.11: Continued (44-86 m).



Figure 2.12: A field view of thick bedded limestone at the top of the studied section.



Figure 2.13: A close view of thick bedded limestone and intercalation of shale represents different sample numbers.



Figure 2.14: A photograph showing intraclast in rudstone microfacies of thick bedded limestone.

CHAPTER 3

MICROFACIES ANALYSIS

3.1 SEDIMENTOLOGICAL STUDIES

The measured stratigraphic section comprises Upper Devonian - Lower Carboniferous strata of the Yılanlı Formation. The samples were taken from almost every bed layer. The sedimentological study is based on the field observations and laboratory studies. These studies include identification of lithology and sedimentary structure. Microfacies analysis include petrographic determinations, point counting, grain size measurements and their statistical interpretation. These analysis are used to classify the facies, understand the carbonate depositional environment and interpret possible conditions of deposition of the formation in the Gökgöl tunnel section. There are nine different microfacies established in measured section.

3.2. RESULTS OF POINT COUNTING AND MEASUREMENTS

In order to determine the percentage constituents of microfacies, the point counting method has been carried out and results of point counting (Figure 3.1) were used to categorize changes in the composition of the microfacies (Table 3.1).

Through the petrographic studies, different minerals (chlorite, feldspar and muscovite), lithic-clasts, bioclasts, pyrite, hematite, cement and matrix have been recognized and counted per thin section as quantitatively. The point counting quantitative measurement percentage data are represented by Table 3.2.

Grain size of some microfacies were measured (Table 3.3). The grain size is used to indicate the depositional environment and a major factor that effects porosity and permeability values. In this study, concentric, radial, superficial and micritic ooids

were documented. Ooids consisting of tangential laminae indicates high energy marine environment may be oolitic shoals or tidal bars (Flügel, 2004). Micritic ooids are characterized by reduced sedimentation rate and random growth in marine environment. The presence of radial ooids illustrates low-moderate energy condition for the deposition.

The graphic interpretation of intraclast measurements indicate that the formation is deposited at shallow marine. The measurement converted to phi values are used to construct Passega diagram (Figure 3.2). Very few sample values indicate the beach deposition (Flügel 2004, pp 253). The median value in phi scale for intraclast is 2.9 (Passega, 1964).

The point counting data percentage peaks indicate that the bottom part of the measured section has a sudden variation in depositional environment. The peloids and intraclast peaks in Figure 3.3 illustrates that environment is shallow but few high peaks of lime matrix indicate lagoonal to shoal. Low value of benthic forams indicate that water depth increases. The middle of the section represents a stable depth of water as compared to bottom of the section indicated by all allochem and matrix having approximately same values (Figure 3.3). The upper part has almost same depositional condition as bottom but the sample sixty eight represent sudden shallowing of environment.

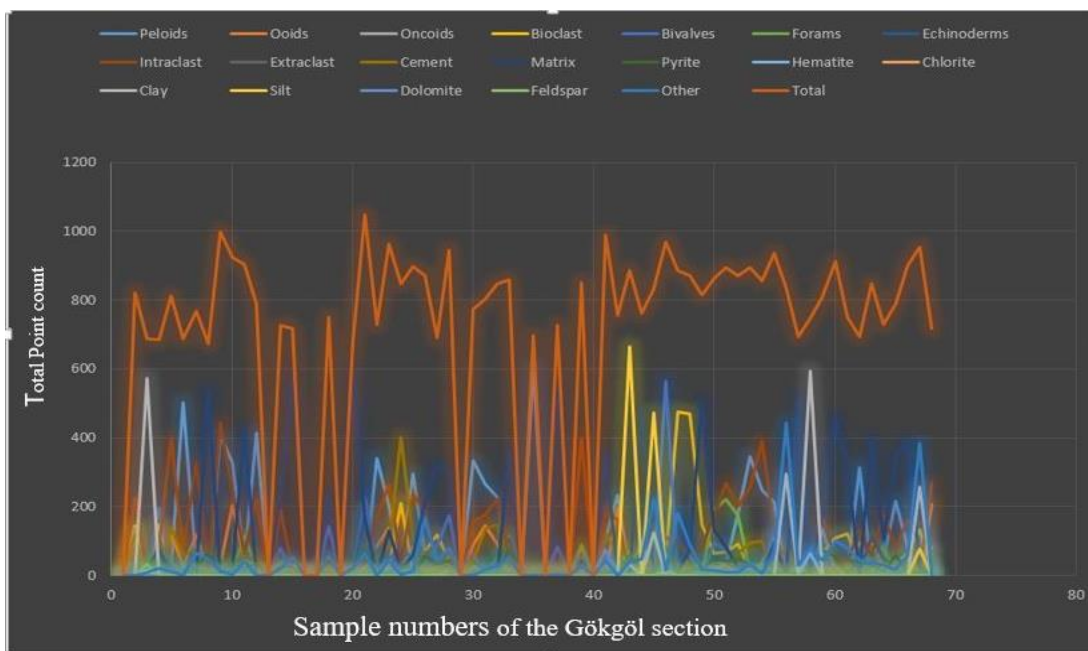


Figure 3.1: Graphic illustration of point counting data of the Gökgöl section.

Table 3.1. Petrographic and point counted data of the Gököl samples (data illustrated in graphic curve as Figure 3.1).

| Sample | Peloids | Ooids | Oncoid | Bioclast | Bivalves | Forams | Echioderm | Intraclast | Extra clast | Cement | Matrix | Pyrite | Hematite | Chlorite | Clay | Silt | Dolomite | Feldspar | Other | Total |
|--------|---------|-------|--------|----------|----------|--------|-----------|------------|-------------|--------|--------|--------|----------|----------|------|------|----------|----------|-------|-------|
| GT 1 | 0 | 0 | 0 | 0 | 0 | 0 | 0 | 0 | 0 | 0 | 0 | 0 | 0 | 0 | 0 | 0 | 0 | 0 | 0 | 0 |
| GT 2 | 110 | 39 | 0 | 145 | 0 | 137 | 35 | 0 | 2 | 0 | 0 | 10 | 0 | 0 | 0 | 0 | 0 | 0 | 0 | 822 |
| GT 3 | 0 | 0 | 0 | 0 | 0 | 0 | 0 | 0 | 0 | 3 | 24 | 27 | 0 | 0 | 573 | 16 | 0 | 34 | 10 | 687 |
| GT 4 | 4 | 8 | 0 | 148 | 195 | 35 | 62 | 84 | 0 | 0 | 78 | 50 | 0 | 0 | 0 | 0 | 0 | 0 | 21 | 685 |
| GT 5 | 23 | 126 | 0 | 31 | 14 | 32 | 28 | 0 | 6 | 0 | 0 | 4 | 0 | 0 | 0 | 0 | 0 | 0 | 14 | 812 |
| GT 6 | 502 | 27 | 2 | 5 | 9 | 0 | 0 | 68 | 0 | 60 | 0 | 16 | 0 | 0 | 0 | 0 | 0 | 0 | 0 | 689 |
| GT 7 | 26 | 118 | 0 | 33 | 47 | 23 | 22 | 0 | 1 | 74 | 2 | 26 | 0 | 0 | 0 | 0 | 0 | 0 | 67 | 768 |
| GT 8 | 0 | 4 | 0 | 2 | 0 | 0 | 0 | 9 | 0 | 12 | 537 | 62 | 0 | 0 | 0 | 0 | 0 | 0 | 48 | 674 |
| GT 9 | 409 | 31 | 0 | 14 | 25 | 0 | 8 | 0 | 0 | 43 | 0 | 12 | 0 | 0 | 0 | 0 | 0 | 0 | 12 | 998 |
| GT 10 | 327 | 204 | 0 | 19 | 0 | 12 | 15 | 0 | 1 | 40 | 18 | 34 | 0 | 0 | 0 | 0 | 0 | 0 | 5 | 923 |
| GT 11 | 42 | 48 | 0 | 29 | 38 | 115 | 17 | 64 | 6 | 55 | 423 | 22 | 0 | 1 | 0 | 0 | 1 | 0 | 42 | 903 |
| GT 12 | 415 | 29 | 0 | 18 | 11 | 16 | 0 | 0 | 0 | 45 | 0 | 33 | 0 | 0 | 0 | 0 | 0 | 0 | 0 | 790 |
| GT 13 | 0 | 0 | 0 | 0 | 0 | 0 | 0 | 0 | 0 | 0 | 0 | 0 | 0 | 0 | 0 | 0 | 0 | 0 | 0 | 0 |
| GT 14 | 43 | 29 | 0 | 29 | 80 | 10 | 27 | 0 | 12 | 25 | 232 | 27 | 0 | 0 | 0 | 0 | 0 | 0 | 22 | 726 |
| GT 15 | 2 | 0 | 0 | 33 | 0 | 0 | 5 | 15 | 0 | 15 | 572 | 23 | 0 | 0 | 0 | 0 | 0 | 0 | 54 | 719 |
| GT 16 | 0 | 0 | 0 | 0 | 0 | 0 | 0 | 0 | 0 | 0 | 0 | 0 | 0 | 0 | 0 | 0 | 0 | 0 | 0 | 0 |
| GT 17 | 0 | 0 | 0 | 0 | 0 | 0 | 0 | 0 | 0 | 0 | 0 | 0 | 0 | 0 | 0 | 0 | 0 | 0 | 0 | 0 |
| GT 18 | 60 | 42 | 0 | 41 | 143 | 0 | 63 | 34 | 0 | 26 | 237 | 45 | 0 | 0 | 0 | 0 | 1 | 0 | 58 | 750 |
| GT 19 | 0 | 0 | 0 | 0 | 0 | 0 | 0 | 0 | 0 | 0 | 0 | 0 | 0 | 0 | 0 | 0 | 0 | 0 | 0 | 0 |
| GT 20 | 0 | 0 | 0 | 5 | 0 | 0 | 0 | 9 | 0 | 7 | 607 | 21 | 0 | 0 | 0 | 0 | 5 | 0 | 22 | 676 |
| GT 21 | 0 | 27 | 0 | 190 | 224 | 0 | 173 | 36 | 91 | 6 | 163 | 72 | 0 | 1 | 0 | 0 | 0 | 0 | 66 | 0 |
| GT 22 | 339 | 87 | 0 | 19 | 36 | 0 | 12 | 0 | 1 | 54 | 0 | 16 | 0 | 0 | 0 | 0 | 0 | 0 | 0 | 729 |
| GT 23 | 205 | 139 | 0 | 24 | 48 | 13 | 5 | 0 | 2 | 85 | 130 | 5 | 0 | 0 | 0 | 0 | 0 | 0 | 42 | 964 |
| GT 24 | 26 | 18 | 0 | 211 | 86 | 0 | 35 | 37 | 10 | 0 | 19 | 0 | 0 | 0 | 0 | 0 | 0 | 0 | 5 | 849 |
| GT 25 | 295 | 84 | 0 | 13 | 48 | 23 | 15 | 0 | 0 | 0 | 59 | 4 | 0 | 0 | 0 | 0 | 0 | 0 | 13 | 899 |
| GT 26 | 59 | 6 | 0 | 72 | 23 | 0 | 7 | 0 | 68 | 11 | 212 | 58 | 0 | 0 | 0 | 0 | 1 | 0 | 166 | 870 |
| GT 27 | 3 | 6 | 0 | 119 | 85 | 0 | 15 | 40 | 5 | 20 | 323 | 34 | 0 | 0 | 0 | 0 | 0 | 0 | 42 | 692 |
| GT 28 | 60 | 15 | 0 | 46 | 175 | 0 | 35 | 69 | 77 | 35 | 308 | 45 | 0 | 0 | 0 | 0 | 0 | 0 | 81 | 946 |
| GT 29 | 0 | 0 | 0 | 0 | 0 | 0 | 0 | 0 | 0 | 0 | 0 | 0 | 0 | 0 | 0 | 0 | 0 | 0 | 0 | 0 |
| GT 30 | 335 | 90 | 0 | 29 | 65 | 0 | 38 | 0 | 0 | 44 | 8 | 10 | 0 | 0 | 0 | 0 | 0 | 0 | 0 | 775 |
| GT 31 | 267 | 145 | 0 | 20 | 0 | 0 | 17 | 0 | 0 | 5 | 14 | 0 | 0 | 0 | 0 | 0 | 0 | 0 | 18 | 802 |
| GT 32 | 228 | 92 | 0 | 11 | 5 | 52 | 35 | 0 | 17 | 0 | 13 | 0 | 0 | 0 | 0 | 0 | 0 | 0 | 27 | 849 |
| GT 33 | 4 | 6 | 0 | 114 | 59 | 0 | 110 | 47 | 3 | 26 | 361 | 77 | 0 | 0 | 0 | 0 | 0 | 0 | 53 | 860 |
| GT 34 | 0 | 0 | 0 | 0 | 0 | 0 | 0 | 0 | 0 | 0 | 0 | 0 | 0 | 0 | 0 | 0 | 0 | 0 | 0 | 0 |
| GT 35 | 0 | 0 | 0 | 0 | 0 | 0 | 0 | 0 | 0 | 37 | 0 | 46 | 0 | 0 | 0 | 0 | 0 | 0 | 1 | 697 |
| GT 36 | 0 | 0 | 0 | 0 | 0 | 0 | 0 | 0 | 0 | 0 | 0 | 0 | 0 | 0 | 0 | 0 | 0 | 0 | 0 | 0 |
| GT 37 | 0 | 0 | 0 | 24 | 84 | 0 | 17 | 34 | 0 | 3 | 548 | 15 | 0 | 0 | 0 | 0 | 0 | 0 | 3 | 728 |
| GT 38 | 0 | 0 | 0 | 0 | 0 | 0 | 0 | 0 | 0 | 0 | 0 | 0 | 0 | 0 | 0 | 0 | 0 | 0 | 0 | 0 |
| GT 39 | 45 | 82 | 0 | 21 | 60 | 89 | 11 | 0 | 11 | 39 | 42 | 26 | 0 | 0 | 0 | 0 | 0 | 0 | 26 | 852 |
| GT 40 | 0 | 0 | 0 | 0 | 0 | 0 | 0 | 0 | 0 | 0 | 0 | 0 | 0 | 0 | 0 | 0 | 0 | 0 | 0 | 0 |
| GT 41 | 111 | 0 | 0 | 27 | 11 | 35 | 18 | 0 | 0 | 0 | 357 | 7 | 0 | 0 | 0 | 0 | 74 | 0 | 46 | 988 |
| GT 42 | 233 | 196 | 0 | 31 | 17 | 43 | 0 | 0 | 0 | 70 | 0 | 2 | 0 | 0 | 0 | 0 | 0 | 0 | 0 | 755 |
| GT 43 | 0 | 0 | 0 | 68 | 0 | 0 | 0 | 10 | 0 | 0 | 64 | 0 | 0 | 34 | 666 | 0 | 4 | 39 | 885 | |
| GT 44 | 101 | 3 | 0 | 8 | 7 | 0 | 0 | 72 | 0 | 12 | 485 | 24 | 0 | 0 | 0 | 0 | 2 | 0 | 49 | 763 |
| GT 45 | 0 | 0 | 0 | 1 | 0 | 0 | 0 | 0 | 11 | 0 | 1 | 0 | 0 | 125 | 474 | 0 | 0 | 0 | 221 | 833 |
| GT 46 | 15 | 19 | 0 | 51 | 563 | 0 | 0 | 7 | 1 | 81 | 85 | 16 | 0 | 0 | 0 | 0 | 0 | 0 | 16 | 968 |
| GT 47 | 0 | 0 | 0 | 475 | 0 | 0 | 110 | 90 | 8 | 7 | 11 | 3 | 0 | 0 | 0 | 0 | 0 | 0 | 182 | 886 |
| GT 48 | 57 | 6 | 0 | 470 | 0 | 0 | 42 | 64 | 6 | 43 | 77 | 16 | 0 | 0 | 0 | 0 | 0 | 0 | 89 | 870 |
| GT 49 | 2 | 8 | 0 | 147 | 0 | 0 | 11 | 83 | 0 | 19 | 506 | 20 | 0 | 0 | 0 | 0 | 1 | 0 | 17 | 814 |
| GT 50 | 46 | 21 | 0 | 66 | 95 | 190 | 55 | 0 | 13 | 8 | 134 | 44 | 0 | 0 | 0 | 0 | 0 | 0 | 15 | 863 |
| GT 51 | 32 | 29 | 0 | 69 | 74 | 223 | 41 | 0 | 11 | 12 | 84 | 41 | 0 | 0 | 0 | 0 | 0 | 0 | 11 | 896 |
| GT 52 | 180 | 0 | 0 | 92 | 47 | 174 | 15 | 0 | 13 | 67 | 24 | 47 | 0 | 0 | 0 | 0 | 0 | 0 | 11 | 870 |
| GT 53 | 347 | 25 | 0 | 13 | 36 | 13 | 0 | 0 | 12 | 95 | 30 | 32 | 0 | 0 | 0 | 0 | 0 | 0 | 33 | 894 |
| GT 54 | 250 | 14 | 0 | 35 | 15 | 28 | 12 | 0 | 0 | 0 | 4 | 0 | 0 | 0 | 0 | 0 | 2 | 0 | 8 | 858 |
| GT 55 | 214 | 54 | 0 | 110 | 138 | 38 | 59 | 0 | 5 | 2 | 98 | 16 | 0 | 0 | 0 | 0 | 0 | 0 | 65 | 937 |
| GT 56 | 0 | 0 | 0 | 1 | 0 | 0 | 0 | 0 | 0 | 89 | 0 | 3 | 0 | 0 | 297 | 2 | 0 | 0 | 444 | 836 |
| GT 57 | 0 | 9 | 0 | 26 | 15 | 0 | 11 | 66 | 0 | 14 | 515 | 8 | 0 | 0 | 0 | 0 | 0 | 0 | 31 | 695 |
| GT 58 | 0 | 0 | 0 | 0 | 0 | 0 | 0 | 0 | 0 | 0 | 7 | 66 | 0 | 594 | 0 | 0 | 0 | 0 | 79 | 746 |
| GT 59 | 136 | 37 | 0 | 65 | 35 | 0 | 45 | 0 | 0 | 21 | 179 | 75 | 0 | 0 | 0 | 0 | 0 | 0 | 45 | 809 |
| GT 60 | 9 | 3 | 0 | 110 | 17 | 0 | 95 | 48 | 0 | 9 | 463 | 55 | 0 | 0 | 0 | 0 | 2 | 0 | 101 | 912 |
| GT 61 | 9 | 26 | 0 | 121 | 19 | 0 | 55 | 41 | 40 | 31 | 318 | 8 | 0 | 0 | 0 | 0 | 0 | 0 | 81 | 749 |
| GT 62 | 313 | 95 | 0 | 29 | 14 | 0 | 18 | 0 | 0 | 3 | 0 | 40 | 0 | 0 | 0 | 0 | 1 | 0 | 46 | 694 |
| GT 63 | 16 | 17 | 0 | 108 | 44 | 0 | 110 | 57 | 0 | 23 | 403 | 32 | 0 | 0 | 0 | 0 | 0 | 0 | 38 | 848 |
| GT 64 | 44 | 46 | 0 | 9 | 95 | 85 | 51 | 0 | 39 | 36 | 105 | 14 | 0 | 0 | 0 | 0 | 0 | 0 | 29 | 730 |
| GT 65 | 217 | 8 | 0 | 36 | 0 | 0 | 0 | 77 | 0 | 32 | 342 | 59 | 0 | 0 | 0 | 0 | 0 | 0 | 19 | 790 |
| GT 66 | 84 | 9 | 0 | 63 | 26 | 0 | 35 | 0 | 6 | 54 | 393 | 9 | 0 | 0 | 0 | 0 | 0 | 0 | 61 | 902 |
| GT 67 | 0 | 0 | 0 | 134 | 70 | 0 | 0 | 0 | 0 | 2 | 22 | 8 | 0 | 0 | 258 | 76 | 0 | 0 | 383 | 953 |
| GT 68 | 81 | 206 | 0 | 11 | 25 | 24 | 22 | 0 | 0 | 75 | 0 | 0 | 0 | 0 | 0 | 0 | 0 | 0 | 4 | 718 |

Table 3 2. Percentage data of the quantitative analysis using point count data for the measured Gökgöl section (data illustrated in graphic curves as well as in ternary diagrams).

| Sample | Peloid% | Ooids % | Oncoid % | Bioclast % | Intraclast % | Extra clast % | Cement % | Matrix % | Pyrite % | Silt % | Clay % | Dolomite % | Other % | Total |
|--------|---------|---------|----------|------------|--------------|---------------|----------|----------|----------|--------|--------|------------|---------|-------|
| GT 1 | 0 | 0 | 0 | 0 | 0 | 0 | 0 | 0 | 0 | 0 | 0 | 0 | 0 | 0 |
| GT 2 | 13.4 | 4.7 | 0 | 20.9 | 27.37 | 0.24 | 14.5 | 0 | 1.2 | 0 | 0 | 0 | 0 | 100 |
| GT 3 | 0 | 0 | 0 | 0 | 0 | 0 | 0.44 | 3.49 | 3.9 | 2.33 | 83.41 | 0 | 1.46 | 100 |
| GT 4 | 0.58 | 1.2 | 0 | 42.6 | 12.26 | 0 | 0 | 11.4 | 7.3 | 0 | 0 | 0 | 3.07 | 100 |
| GT 5 | 2.83 | 16 | 0 | 9.11 | 49.01 | 0.74 | 16.7 | 0 | 0.5 | 0 | 0 | 0 | 1.72 | 100 |
| GT 6 | 72.9 | 3.9 | 0.3 | 1.31 | 9.869 | 0 | 8.71 | 0 | 2.3 | 0 | 0 | 0 | 0 | 100 |
| GT 7 | 3.39 | 15 | 0 | 12 | 42.84 | 0.13 | 9.64 | 0.26 | 3.4 | 0 | 0 | 0 | 8.72 | 100 |
| GT 8 | 0 | 0.6 | 0 | 0 | 1.335 | 0 | 1.78 | 79.7 | 9.2 | 0 | 0 | 0 | 7.12 | 100 |
| GT 9 | 41 | 3.1 | 0 | 3.31 | 44.49 | 0 | 4.31 | 0 | 1.2 | 0 | 0 | 0 | 1.2 | 100 |
| GT 10 | 35.4 | 22 | 0 | 2.93 | 26.87 | 0.11 | 4.33 | 1.95 | 3.7 | 0 | 0 | 0 | 0.54 | 100 |
| GT 11 | 4.65 | 5.3 | 0 | 18.8 | 7.087 | 0.66 | 6.09 | 46.8 | 2.4 | 0 | 0 | 0.11 | 4.65 | 100 |
| GT 12 | 52.5 | 3.7 | 0 | 3.42 | 28.23 | 0 | 5.7 | 0 | 4.2 | 0 | 0 | 0 | 0 | 100 |
| GT 13 | 0 | 0 | 0 | 0 | 0 | 0 | 0 | 0 | 0 | 0 | 0 | 0 | 0 | 0 |
| GT 14 | 5.92 | 4 | 0 | 16.1 | 26.17 | 1.65 | 3.44 | 32 | 3.7 | 0 | 0 | 0 | 3.03 | 100 |
| GT 15 | 0.28 | 0 | 0 | 0.7 | 2.086 | 0 | 2.09 | 79.6 | 3.2 | 0 | 0 | 0 | 7.51 | 100 |
| GT 16 | 0 | 0 | 0 | 0 | 0 | 0 | 0 | 0 | 0 | 0 | 0 | 0 | 0 | 0 |
| GT 17 | 0 | 0 | 0 | 0 | 0 | 0 | 0 | 0 | 0 | 0 | 0 | 0 | 0 | 0 |
| GT 18 | 8 | 5.6 | 0 | 27.5 | 4.533 | 0 | 3.47 | 31.6 | 6 | 0 | 0 | 0.13 | 7.73 | 100 |
| GT 19 | 0 | 0 | 0 | 0 | 0 | 0 | 0 | 0 | 0 | 0 | 0 | 0 | 0 | 0 |
| GT 20 | 0 | 0 | 0 | 0 | 1.331 | 0 | 1.04 | 89.8 | 3.1 | 0 | 0 | 0.74 | 3.25 | 100 |
| GT 21 | 0 | 2.6 | 0 | 37.8 | 3.432 | 8.67 | 0.57 | 15.5 | 6.9 | 0 | 0 | 0 | 6.29 | 100 |
| GT 22 | 46.5 | 12 | 0 | 6.58 | 22.63 | 0.14 | 7.41 | 0 | 2.2 | 0 | 0 | 0 | 0 | 100 |
| GT 23 | 21.3 | 14 | 0 | 6.85 | 27.59 | 0.21 | 8.82 | 13.5 | 0.5 | 0 | 0 | 0 | 4.36 | 100 |
| GT 24 | 3.06 | 2.1 | 0 | 14.3 | 4.358 | 1.18 | 47.3 | 2.24 | 0 | 0 | 0 | 0 | 0.59 | 100 |
| GT 25 | 32.8 | 9.3 | 0 | 9.57 | 26.47 | 0 | 11.9 | 6.56 | 0.4 | 0 | 0 | 0 | 1.45 | 100 |
| GT 26 | 6.78 | 0.7 | 0 | 3.45 | 21.49 | 7.82 | 1.26 | 24.4 | 6.7 | 0 | 0 | 0.11 | 19.1 | 100 |
| GT 27 | 0.43 | 0.9 | 0 | 14.5 | 5.78 | 0.72 | 2.89 | 46.7 | 4.9 | 0 | 0 | 0 | 6.07 | 100 |
| GT 28 | 6.34 | 1.6 | 0 | 22.2 | 7.294 | 8.14 | 3.7 | 32.6 | 4.8 | 0 | 0 | 0 | 8.56 | 100 |
| GT 29 | 0 | 0 | 0 | 0 | 0 | 0 | 0 | 0 | 0 | 0 | 0 | 0 | 0 | 0 |
| GT 30 | 43.2 | 12 | 0 | 13.3 | 20.13 | 0 | 5.68 | 1.03 | 1.3 | 0 | 0 | 0 | 0 | 100 |
| GT 31 | 33.3 | 18 | 0 | 2.12 | 22.32 | 0 | 17.1 | 0.62 | 1.7 | 0 | 0 | 0 | 2.24 | 100 |
| GT 32 | 26.9 | 11 | 0 | 10.8 | 26.15 | 2 | 17.3 | 0 | 1.5 | 0 | 0 | 0 | 3.18 | 100 |
| GT 33 | 0.47 | 0.7 | 0 | 19.7 | 5.465 | 0.35 | 3.02 | 42 | 9 | 0 | 0 | 0 | 6.16 | 100 |
| GT 34 | 0 | 0 | 0 | 0 | 0 | 0 | 0 | 0 | 0 | 0 | 0 | 0 | 0 | 0 |
| GT 35 | 0 | 0 | 0 | 0 | 0 | 0 | 5.31 | 0 | 6.6 | 0 | 0 | 87.9 | 0.14 | 100 |
| GT 36 | 0 | 0 | 0 | 0 | 0 | 0 | 0 | 0 | 0 | 0 | 0 | 0 | 0 | 0 |
| GT 37 | 0 | 0 | 0 | 13.9 | 4.67 | 0 | 0.41 | 75.3 | 2.1 | 0 | 0 | 0 | 0.41 | 100 |
| GT 38 | 0 | 0 | 0 | 0 | 0 | 0 | 0 | 0 | 0 | 0 | 0 | 0 | 0 | 0 |
| GT 39 | 5.28 | 9.6 | 0 | 18.8 | 46.95 | 1.29 | 4.58 | 4.93 | 3.1 | 0 | 0 | 0 | 3.05 | 100 |
| GT 40 | 0 | 0 | 0 | 0 | 0 | 0 | 0 | 0 | 0 | 0 | 0 | 0 | 0 | 0 |
| GT 41 | 11.2 | 0 | 0 | 6.48 | 18.62 | 0 | 11.9 | 36.1 | 0.7 | 0 | 0 | 7.49 | 4.66 | 100 |
| GT 42 | 30.9 | 26 | 0 | 7.95 | 21.59 | 0 | 9.27 | 0 | 0.3 | 0 | 0 | 0 | 0 | 100 |
| GT 43 | 0 | 0 | 0 | 0 | 1.13 | 0 | 0 | 0 | 7.2 | 75.3 | 3.842 | 0 | 4.41 | 100 |
| GT 44 | 13.2 | 0.4 | 0 | 0.92 | 9.436 | 0 | 1.57 | 63.6 | 3.1 | 0 | 0 | 0.26 | 6.42 | 100 |
| GT 45 | 0 | 0 | 0 | 0 | 0 | 0 | 1.32 | 0 | 0.1 | 56.9 | 15.01 | 0 | 26.5 | 100 |
| GT 46 | 1.55 | 2 | 0 | 58.2 | 11.78 | 0.72 | 0.1 | 8.37 | 8.8 | 0 | 0 | 0 | 1.65 | 100 |
| GT 47 | 0 | 0 | 0 | 12.4 | 10.16 | 0.9 | 0.79 | 1.24 | 0.3 | 0 | 0 | 0 | 20.5 | 100 |
| GT 48 | 6.55 | 0.7 | 0 | 4.83 | 7.356 | 0.69 | 4.94 | 8.85 | 1.8 | 0 | 0 | 0 | 10.2 | 100 |
| GT 49 | 0.25 | 1 | 0 | 1.35 | 10.2 | 0 | 2.33 | 62.2 | 2.5 | 0 | 0 | 0.12 | 2.09 | 100 |
| GT 50 | 5.33 | 2.4 | 0 | 39.4 | 20.39 | 1.51 | 0.93 | 15.5 | 5.1 | 0 | 0 | 0 | 1.74 | 100 |
| GT 51 | 3.57 | 3.2 | 0 | 37.7 | 30.02 | 1.23 | 1.34 | 9.38 | 4.6 | 0 | 0 | 0 | 1.23 | 100 |
| GT 52 | 20.7 | 0 | 0 | 27.1 | 22.99 | 1.49 | 7.7 | 2.76 | 5.4 | 0 | 0 | 0 | 1.26 | 100 |
| GT 53 | 38.8 | 2.8 | 0 | 5.48 | 28.86 | 1.34 | 10.6 | 3.36 | 3.6 | 0 | 0 | 0 | 3.69 | 100 |
| GT 54 | 29.1 | 1.6 | 0 | 6.41 | 45.34 | 0 | 11.8 | 0 | 0.5 | 0 | 0 | 0.23 | 0.93 | 100 |
| GT 55 | 22.8 | 5.8 | 0 | 25.1 | 14.73 | 0.53 | 0.21 | 10.5 | 1.7 | 0 | 0 | 0 | 6.94 | 100 |
| GT 56 | 0 | 0 | 0 | 0 | 0 | 0 | 10.6 | 0 | 0.4 | 0.24 | 35.53 | 0 | 53.1 | 100 |
| GT 57 | 0 | 1.3 | 0 | 3.74 | 9.496 | 0 | 2.01 | 74.1 | 1.2 | 0 | 0 | 0 | 4.46 | 100 |
| GT 58 | 0 | 0 | 0 | 0 | 0 | 0 | 0 | 0 | 0.9 | 0 | 79.62 | 0 | 10.6 | 100 |
| GT 59 | 16.8 | 4.6 | 0 | 9.89 | 21.14 | 0 | 2.6 | 22.1 | 9.3 | 0 | 0 | 0 | 5.56 | 100 |
| GT 60 | 0.99 | 0.3 | 0 | 12.3 | 5.263 | 0 | 0.99 | 50.8 | 6 | 0 | 0 | 0.22 | 11.1 | 100 |
| GT 61 | 1.2 | 3.5 | 0 | 9.88 | 5.474 | 5.34 | 4.14 | 42.5 | 1.1 | 0 | 0 | 0 | 10.8 | 100 |
| GT 62 | 45.1 | 14 | 0 | 4.61 | 19.45 | 0 | 0.43 | 0 | 5.8 | 0 | 0 | 0.14 | 6.63 | 100 |
| GT 63 | 1.89 | 2 | 0 | 18.2 | 6.722 | 0 | 2.71 | 47.5 | 3.8 | 0 | 0 | 0 | 4.48 | 100 |
| GT 64 | 6.03 | 6.3 | 0 | 31.6 | 24.25 | 5.34 | 4.93 | 14.4 | 1.9 | 0 | 0 | 0 | 3.97 | 100 |
| GT 65 | 27.5 | 1 | 0 | 0 | 9.747 | 0 | 4.05 | 43.3 | 7.5 | 0 | 0 | 0 | 2.41 | 100 |
| GT 66 | 9.31 | 1 | 0 | 6.76 | 17.96 | 0.67 | 5.99 | 43.6 | 1 | 0 | 0 | 0 | 6.76 | 100 |
| GT 67 | 0 | 0 | 0 | 7.35 | 0 | 0 | 0.21 | 2.31 | 0.8 | 7.97 | 27.07 | 0 | 40.2 | 100 |
| GT 68 | 11.3 | 29 | 0 | 9.89 | 37.6 | 0 | 10.4 | 0 | 0 | 0 | 0 | 0 | 0.56 | 100 |

Table 3.3. Grain size measurement of some samples of the Gököl section.

| Sample No. | Ooids | | | | | | Intraclast | | | | | | Peloids | | | | | |
|------------|---------------|-------------|-----------|-------|----------------|---------|------------|-----------|-------|-----------|------|--------|---------|---------|------|---------|-------|-------|
| | spherical | ellipsoidal | length mm | | type of nuclei | mm | lamine | Min. (mm) | | Max. (mm) | | | | Min. mm | | Max. mm | | |
| | Diameter (mm) | Cortex (mm) | X | Y | | Nucleus | Numbers | X | Y | X | Y | Shape | Content | X | Y | X | Y | Shape |
| GT 2 | 0.09 | 0.02 | | | | 0.05 | | 0.21 | 0.31 | 0.17 | 0.23 | S A | M | | | 0.043 | 0.12 | RO |
| GT 4 | | | | | | | | | | 0.306 | 0.17 | S A | M | | | | | |
| GT 5 | 0.219 | 0.044 | | | M | 0.19 | 1 | 0.239 | 0.589 | 0.34 | 0.69 | S R | M | | | 0.115 | 0.289 | RO |
| | 0.029 | 0.224 | 0.319 | | M | 0.195 | 2 | 0.297 | 0.237 | 0.9 | 2.1 | S A | M | | | 0.08 | 0.332 | |
| | 0.047 | 0.176 | 0.325 | | M | 0.1 | 2 | 0.247 | 0.296 | 0.45 | 2.33 | S A | M | | | 0.097 | 0.504 | R |
| GT 6 | 0.14 | | | | M | 0.061 | | 0.218 | 0.265 | | | S A | M | | | 0.127 | 0.34 | R |
| | | | | | | | | | | | | | | | | 0.105 | 0.162 | RO |
| | | 0.031 | 0.129 | 3.1 | M | 0.28 | | 0.328 | 0.408 | | | S A | M | | | 0.089 | 0.138 | R |
| | | | | | | | | 0.214 | 0.315 | | | | | | | 0.135 | 0.724 | R |
| GT 7 | 0.218 | 0.03 | | | M | 0.15 | | 0.257 | 0.287 | 0.501 | 0.6 | S A | M | | | | | |
| | | | | | | | | 0.256 | 0.419 | 0.369 | 0.8 | S A | M | | | | | |
| | 0.26 | 0.048 | 0.167 | 0.215 | M | 0.071 | 2 | 0.286 | 0.388 | 0.561 | 2.99 | | | | | 0.134 | 0.407 | R |
| | | | | | M | 0.186 | | 0.081 | 0.137 | | | | | | | | | |
| GT 9 | | 0.002 | 0.071 | 0.583 | M | 0.003 | 1 | 0.662 | 0.648 | 0.394 | 2.77 | S A/SR | M | | | 0.149 | 0.108 | R |
| | | 0.075 | 0.281 | 0.415 | M | 0.151 | 2 | | | | | | | | | | | |
| | | 0.043 | 0.176 | 0.235 | M | 0.095 | 2 | 0.101 | 0.155 | 1.326 | 3.09 | S A/SR | M | | | 0.183 | 0.675 | R |
| GT 10 | 0.251 | 0.049 | | | M | 0.176 | | 0.061 | 0.157 | | | | | | | | | |
| | | 0.005 | 0.091 | 0.563 | M | 0.004 | 1 | 0.521 | 0.648 | 0.394 | 0.94 | S A/SR | M | | | 0.149 | 0.108 | RO |
| | | 0.076 | 0.297 | 0.422 | M | 0.157 | 1 | | | 0.35 | 0.49 | | | | | | | |
| | | 0.044 | 0.179 | 0.238 | M | 0.087 | 1 | 0.091 | 0.181 | 0.557 | 0.62 | SR | M | | | 0.183 | 0.675 | R |
| GT 12 | 0.196 | | | | | 0.074 | | 0.268 | 0.234 | 0.162 | 0.98 | S A/SR | | 0.045 | 0.17 | 0.08 | 0.435 | R |
| | | 0.038 | 0.182 | 0.311 | | 0.147 | 2 | 0.177 | 0.19 | 0.184 | 0.31 | S A/SR | | 0.092 | 0.27 | 0.144 | 0.867 | R |
| | | | | | | | | | | 0.208 | 0.53 | | | | | | | |
| GT 14 | 0.121 | 0.011 | | | M | 0.088 | 1 | 1.175 | 1.034 | 3.023 | 2.81 | | AM | 0.171 | 0.06 | 0.303 | 0.061 | R |
| | | | | | | | | 0.207 | 0.313 | 2.961 | 1.85 | | M | 0.078 | 0.31 | 0.087 | 0.024 | R |
| | | | | | | | | 0.13 | 0.258 | | | | M | | | 0.073 | 0.023 | R |
| GT 21 | | | | | | | | 0.032 | 0.087 | 0.601 | 0.05 | SR | M | | | | | |
| GT 22 | 0.16 | 0.042 | | | | 0.078 | | | | 0.406 | 0.23 | A | M | 0.067 | 0.14 | 0.142 | 0.362 | R |
| | 0.1 | 0.044 | | | | 0.034 | | 0.169 | 0.376 | 0.201 | 0.71 | A | M | | | | | |
| | 0.195 | 0.026 | 0.189 | 0.425 | | 0.367 | | | | 0.597 | 0.32 | | | | | | | |
| | | 0.068 | | | | 0.094 | | | | 0.355 | 0.22 | A | M | 0.096 | 0.09 | 0.45 | 0.131 | SRO |
| GT 23 | | 0.023 | 0.189 | 0.425 | | 0.347 | | | | 0.478 | 0.29 | SR | M | 0.069 | 0.19 | 0.38 | 0.391 | R |
| | | | | | | | | 0.15 | 0.262 | 0.57 | 0.63 | SR | | 0.103 | 0.22 | 0.29 | 0.268 | RO |
| | | | | | | | | 0.097 | 0.302 | | | A | | | | 0.06 | 0.04 | RO |
| | | | | | | | | 0.297 | 0.347 | 0.9 | 0.62 | SA | M | | | 0.084 | 0.35 | R |
| GT 25 | | | | | | | | 0.192 | 0.272 | 0.54 | 0.88 | SA | M | | | 0.069 | 0.511 | R |
| | | | | | | | | 0.341 | 0.265 | 0.22 | 0.57 | A | M | | | 0.15 | 0.32 | SRO |
| | | | | | | | | 0.482 | 0.211 | 0.67 | 0.34 | | | | | 0.069 | 0.03 | |
| | | | | | | | | 0.304 | 0.08 | 0.325 | 0.26 | A | M | 0.052 | 0.09 | 0.57 | 0.121 | SRO |
| GT 26 | 0.15 | 0.032 | | | M | 0.074 | 1 | 0.444 | 1.102 | 0.801 | 3.08 | SR | | 0.118 | 0.2 | 0.14 | 0.087 | R |
| | | | | | | | | | | 0.554 | 0.64 | SR | AM | | | 0.321 | 0.04 | RO |
| | | | | | | | | 0.662 | 0.621 | | | SR | P | | | | | |
| | | | | | | | | | | 0.211 | 0.22 | SR | M | | | | | |
| GT 30 | 0.055 | 0.014 | | | | 0.03 | 2 | 0.193 | 0.157 | 0.241 | 0.21 | SA | M | 0.047 | 0.07 | 0.084 | 0.195 | SR |
| | 0.041 | | 0.199 | 0.174 | | 0.071 | | | | 0.118 | 0.24 | SA | | 0.078 | 0.14 | 0.101 | 0.187 | SRO |
| | 0.071 | 0.012 | | | | 0.048 | 2 | | | 0.159 | 0.22 | | M | | | | | |
| GT 31 | 0.26 | 0.044 | | | M | 0.073 | 1 | 0.53 | 0.39 | 0.35 | 0.69 | A | M | 0.09 | 0.35 | 0.22 | 0.57 | SR |
| GT 32 | | | | | | | | 0.32 | 0.199 | 0.21 | 0.42 | A | M | | | 0.069 | 0.05 | |
| GT 39 | 0.128 | 0.025 | | | M | 0.071 | 1 | 1.751 | 2.796 | 1.561 | 3.71 | SA | M | 0.054 | 0.1 | | | rod |
| | 0.0182 | 0.046 | | | M | 0.09 | 1 | 1.160 | 0.155 | 0.347 | 0.93 | SA | M | 0.07 | 0.06 | | | rod |
| | 0.097 | 0.022 | | | M | 0.057 | 1 | 0.211 | 0.279 | | | SR | M | 0.049 | 0.04 | | | R |
| | | | | | | | | 0.2 | 0.421 | | | SR | M | | | | | |
| GT 41 | | | | | | | | 0.07 | 0.08 | | | A | M | 0.005 | 0.09 | 0.15 | 0.076 | SR |
| | | 0.035 | 0.139 | 0.189 | | 0.077 | 1 | | | 0.182 | 0.52 | | M | 0.059 | 0.09 | 0.058 | 0.09 | |
| GT 42 | 0.108 | 0.038 | | | | 0.052 | 10 | | | 0.11 | 0.21 | | M | 0.047 | 0.09 | 0.336 | 0.08 | |
| | | 0.041 | 0.192 | 0.266 | | 0.124 | R1 | | | 0.276 | 0.39 | A | M | | | 0.074 | 0.096 | RO |
| | 0.189 | 0.045 | | | | 0.084 | R1 | | | 0.174 | 0.09 | SA | M | | | 0.094 | 0.401 | R |
| | | 0.025 | 0.112 | 0.144 | M | 0.063 | R2 | | | | | | | | | | | |
| | 0.224 | 0.055 | | | M | 0.115 | 2 | | | | | | | | | | | |
| GT 50 | | | | | | | | 0.016 | 0.08 | 0.15 | 0.26 | SA | M | 0.02 | 0.06 | 0.04 | 0.09 | |
| GT 51 | | | | | | | | | | 0.27 | 0.32 | A | M | | | | | |
| GT 52 | | | | | | | | | | 0.218 | 0.47 | SA | M | 0.09 | 0.91 | 0.072 | 0.036 | R |
| GT 53 | | | | | | | | 0.072 | 0.09 | | | SA | | 0.059 | 0.02 | 0.077 | 0.08 | SRO |
| GT 54 | 0.19 | 0.032 | | | M | 0.118 | 2 | 0.122 | 0.018 | 0.239 | 0.67 | | | 0.072 | 0.04 | 0.098 | 0.049 | R |
| | 0.12 | 0.017 | | | M | 0.083 | R4 | | | 0.163 | 0.38 | S A/SR | | 0.054 | 0.07 | 0.141 | 0.061 | RO |
| | 0.124 | 0.011 | | | M | 0.097 | 2 | | | 2.302 | 0.57 | SA | | | | | | |
| | | | | | | | | | | 0.276 | 0.5 | SA | | | | | | |
| GT 62 | 0.114 | 0.015 | | | | 0.055 | R1 | | | 0.175 | 0.11 | SA | M | 0.057 | 0.06 | 0.053 | 0.131 | RO |
| | 0.118 | 0.023 | | | | 0.07 | R2 | | | | | | | 0.055 | 0.06 | 0.088 | 0.27 | SRO |
| | 0.104 | 0.034 | | | M | 0.045 | 2 | | | | | | | | | | | |
| GT 64 | | | | | | | | 0.214 | 0.187 | 0.09 | 0.24 | SR | | 0.084 | 0.36 | 0.33 | 0.128 | R |
| GT 68 | 0.44 | 0.131 | | | | 0.19 | R | | | 0.357 | 0.33 | A | M | 0.086 | 0.28 | 0.13 | 0.329 | R |
| | 0.18 | 0.056 | | | | 0.065 | R2 | 0.392 | 0.257 | 1.359 | 3.29 | SA | M | 0.134 | 0.06 | 0.079 | 0.253 | R |
| | | 0.019 | 0.246 | 0.353 | | 0.267 | S | 0.175 | 0.193 | 1.14 | 0.89 | A | M | | | 0.051 | 0.313 | R |
| | | 0.051 | 0.31 | 0.396 | | 0.309 | 4 | | | | | | | | | | | |
| | | 0.063 | 0.28 | 0.398 | M | 0.31 | 3 | | | | | | | | | | | |
| | | 0.027 | 0.181 | 0.351 | M | 0.123 | 2 | | | | | | | | | | | |

Symbols of table 3.6 micrite (M), rounded (R), sub-angular (SA), angular (A), subrounded (SR), rod (RO).

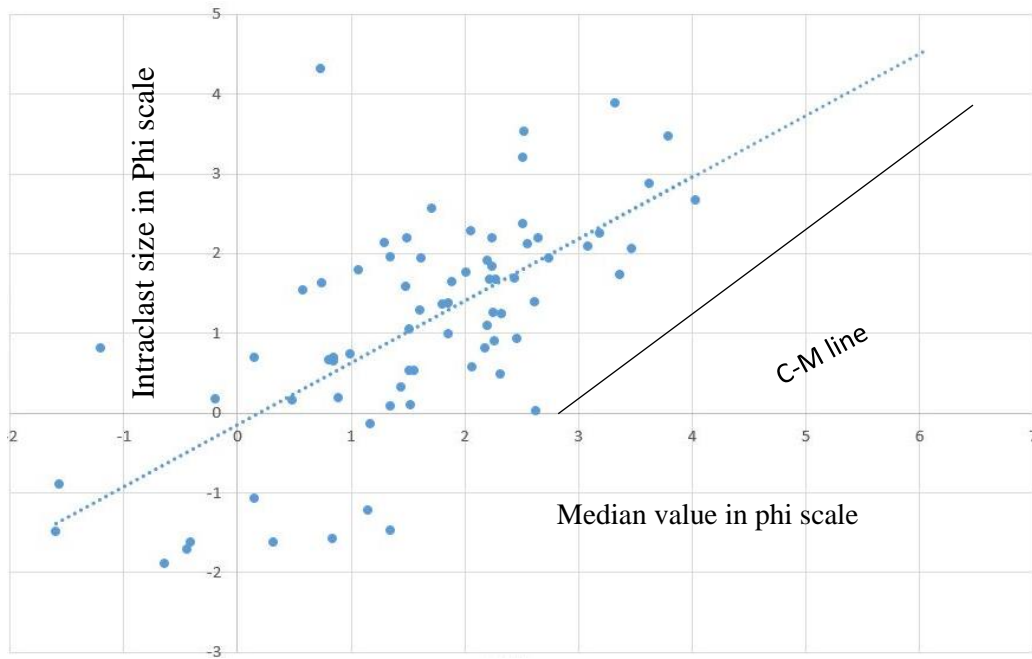


Figure 3.2: Passega diagram. The area included by the black straight line is the pattern based on median (Coarse grain: C, median: M 2.9 phi value).

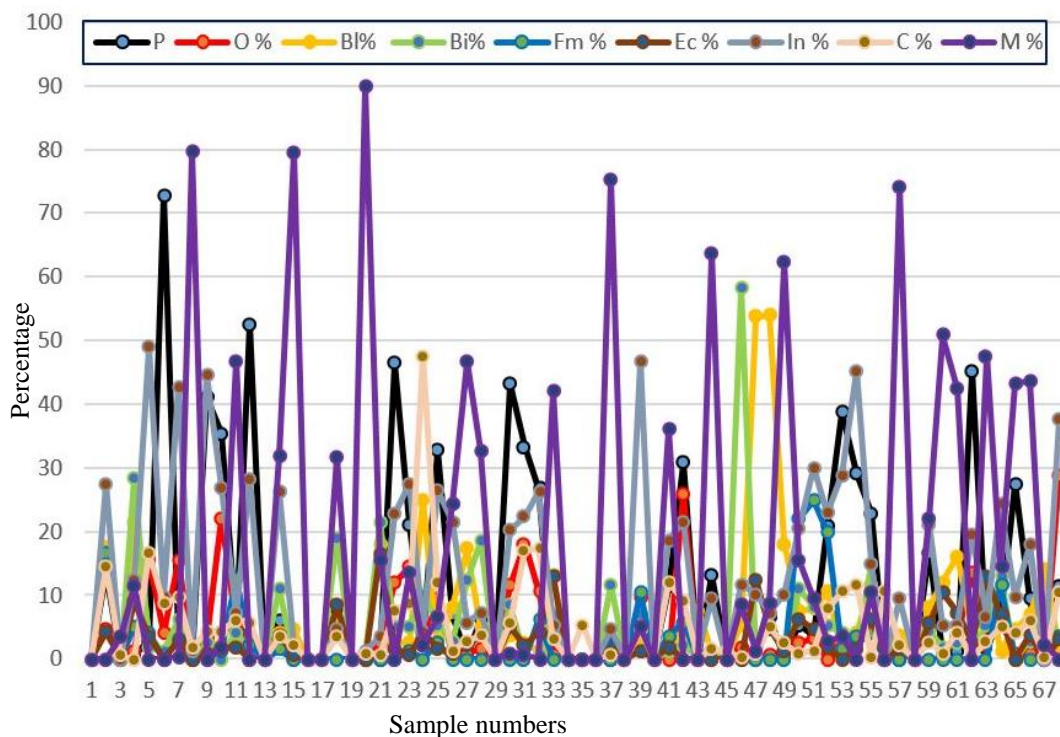


Figure 3.3: Graphic representation of percentage of different allochem, lime matrix and cement of the Gökğöl section (peloids (P), ooids (O), bioclast (BI), bivalve (Bi), forams (Fm), echinoderms (Ec), intraclast (In), cement (C) and (M) matrix).

3.3. MICROFACIES OF GÖKGÖL TUNNEL SECTION

In the Gökgöl tunnel section, total sixty eight samples were collected almost from every bed. Thin section of some samples were not prepared because of fissile nature and very thin size. Nine microfacies of the Yılanlı Formation (MYF) are recognized on the basis of outcrops and microscopic studies. These microfacies have been identified on the basis of compositional and textural classifications, and percentage composition of different minerals. Percentage composition have been determined by using visual estimation charts as well as by point counting percentages, both percentages are correlate with each other to get precise results of microfacies. The microfacies of the Yılanlı Formation (MYF) are described in (Table 3.4). These are as follows;

Table 3.4: Microfacies and sub-microfacies of the Yılanlı Formation.

| S.# | Microfacies | Sub-Microfacies Type | Sample Numbers | Environment of Deposition |
|-----|-------------|------------------------|--|--|
| 1. | Grainstone | Peloidal | GT12,GT22, GT30, GT42, GT62, | Intertidal – sub tidal shallow marine |
| 2. | Packstone | Bioclastic | GT2, GT4, GT21, GT50, GT51, GT52, GT55 , GT64 | Shallow marine subtidal to restricted lagoon |
| | | Intraclastic | GT5, GT7, GT19 | |
| | | Peloidal | GT10, GT25, GT31, GT32, GT53 | |
| | | Bivalve | GT46 | |
| 3. | Wackestone | Peloidal | GT44, GT65 | Restricted lagoon to open marine |
| | | Bioclastic | GT11, GT18, GT24, GT27, GT28,GT33, GT37, GT49, GT60, GT61, GT63, | |
| | | Intraclastic | GT57, GT59, GT66 | |
| 4. | Mudstone | Burrowed Lime mudstone | GT8, GT15, GT16, , GT29, | Shallow marine to restricted lagoon. |
| | | Brecciated | GT20 | |
| 5. | Bindstone | | GT23, GT41, GT47, GT48, | Intertidal to restricted lagoon. |
| 6. | Rudstone | | GT6, GT9, GT14, GT26, GT39, ,GT54, GT68 | Subtidal to lagoon. |
| 7. | Shale | Clayey | GT1, GT13, GT17, GT34, GT36, , GT67 | Shallow marine to restricted lagoon. |
| | | Silty | GT43 | |
| | | Black | GT40, GT56 | |
| 8. | Claystone | Claystone | GT3, GT38, GT58, | Shallow marine to restricted lagoon. |
| | | Silty | GT45 | |
| 9. | Dolomite | | GT35 | Shallow marine to lagoon. |

The adopted classification here to propose microfacies of carbonate rocks are based on Dunham (1962), Embry and Klovan (1971), James (1984) and Kendal (2005) (Figure 3.4). The modified classification of Folk by Strohmenger and Wirsing (1991) is used to classify microfacies after Folk (1959, 1962) classifications (Figures 3.5, 3.6 and 3.7). Dunham (1962) classified the carbonate rocks on basis of primary constituents and modified by Kendal (2005). Embry and Klovan (1971) and James (1984) classify rocks on the basis of texture primary based on allochthonous and autochthonous organisms. Flügel and Haditsch (1975), Langbein et al. (1982), Oates (1998) classified the limestone on the basis of mineralogical or chemical composition of rock. It can be expressed in percentage. The basic element or mineral is calcite and dolomite along with non-carbonate Oates (1998) (Figure 3.8). The Wilson (1975) model is used to classify microfacies and sub-microfacies of carbonate. Standard microfacies types are fundamental classifications that use identical criteria to define facies and their depositional environment. Mostly standard microfacies types (SMF) are classified on the basis of dominant characteristic including grain types, biota (bioclast) or depositional texture. Standard microfacies (SMF) can be used to understand the facies distribution along the depositional profile and interpret the possible depositional condition or environment for the facies. The interpretation of microfacies compare to SMF are put in the ramp type depositional model of Wilson (1975) (Figures 3.9 and 3.10).

Baccelle and Bosellini (1965) charts are used for visual estimation (Figure 3.11). The point counting data is used to generate carbonate microfacies model in the context of high-frequency dynamic relative sea-level changes. The combined classification of modified Dunham and Folk were used to categorize the microfacies and their sub-microfacies of carbonates.

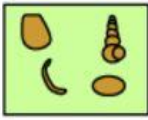
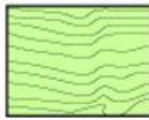
| | | | | |
|--|--|---|---|--|
| Original components not bound together at deposition | | | | Original components bound together at deposition. Intergrown skeletal material, lamination contrary to gravity, or cavities floored by sediment, roofed over by organic material but too large to be interstices |
| Contains mud (particles of clay and fine silt size) | | Lacks Mud | | |
| Mud-supported | | Grain-supported | | |
| Less than 10% Grains | More than 10% Grains | | | |
| Mudstone  | Wackestone  | Packstone  | Grainstone  | Boundstone  |
| C. G. St. C. Kendall, 2005 (after Dunham, 1962, AAPG Memoir 1) | | | | |

Figure 3.4: Classification of carbonate rocks proposed by Kendall (2005) after Dunham (1962).

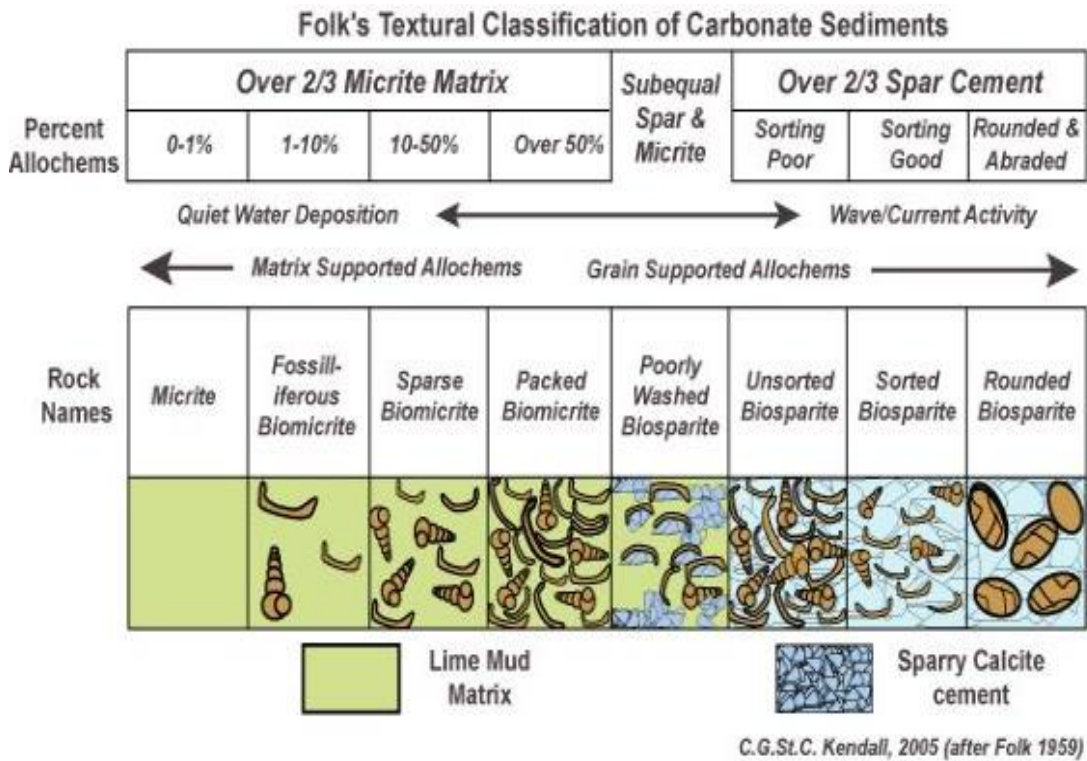


Figure 3.5: Textural classification of carbonate rocks by Folk's and improved by Kendall (2005) after Folk (1959).

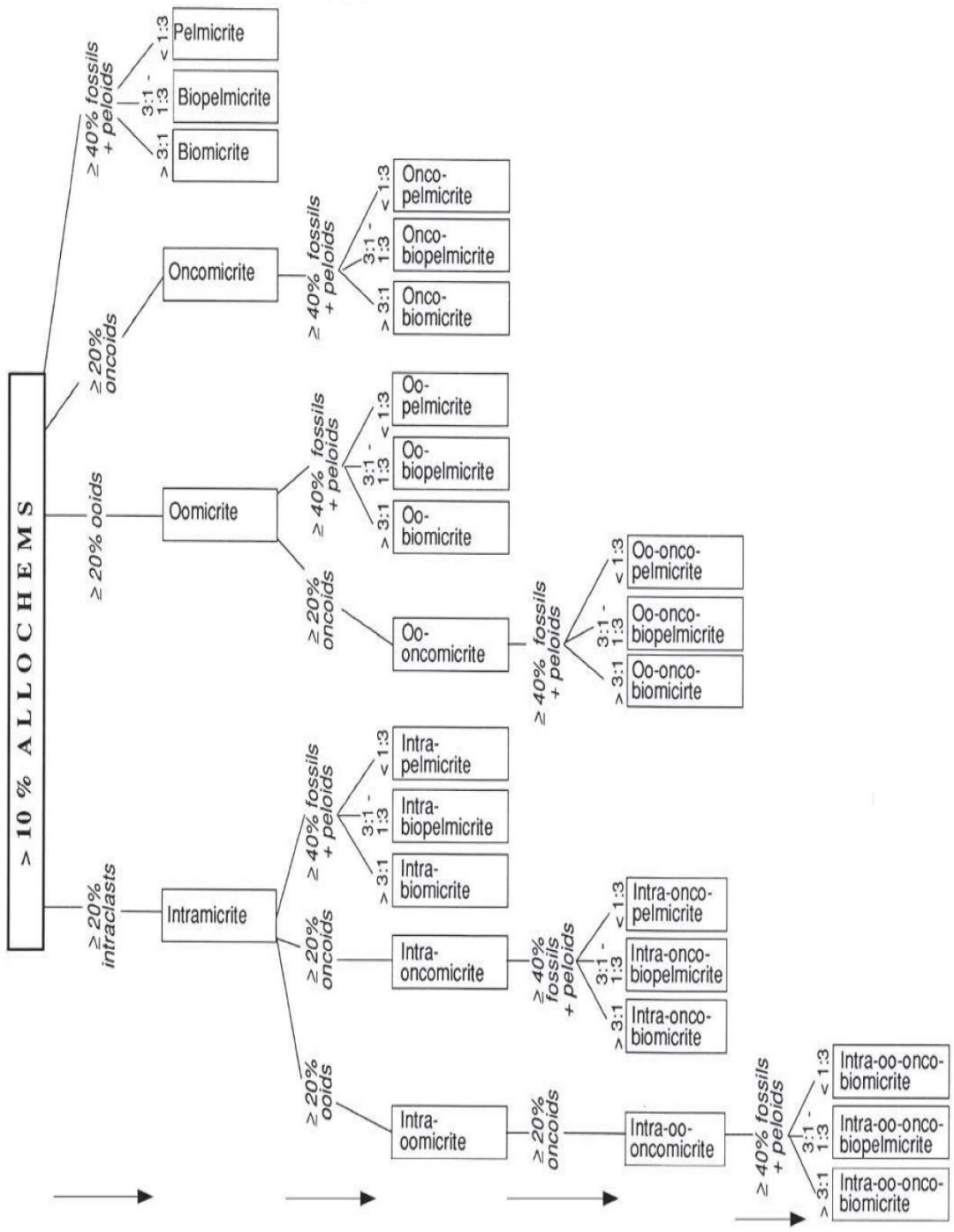


Figure 3.6: Classification of carbonate rocks based on crystal texture Strohmenger and Wirsing (1991) after Folk (1959).

| Allochthonous | | Autochthonous | | |
|---|-----------------------------|---|------------------------------------|---|
| Original components not bound organically at deposition | | Original components bound organically at deposition | | |
| >10% grains >2mm | | | | |
| Matrix supported | Supported by >2mm component | By organisms that act as baffles | By organisms that encrust and bind | By organisms that build a rigid framework |
| Floatstone | Rudstone | Bafflestone | Bindstone | Framestone |

Figure 3.7: Textural classification of carbonate rocks by Folk and improved by Kendall (2005) after Folk (1959).

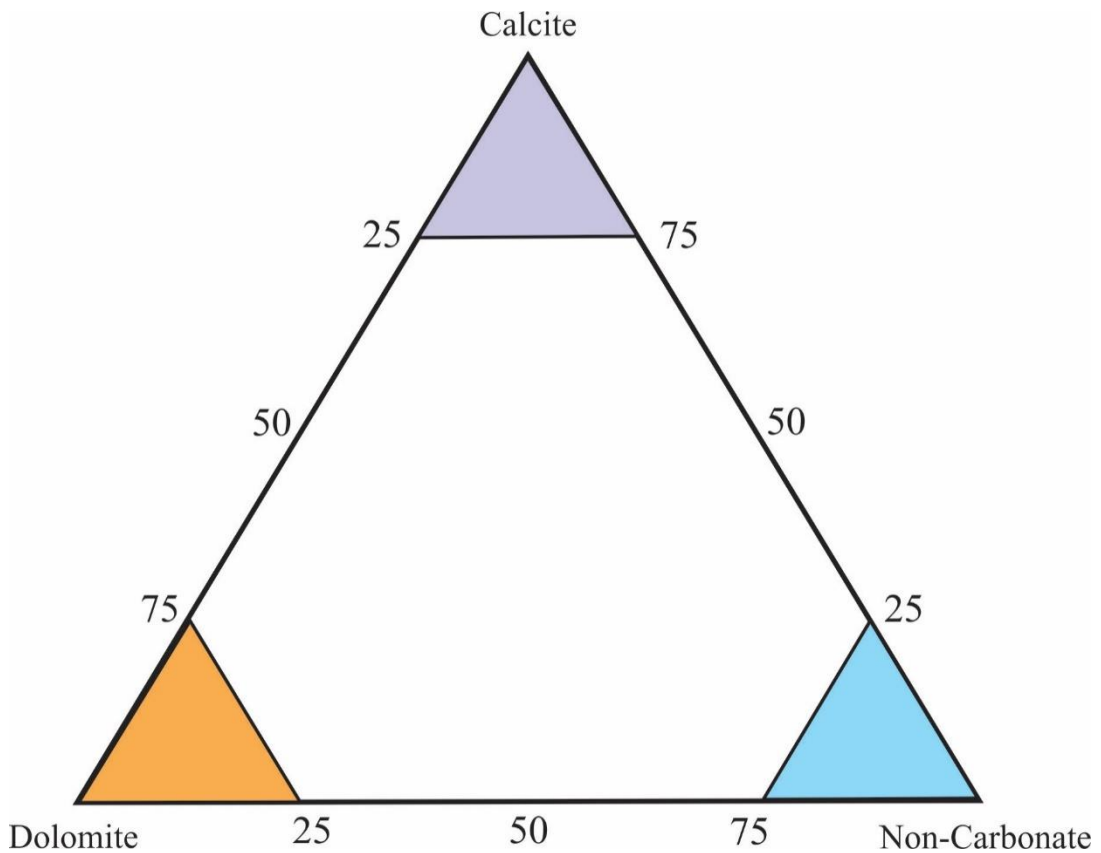


Figure 3.8: Limestone classification on the basis of composition (Flügel and Haditsch, 1975; Oates, 1998).

| | |
|-----------------------|--|
| SMF 1: | Spiculite wackestone/packstone |
| SMF 2: | Microbioclastic peloidal calcisiltite |
| SMF 3: | Pelagic mudstone/wackestone |
| SMF 4: | Microbreccia, bio-lithoclastic packstone |
| SMF 5: | Allochthonous bioclastic grainstone/ rudstone/packstone/floatstone, breccia |
| SMF 6: | Densely packed reef rudstone |
| SMF 7: | Organic boundstone, platform-margin 'reef' |
| SMF 8: | Whole fossil wackestone/floatstone |
| SMF 9: | Burrowed bioclastic wackestone |
| SMF 10: | Bioclastic packstone/wackestone with worn skeletal grains |
| SMF 11: | Coated bioclastic grainstone |
| SMF 12-S: | Limestone with shell concentrations |
| SMF 12-CRIN: | Limestones with crinoid concentrations |
| SMF 13: | Oncoid rudstone/grainstone |
| SMF 14: | Lag deposits (found in different facies zones) |
| SMF 15-C: | Ooid grainstone with concentric ooids |
| SMF 15-R: | Ooid grainstone with radial ooids |
| SMF 15-M: | Ooid grainstone with micritic ooids |
| SMF 16-NON-LAMINATED: | Peloidal grainstone/packstone |
| SMF 16-LAMINATED: | Peloidal bindstone |
| SMF 17: | Aggregate-grain grainstone |
| SMF 18: | Grainstone/packstone with abundant foraminifera or algae |
| SMF 19: | Densely laminated bindstone |
| SMF 20: | Laminated stromatolitic bindstone/mudstone |
| SMF 21: | Fenestral packstone/bindstone |
| SMF 22: | Oncoid floatstone/packstone |
| SMF 23: | Homogeneous, non-fossiliferous micrite |
| SMF 24: | Lithoclastic floatstone/rudstone/breccia |
| SMF 25: | Laminated evaporite-carbonate mudstone |
| SMF 26: | Pisoid cementstone/rudstone/packstone |

Figure 3.9: List of standard microfacies types of the Wilson Model going from the basal SMF type 1 to sub-aerial SMF 26 (Wilson, 1975).

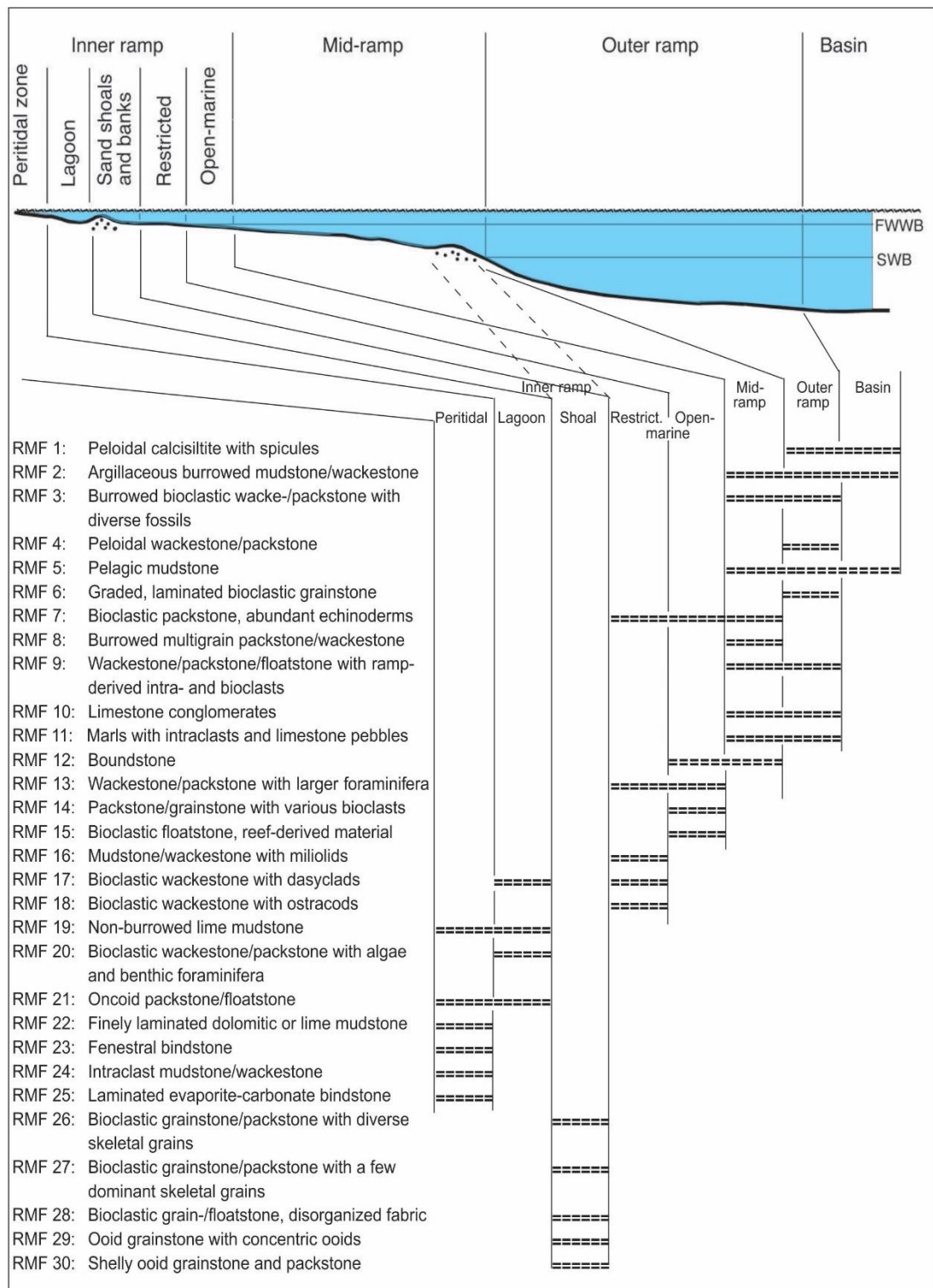


Figure 3.10: List of ramp microfacies types and depositional profile of the Wilson Model in different parts of a carbonate ramp (Wilson, 1975).

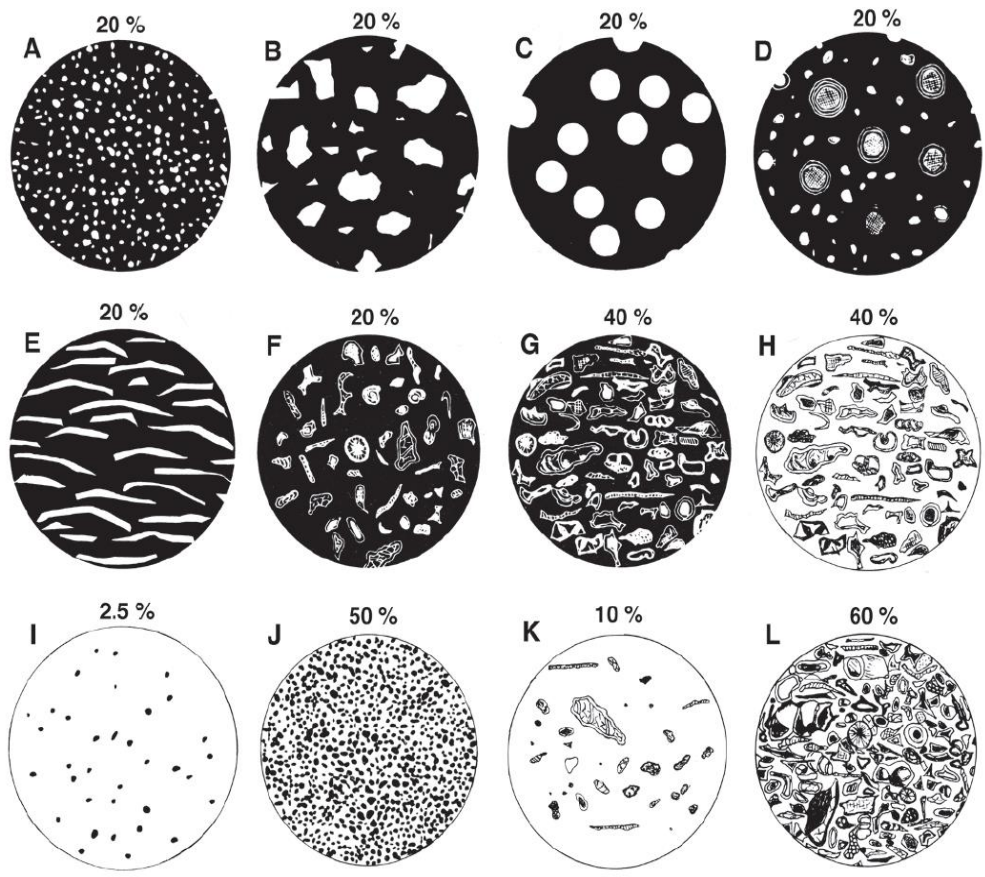


Figure 3.11: The comparison charts for visual percentage estimation for limestone's (Baccelle and Bosellini, 1965). The charts represents A - silt-sized and fine-sand sized particles, e.g. peloids, small intraclasts, or microfossils; B - coarse angular and subangular particles, e.g. intraclasts and angular skeletal grains; C - equal-sized ooids; D - differently sized ooids or peloids; E - oriented shells, e.g. bivalves; F - associations of various grains, here predominantly bioclasts, a few coated grains and peloids. G and H display the same percentage of skeletal grains with a black and with a white background. Low and high values: Most charts start with images at 10%; only the charts for the groups A and B show images below 10%. The largest percentage value shown is 50 or 60%. I and J: Few and abundant peloids contrasted; K and L: Few and abundant bioclasts (Baccelle and Bosellini, 1965).

3.3.1. MYF-I GRAINSTONE MICROFACIES

The sub-microfacies of grainstone of the Yılanlı Formation is identified on the basis of primary constituent and texture (Dunham, 1962; Folk, 1962; Strohmenger and Wirsing, 1991; Kendall, 2005), during petrographic studies one sub-microfacies is identified (Figures 3.4, 3.5 and 3.9).

- i) Peloidal Grainstone – Pel-intra-oosparite

3.3.1.1. S-MYF I PELOIDAL GRAINSTONE – PEL-INTRA-OOSPARITE

The samples GT12, GT22, GT30, GT42 and GT62 show peloidal grainstone sub-microfacies (Plate 1). Allochem include mainly peloids, bioclasts, ooids and intraclast. The grain size of peloid, ooid and intraclast are measured (Table 3.3).

The peloids present in this grainstone sub-microfacies represent 45 %. Peloids are rounded elongate, rod-shaped and the average size of rounded peloid ranges from 0.055 – 0.455 mm and rod like peloids have 0.206–0.785 mm in size, dark color, homogenous and spherical pellets are shown in Plate 1 that indicate fecal pellets type of peloids. Mud peloids, algal peloids and cortoid are rare (Plate 1, A-D).

Besides peloids, ooids (11.1 %) in the grainstone sub-microfacies are radial-fibrous, concentric, superficial, tangential and micritized microfabrics. The radial ooids and superficial ooids are common. These generally display moderate sorting and 0.041-0.224 mm diameter size, with overall size uniformity. The nucleus of ooids is composed of shell fragments, micritized particles. The cortex size ranges from 0.021–0.055 mm. Bioclasts (10.5 %) include ostracods, foraminifers, gastropods, bivalves, corals, calcisphere, algae, charophyta (gyrogonite) and bryozoan (Plate 1, A-F).

The intraclast are angular to sub-angular and their size ranges from (X: 0.177 – 0.406 mm and Y: 0.234 – 0.712 mm) and poorly sorted. Lithoclast and grains are reworked by storm/wave and modified by cyanobacteria. Calcite vein, stylolite, fractures, aggregate, intraclast, organic matter, oil remains and pyrite are present.

The allochems to cement ratio in the grainstone microfacies is 4:1 approximately according to visual estimation. Peloids represents 45 %, ooids 11.1 % cement 5.7 % and

intraclast 23 % and 11 % bioclast. This sub-microfacies is similar to SMF 15, SMF16, SMF17 and SMF 18 of Wilson's (1975) SMF model and equivalent to RMF 6, and RMF 14 of ramp model of Wilson's (Figure 3.10).

3.3.1.2. INTERPRETATION

The diagnostic features of microfacies are characterized by:

- i) Predominantly peloid and intraclast as allochem,
- ii) Bioclasts includes mainly ostracods, foraminifera, bivalves, gastropods, calcisphere and charophyta.

This microfacies is primarily represented by fecal pellets (Plate 1) of biotic origin in the form of rounded, elongated, ovoid dark color micritic grains, algal structures and minor bioturbation. Fecal pellets are produced in tropical- marine environment and preserved in sub-tidal to intertidal platform (Flügel, 2004).

Intraclast mainly consists of black pebbles and reworked clast indicated by poor sorting and angular to sub-rounded grains that represents shallow marine condition. Ooids of tangential, radial, micritized can be seen and represent high energy environment along with bioclasts abundantly ostracods, foraminifera, bivalves, gastropods. This microfacies is interpreted to have deposited in a high energy, wave dominated intertidal to sub-tidal marine environment.

The presence of foraminifera and ostracods represents open-marine conditions of normal salinity and gyrogonite green algae indicate shallow brackish and sunlight water.

So the microfacies represent wave dominated, shallow water of normal salinity marine conditions, intertidal to sub-tidal, shoals and restricted on the inner ramp type carbonate platform.

3.3.2. MYF-II PACKSTONE MICROFACIES

On the basis of constituent and texture Dunham (1962), Folk (1962), Kendall (2005), Strohmenger and Wirsing (1991), four sub-microfacies of packstone of the Yılanlı Formation are identified during petrographic studies. Allochem measurement are represented by Table 3.3.

- i) Bioclastic Packstone – Bio-pelmicrite
- ii) Intraclastic Packstone – Intra-oo-biomicrorite
- iii) Peloidal Packstone – Pel-intra-biomicrorite
- iv) Bivalve Packstone – Biomicrorite

3.3.2.1. S-MYF I BIOCLASTIC PACKSTONE – BIO-PELMICRITE

The samples GT2, GT4, GT21, GT50, GT51, GT52, GT55 and GT64 represents bioclastic packstone sub-microfacies. The bioclasts (44.8 %) dominantly comprise ostracods, foraminifers and gastropods. The other bioclasts are bivalves, green algae, charophyta, echinoids, calcisphere and fossil fragments (Plate 2).

Along with bioclasts in this packstone sub-microfacies, peloids, intraclast and ooids. Algal type and fecal pellet are documented. Organic matter, micro fractures, calcite vein, sparite, stylolite with oil remnants and pyrite are present. Bioturbation and stromatolite are present. Micritic layer have lamination.

This sub-microfacies corresponds to SMF 2, SMF 4 and SMF 10 of Wilson's (1975) SMF Model and equivalent to RMF 7.

3.3.2.2. S-MYF II INTRACLASTIC PACKSTONE – INTRA-OO-BIOMICRITE

The samples GT5, GT7 and GT19 represents intraclastic packstone sub-microfacies. Intraclast (47 %) and bioclast (13 %) are mainly composed of bivalve, ostracods, corals, algae, micritized peloids (3.1 %), and ooids (15.1 %). Fossil fragments, organic matter, stylolite and pyrite. Minor fracturing is also present (Plate 3, A). This sub-microfacies is similar to SMF 4 of Wilson's (1975) SMF Model.

3.3.2.3. S-MYF III PELOIDAL PACKSTONE – PEL-INTRA-BIOMICRITE

The samples GT10, GT25, GT31, GT32 and GT53 displays peloidal packstone sub-microfacies. This sub-microfacies dominantly consists of peloids (34 %). The peloids are oblate, elongate to rarely rounded range in size from 0.048 mm to 0.112 mm and peloids are of fecal pellet origin (Plate 3, B-D).

The ooids are associated with peloids but their frequency is less. Ooids (12.7 %) are commonly tangential, radial and micritized. Superficial ooids are rare.

The bioclasts (7 %) consist of ostracods, gastropods, foraminifera, bivalve and other fossil fragments. Intraclast (26 %), calcisphere, calcite vein, organic matter, stylolite with oil remains, iron oxide may be hematite and pyrite are also present.

This sub-microfacies corresponds to SMF 16 of Wilson's (1975) SMF Model and approximately equal to RMF 4.

3.3.2.4. S-MYF IV BIVALVE PACKSTONE - BIOMICRITE

The sample GT46 illustrate bivalve packstone sub-microfacies. Allochem mainly comprises bivalve (58 %), bioclasts and peloids.

The allochems include ostracods, bivalves and fossil fragments (Plate 3, F). This sub-microfacies is similar to SMF 10 (RMF 7) of Wilson's (1975) SMF Model.

3.3.2.5. INTERPRETATION

Salient features of packstone microfacies are characterized by:

- i) Presence of micrite as matrix,
- ii) Predominantly bioclasts of ostracods, foraminifera, gastropods, bivalve, calcisphere and green algae,
- iii) Peloids of fecal origin, algal peloids and micritized grain,
- iv) Presence of intraclast reworked wave/storm and modified by cyanobacteria.

The packstone microfacies is mainly characterized by a diversity of bioclasts along with peloids, intraclast and micritized grain. Bioclasts comprises abundantly foraminifers, bivalves, ostracods and relatively low frequency gastropods, calcisphere, green algae, echinoid, tangential ooids, radial ooids and lime mud as matrix indicates low energy condition of deposition may be shallow to open shelf platform.

Textural relationship indicates restricted platform to open-marine platform below fair weather wave base on the basis of radial peloids, ooids and bioclasts embedded in micrite as matrix.

Intraclasts represent reworking and redeposition achieved through occasional intense activity at sediment-water interface and their presence indicates storm/wave event. Partial dolomitization and calcite vein shows recrystallization.

This microfacies shows shallow marine, shoals to open marine environment of inner ramp carbonate setting.

3.3.3. MYF-III WACKESTONE MICROFACIES

During petrographic study three sub-microfacies of Wackestone of the Yılanlı Formation are identified on the basis of texture and constituents Dunham (1962), Folk (1962), Kendall (2005), Strohmenger and Wirsing (1991).

- i) Peloidal Wackestone – Pel-intramicrorite
- ii) Bioclastic Wackestone – Bio-intramicrorite
- iii) Intraclastic Wackestone – Intra-pelmicrorite

3.3.3.1. S-MYF I PELOIDAL WACKESTONE – PEL-INTRAMICRITE

The samples GT44 and GT65 show peloidal wackestone sub-microfacies. Allochem consists of primarily peloids (20.4 %) along with intraclast (9.5 %) and bioclasts (3.2 %). Micritic type of matrix consists of 53.4 %.

The peloids are elongated to rounded, poorly sorted and mud peloid origin (Plate 4, A-B). This sub-microfacies consist of some bioclasts like ostracods, bivalves, gastropods, calcisphere, fossil fragments. Calcite vein, fractures, organic matter, burrowing, stylolite may be with oil remnants and pyrite are also present.

The peloidal wackestone sub-microfacies is similar to SMF 2 and SMF 9 of Wilson's (1975) SMF Model and corresponds to RMF 4.

3.3.3.2. S-MYF II BIOCLASTIC WACKESTONE – BIO-INTRAMICRITE

The samples GT11, GT18, GT24, GT27, GT28, GT33, GT37, GT49, GT60, GT61 and GT63 represent bioclastic wackestone sub-microfacies. Allochem include mainly bioclasts (27 %) (ostracods) along with intraclast (6 %) and consists of approximately 43 % of matrix and cement (7 %).

This microfacies is mainly consists of ostracods, bivalves (pelecypods), gastropods and calcisphere. The other bioclasts occur in relatively low frequency like foraminifera, algae (charophyta) and fossil fragments (Plate 4, C-F).

Intraclast (limeclast, siliciclast), calcite vein, fractures, bioturbation, organic matter, stylolite, fractures, pyrite, rhombohedral crystal of dolomite and heavy oil remnants are present (Plate 5, A, D and E).

The bioclastic wackestone sub-microfacies corresponds to SMF 8 and SMF 9 of Wilson's (1975) SMF Model and similar to RMF 3 and RMF 20 (Figure 3.9 and 3.10).

3.3.3.3. S-MYF III INTRACLASTIC WACKESTONE – INTRA-PELMICRITE

The samples GT57, GT59 and GT66 show intraclastic wackestone sub-microfacies. Allochems include mainly intraclast (16 %) along with bioclasts (12 %) (Bivalve, ostracods, foraminifera) and consists of approximately 46.5 % of matrix.

Intraclast are composed of black limestone pebbles, dark grey color angular to sub-rounded limestone pebble 0.02 – 0.8 mm in size. Plate 4 illustrated intraclasts and bioclast.

The intraclastic wackestone sub-microfacies corresponds to SMF 9 and SMF 10 of Wilson's (1975) SMF Model and similar to RMF 24 (Figure 3.9 and 3.10).

3.3.3.4. INTERPRETATION

This microfacies is characterized by following diagnostic features:

- i) Presence of micrite as matrix,
- ii) Bioclasts mainly consist of ostracods, gastropods, bivalve and calcisphere,
- iii) Presence of bioturbation and burrowing.

This microfacies is dominantly characterized by a diversity of bioclasts along with peloids and micritized grain. Bioclasts consists of abundant ostracods, gastropods, pelecypods, calcisphere and relatively low frequency foraminifers, bivalves, fossil fragments. The greater number of bivalve indicate shallow lagoon environment of deposition.

Burrowing process diminute the skeletal grain that indicate deep open shelf environment (Taylor and Goldring, 1993). Small size bioclasts (shell debris) having strong burrowing matrix represents open sea. Partial dolomitization, crystal of dolomite and sparite vein may because of recrystallization or burial diagenesis. The presence of gastropods composition indicate open marine to restricted conditions.

The microfacies may be represents as restricted shallow lagoonal to open marine condition of inner to middle ramp carbonate platform environment.

3.3.4. MYF-IV MUDSTONE MICROFACIES

Two sub-micro facies of mudstone of the Yılanlı Formation are identified on the basis of texture and constituents Dunham (1962), Folk (1962), Kendall (2005), Strohmenger and Wirsing (1991) during petrographic studies.

- i) Burrowed lime mudstone
- ii) Brecciated mudstone

3.3.4.1. S-MYF I BURROWED LIME MUDSTONE

The samples GT8, GT15, GT16 and GT29 represent burrowed lime mudstone sub-microfacies. This sub-microfacies consists of approximately 80 % of lime mud as matrix and 2 % cement.

This sub-microfacies comprises dominantly burrows along with some bioclasts (2.6 %). Bioclasts mainly comprises foraminifera, ostracods and bivalves. Very low frequency of gastropods, fossil fragment and peloids.

Calcite vein, fractures, bioturbation, stylolite, organic matter, pyrite, crystal of dolomite are present (Plate 5).

This sub-microfacies is similar to SMF 3, SMF 20 and RMF 16, RMF 19 of Wilson`s (1975) SMF and RMF models (Figure 3.9, 3.10).

3.3.4.2. S-MYF BRECCIATED MUDSTONE

The sample 20 shows brecciated mudstone sub-microfacies. Allochem include dominantly brecciated clast along with some bioclasts and ghost fossil fragment. Breccia is poorly sorted, angular-subangular and subrounded clast of lime origin (Plate 5, B and C).

Calcite vein, fractures, stylolite, pyrite, rhombohedral crystal of dolomite are present. This sub-microfacies is similar to SMF 4 of Wilson`s (1975) SMF model.

3.3.4.3. INTERPRETATION

The important features of mudstone microfacies are characterized by:

- i) Presence of burrows in lime mudstone matrix,
- ii) Bioclasts include mainly foraminifers, bivalves and ostracods,
- iii) Presence of lime brecciated clast.

Dark color lamination and intercalation of bioclastic layer full of bivalve with organic matter represent restricted shallow marine environment. The presence of foraminifera in lime mud matrix and having lamination shows open platform to restricted lagoon environment.

Fine grained microbreccia consisting bioclasts and shells derived from shallow water and previously cemented lithoclast.

The general depositional environment for this microfacies is peritidal, restricted lagoonal to open marine of inner ramp type carbonate platform.

3.3.5. MYF-V BINDSTONE MICROFACIES

During petrographic study microfacies are identified on the basis of texture and constituents Dunham (1962), Folk (1962), Kendall (2005), Strohmenger and Wirsing (1991).

The samples GT23, GT41, GT47 and GT48 illustrates bindstone microfacies. Allochem include mainly peloids (9.7 %), stromatolite, and bioclasts (35 %) along with, ooids (4 %), intraclast (16 %), cement (6.6 %) and matrix (15 %).

The peloids are rounded, oblate, elongate, rod-shaped of fecal pellets origin of peloids. Mud peloids and algal type of peloids were documented. The bioclasts comprises ostracoda, foraminifera, bivalve, gastropods, algae and calcisphere (Plate 6).

Intraclast, oncoid, calcite vein, fractures, silt size organic matter, stylolite, fractures and heavy oil remnants are present. Dolomite crystal vary from subhedral to euhedral, equigranular selective to pervasive dolomite replacing limestone matrix. The dolomite crystals exhibit straight boundaries.

Stromatolites are skeletal type of laterally linked hemispheroids origin (Logan et al., 1964). The size of laminae of stromatolites ranges from 0.5-0.49 mm. and laminae consists of micrite, organic matter, peloids, cements and fossil fragments. Agglutinated type of fabric is present.

This microfacies corresponds to SMF 19, SMF 20 and SMF 21 of Wilson`s (1975) SMF Model.

3.3.5.1. INTERPRETATION

The diagnostic features of microfacies are characterized by:

- i) Skeletal type stromatolite, microbialites
- ii) Bioclasts includes ostracods, bivalves, foraminifers, gastropods and algae,
- iii) Presence of fecal pellets,
- iv) Presence of dolomite.

Planar lamination of fine and coarse grain consisting of some bioclasts and algae shows tidal to intertidal environment.

The overall depositional environment for this microfacies is intertidal, tidal flats, restricted lagoon to open marine of inner ramp carbonate platform.

3.3.6. MYF-VI RUDSTONE MICROFACIES

The microfacies is identified on the basis of texture and constituents Dunham (1962), Folk (1962), Kendall (2005), Strohmenger and Wirsing (1991). The grain size were measured (Table 3.3).

The samples GT6, GT9, GT14, GT26, GT39, GT54 and GT68 represents rudstone microfacies. Allochem include dominantly intraclast (31 %) along with bioclasts (11.5 %), ooids (7 %) and peloids (27.8 %).

This microfacies is supported by coarse gravel (intraclast) of biogenic origin and lithic clast origin. Poorly sorted, size ranges from 1.561 mm – 3.71 mm. The intraclast are angular, sub-angular to sub-rounded and their size ranges from (X: 0.207 – 3.023 mm and Y: 0.128 – 3.711 mm) and poorly sorted (Plate 7).

Bioclasts includes foraminifera, ostracoda, bivalves, echinoderms, gastropods, green algae and calcisphere. Peloids are elongate, rounded and poorly sorted. The average size of rounded peloid ranges from 0.085 – 0.115 mm and rod like peloids have size from 0.903–0.685 mm.

Ooids in the microfacies are radial, concentric, superficial, and tangential. The ooids shows moderate sorting and 0.097-0.44 mm diameter size, with overall size uniformity. The nucleus of ooids is composed of shell fragments, micritized particles. The cortex size ranges from 0.019–0.075 mm.

Micro-crystalline calcite vein, aggregate grain, burrowing, nodular fabric, matrix consist of organic matter, stylolite and pyrite were documented (Plate 8).

This sub-microfacies is similar to SMF 5, SMF 6 and SMF 24 of Wilson`s (1975) SMF Model.

3.3.6.1. INTERPRETATION

This microfacies is characterized by the following diagnostic features:

- i) Presence lithic and bioclastic gravels,
- ii) Nodular fabric,
- iii) Tangential, superficial and radial ooids.

The presence of carbonate clast and elongated micritic clast indicates platform interior to tidal flat depositional settings. Ooids represent shallow water environment.

So the depositional environment is subtidal to shallow lagoon of inner ramp carbonate platform.

Mud rock is the general term used in are the sedimentary rocks. Fine grains facies are classified on the basis of Folk texture classification (1965) (Table 3.5) and Pettijohn (1975). Fine grains rocks are also (Figure 3.8) classified on the basis of relative proportion of grains (Picard's 1971).

Table 3.5. Folk (1965) classification for fine-grain sedimentary rock on the basis of texture.

| Mud-rock division based upon Texture and Structure | | | |
|--|------|------------------------|--------------------|
| Grain size of mud fraction | Soft | Indurated, Non-fissile | Indurated, Fissile |
| >66 % Silt | Silt | Siltstone | Silt-Shale |
| 33-66 % (Sub-equal silt and clay) | Mud | Mudstone | Mud-Shale |
| >66 % Clay | Clay | Claystone | Clay-Shale |

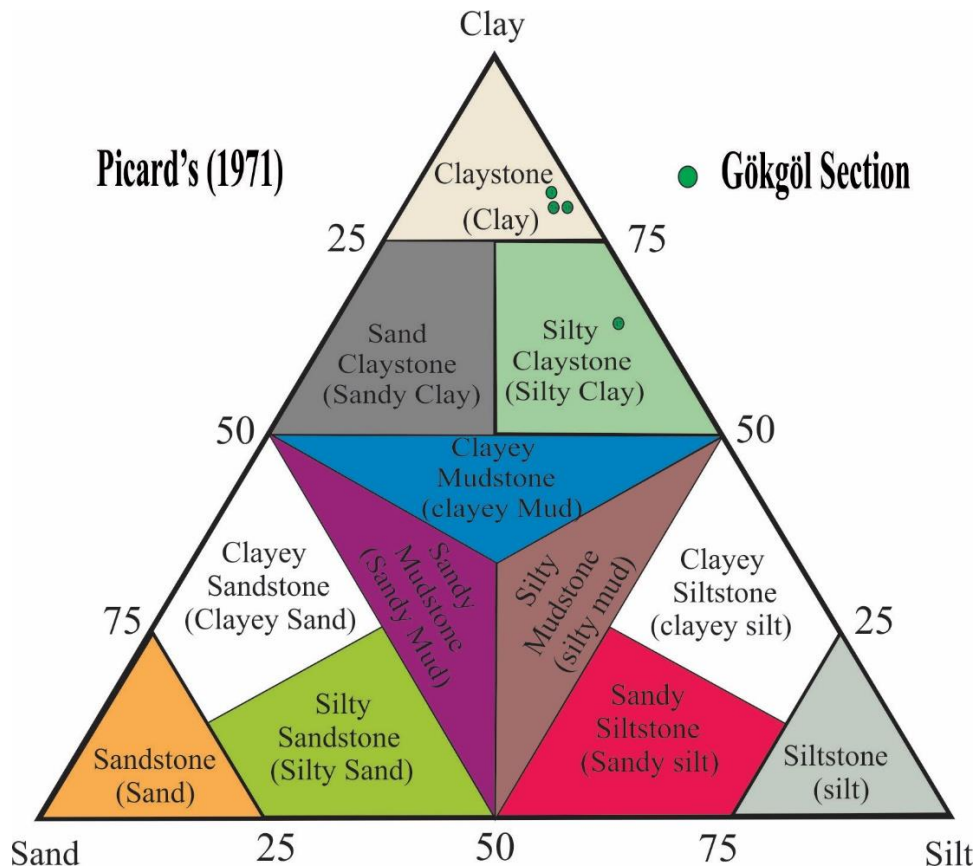


Figure 3.12: Classification of claystone on relative proportions of grains size, showing claystone sample by green sphere (modified from Picard's 1971).

3.3.7. MYF-VII SHALE MICROFACIES

The study of shale under ordinary optical microscope is difficult because of their very fine grain size. In present study, shale is classified on the basis of grains size, amount of clay and silt, induration, fissility, lamination, color and presence of organic matter (Picards, 1971). Three sub-micro facies of shale are recognized on the basis of visual estimation (Baccelle and Bosellini, 1965) during the petrographic studies.

- i) Clayey shale
- ii) Silty shale
- iii) Black shale

3.3.7.1. S-MYF I CLAYEY SHALE

The samples GT1, GT13, GT17, GT34, GT36 and GT67 illustrate clayey shale sub-microfacies. Bioclast (21.3 %) includes bivalve's fragments and ghost fossils. Calcareous cement and hackly fracture is present. Silt size clast rich with organic matter with calcareous matrix (2.3 %). A mesh structure of bivalve was documented (Plate 9).

3.3.7.2. S-MYF II SILTY SHALE

The sample GT43 represents silty shale sub-microfacies. Allochem consists of bioclast (7 %) includes ostracods, bivalves. Parallel lamination is documented. Iron matrix with organic matter and calcite vein. Oil impregnation is seen on fossil (Plate 10).

3.3.7.3. S-MYF III BLACK SHALE

The samples GT40 and GT56 represent black shale sub-microfacies. Organic rich shale with bivalve, fossil fragment, ostracods, corals, iron matrix, replacement of oil. Intraclast include organic matter and quartz. This facies is highly fractured and deformed.

3.3.7.4. INTERPRETATION

This microfacies is characterized by the following diagnostic features:

- i) Mesh structure of bivalves,
- ii) Parallel lamination,
- iii) Rich with organic matter,
- iv) Black shale.

This microfacies is deposited at low energy, calm condition of shallow marine to restricted lagoonal environment.

3.3.8. MYF- VIII CLAYSTONE MICROFACIES

On the basis of grain proportion (Picards, 1971), two sub-microfacies of claystone of the Yılanlı Formation are identified during petrographic studies. Claystone have clay size grain 82 % while silty claystone have approximately 50 % silt size grain and rest clay size (Figure 3.11). Claystone show yellow and black color but the composition and texture is same.

- i) Claystone
- ii) Silty claystone

3.3.8.1. S-MYF I CLAYSTONE

The samples GT3, GT38 and GT58 represent claystone sub-microfacies and characterized by fissile. This facies consists of very fine size grains comprising rare fossils and trace amount of muscovite, feldspar, iron oxide embedded in the clayey matrix. Micro fractures and burrows are occupied by silica. Hematite, organic matter, lamination and pyrite are present (Plate 11).

3.3.8.2. S-MYF II SILTY CLAYSTONE

The sample GT45 represent silty claystone sub-microfacies. The microfacies is full of silt size organic matter. Bioclast include bivalves, ghost fossil fragments, calcite vein, sparite and burrow filled with silica (Plate 12).

3.3.8.3. INTERPRETATION

The diagnostic features of this microfacies are:

- i) Relict of feldspar
- ii) Traces of muscovite

This microfacies may be deposited at shallow marine to lagoon.

3.3.9. MYF-IX DOLOMITE MICROFACIES

A term dolomite is applied to both minerals $Mg(CO_3)_2$ and $CaMg(CO_3)_2$. The sedimentary rock comprises more than 50 % of dolomite $CaMg(CO_3)_2$ mineral sometimes known as Dolostone (Selley, 2001; Flügel, 2004).

3.3.9.1. CLASSIFICATION OF DOLOMITE

Genetically dolostone is classified into three types (Flügel, 2004):

a. SYNGENETIC DOLOSTONE

A rock simultaneously formed within the depositional environment.

b. DIAGENETIC DOLOSTONE

A rock formed by replacement of carbonate sediments or limestone during following consolidation.

c. EPIGENETIC DOLOSTONE

A rock formed by localized replacement along post-depositional faults and fractures.

There is different type of crystal forms, fabrics and mosaics for dolomite. Mostly dolomite are formed by replacement of pre-existing limestone $CaCO_3$. This replacement of limestone by dolomite have wide range from fabric destructive to retentive and from selective fabric to pervasive. In the replacement process, the shapes of dolomite vary from anhedral to euhedral rhombs, with the term xenotopic, idiotopic and hypidiotopic mosaics (Sibley and Gregg, 1987) (Figure 3.13).

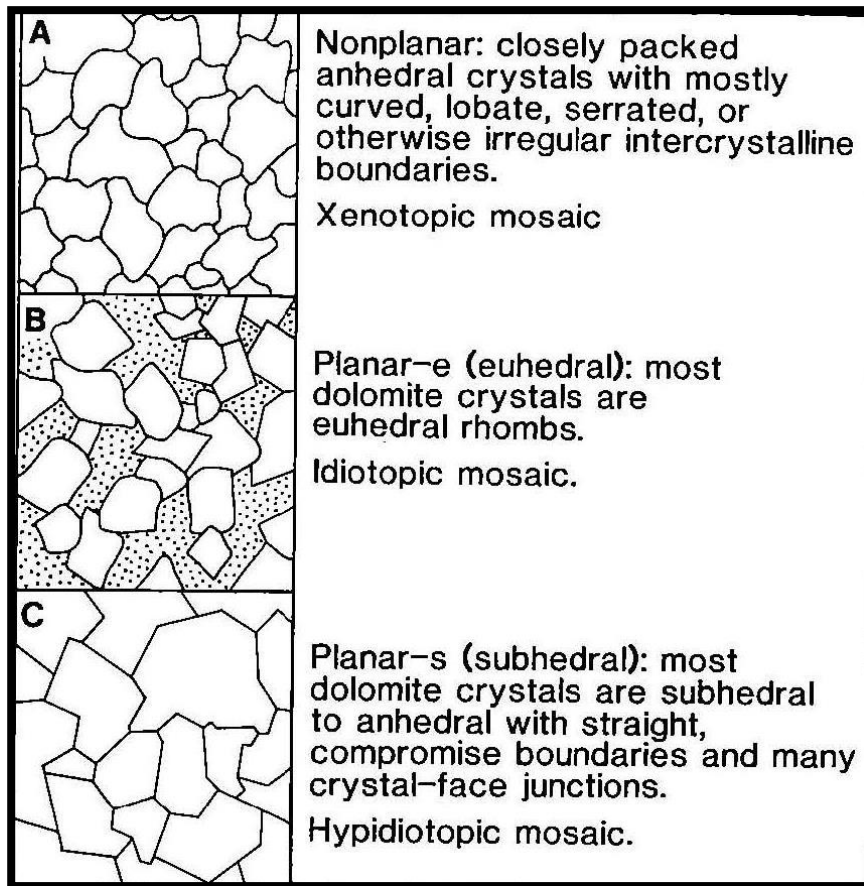


Figure 3.13: Classification of dolomite fabrics by Sibley and Gregg (1987).

The sample GT 35 represent dolomite microfacies. This facies shows a diagenetic dolomite/dolostone type probably formed through replacement or recrystallization of unfossiliferous or scarcely fossiliferous lime mudstone. Bioclasts includes ostracods and ghost fossil (Plate 13).

The lime dolomitized mudstone microfacies consists of finely crystalline, subhedral to euohedral, pervasive to selective dolomite replaced depositional lime fabric. Unimodal planar partial matrix replacement by dolomite (Gregg and Sibley, 1987). The pyrite crystal are also present.

Pervasive to microdolomitization is recognized in the Yılanlı Formation. Xenotopic to hypidiotopic texture is observed. This microfacies is similar to SMF 20 and SMF 23 of Wilson`s (1975) SMF Model.

3.3.9.2. INTERPRETATION

The microfacies is characterized dominantly by subhedral to euhedral dolomite grains. Repeated dolomitization in the formation indicate selective type. Secondary type of dolomite formed by diagenetically alteration of lime mudstone or wackestone. This facies may be deposited at saline condition of tidal flats.

3.4. SEDIMENTARY STRUCTURE IN STRATIGRAPHIC SECTION

Sedimentary structures through the stratigraphic section that have been observed in field and microscopic level are as below.

3.4.1. BEDDING AND LAMINATION

The bedding of the Gökgöl section represents variation from very thin, thick to massive bedded limestone with thin to medium bedded shale and clay alternations. Dolomite in the studied section represent thick bed and located in nearly middle of the studies section. Intercalation of shale, chert and marl are documented at different horizon. Parallel lamination is documented at different interval (Figures 3.14, 3.15, 3.16).

3.4.2. BIOTURBATION

Bioturbation is determined mostly at microscopic level. The filling materials is dark color of clay to silt size grains in burrows (Plate 4, Figure 3.17).

3.4.3. DIAGNOSTIC FOSSILS

Some of the fossils that are identified are shown in Figure 3.18, 3.19 and 3.20.



Figure 3.14: Photograph illustrates lamination in the upper section of studied section.

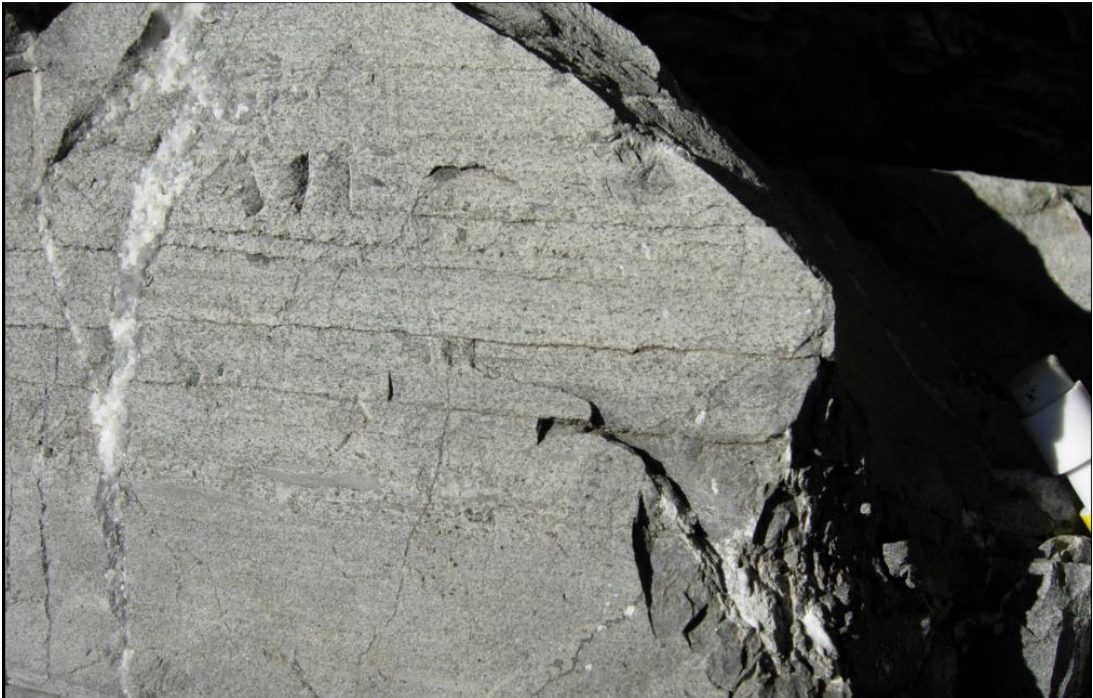


Figure 3.15: Photograph illustrates parallel lamination and calcite vein in the middle of the section.



Figure 3.16: Photograph showing dark color lamination in the upper part of the section.

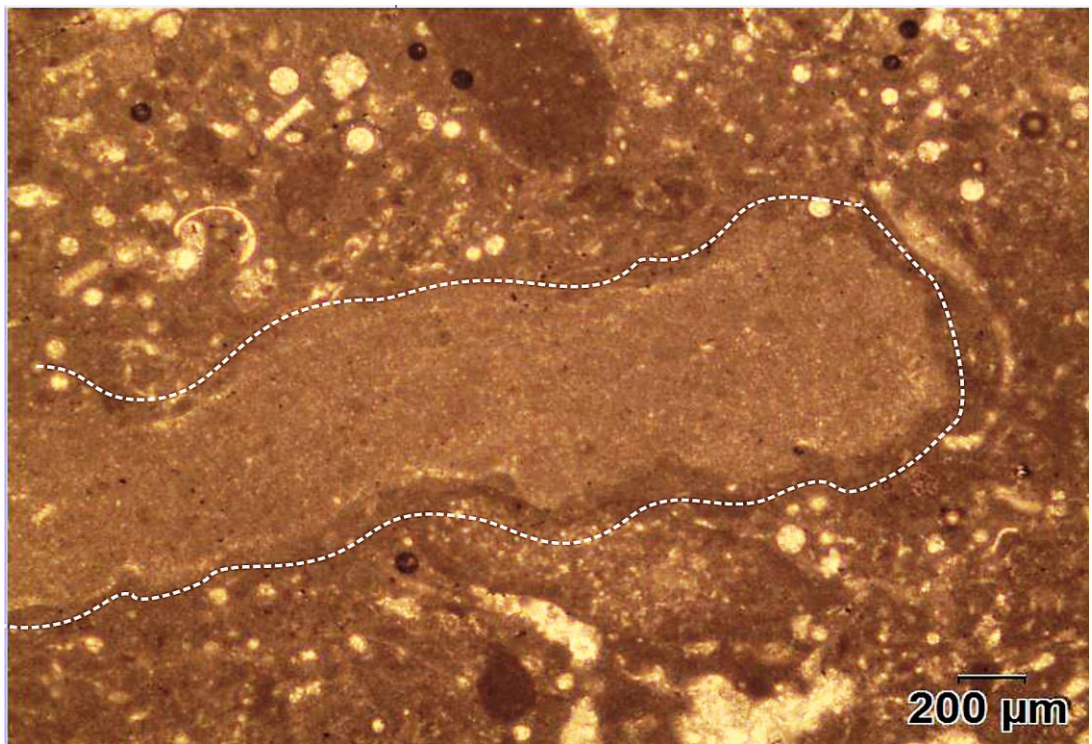


Figure 3.17: Microphotograph illustrating bioturbation area with white dotted line (PPL, 4 X GT/S 64).

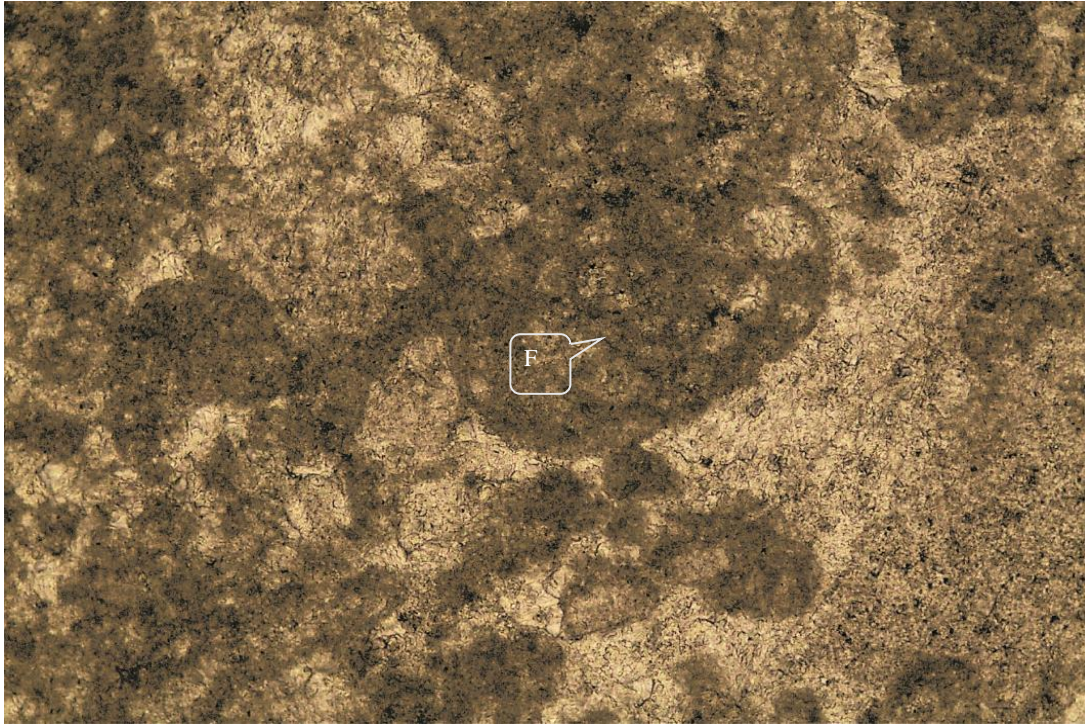


Figure 3.18: Microphotograph showing foraminifers (F) (PPL, 20 X GT/S 2).

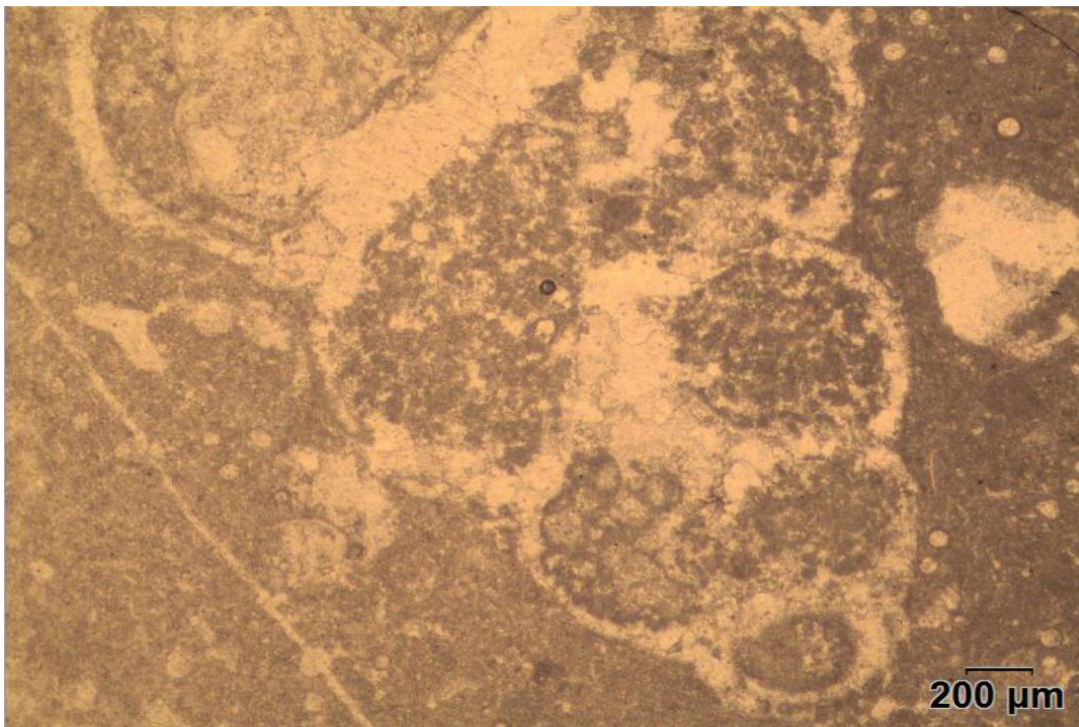


Figure 3.19: Microphotograph showing gastropods shell (PPL, 4 X GT/S 64).

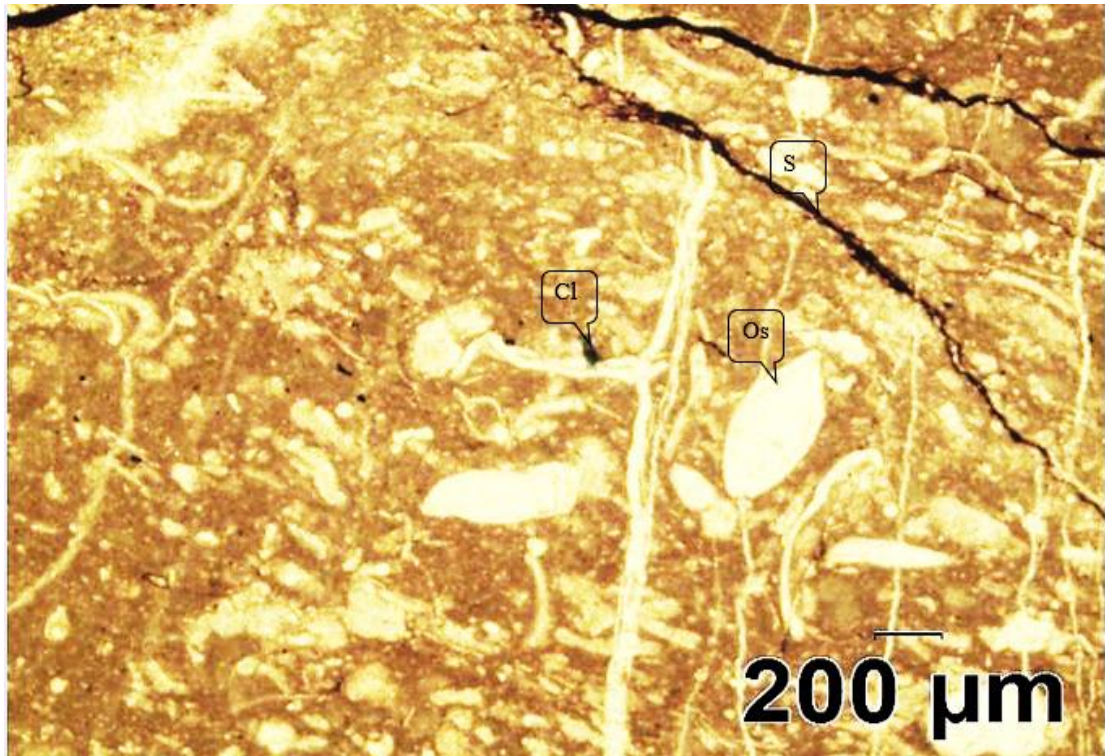


Figure 3.20: Photomicrograph illustrating ostracods (Os), stylolite (S) with organic matter and chlorite (Cl) (PPL, GT/S 21).

3.5. COMPONENT ANALYSIS OF MICROFACIES AND INTERPRETATION OF DEPOSITIONAL CONDITIONS

The relative sea-level and dynamic environmental changes have been known by the geologic past and strongly influenced the evolution of distinct carbonate platforms. The same type of microfacies within these stratigraphic units vary in response to the gradual environmental shifts caused by the relative sea-level changes or water depth. The variation in water depth is the most important factor that controls a wide range of environmental changes comprising water turbulence, light penetration, siliciclastic contamination and nutrient source.

The conceptual methods are used to model limestone microfacies, which will help to identify environmental changes. Standard microfacies models (Flügel, 1982; Wilson, 1975) are widely used to interpret carbonate microfacies. However, the rate at which environmental changes occurred, particularly fluctuations in relative sea level, were supposed to have been slower, therefore the effects of systematic, high-frequency, dynamic environmental changes on the microfacies of individual platforms is ignored

in these models. Same type of microfacies at different interval have variation while different microfacies can exist at similar locations and depths on a platform at different times within a change of relative sea-level cycle. The spatial or temporal orderly shifts / changes in the relative importance of component grains are termed relays (Hennebert and Lees, 1985). Statistics methods are used in the analysis of carbonate microfacies like graphical, triangular diagrams, in order to identifying different sedimentary constituent. Modal compositional data from the Gökgöl tunnel section samples were analyzed using ternary diagrams. Different combinations of parameters are used to recognize populations/ elements in limestones (Dunham, 1962).

3.5.1. INTERPRETATION OF DEPOSITIONAL CONDITIONS OF THE MEASURED SECTION

The ternary diagrams were made for basal, middle and upper part of the measured section of Gökgöl section. Triangular diagrams were drawn among different parameters like texture (allochem, micrite and sparite), modal abundance (micrite, peloids and mollusca) and spatial (benthic foraminifers, echinoderms and mollusca).

The basal part of the section consists of the samples GT1–GT42. Different parameters are used to identify and group the microfacies in a ternary plot (Figure 3.21). The allochem and micrite is abundant while allochems consists of mollusca dominantly with less amount of forams and rare echinoderms. The sample scatter patterns generated can be subdivided into five populations on the basis of the distribution of samples sharing similar sedimentary fabric into distinct groups. These assemblages can be classified as: (a) peloidal/molluscan grainstone microfacies; (b) peloidal/molluscan packstone microfacies; (c) wackestone microfacies. (d) peloidal grainstone; and (e) peloidal/molluscan rudstone microfacies. The high abundance of mollusca and echinoderms and low content of benthic foraminifera indicates a shallow-marine depositional setting.

The middle part of the measured section is displayed by the samples GT43 to GT54. Allochems are rich in number (Figure 3.22). A triangular diagram represents a scatter of plots. On the basis of patterns produced samples can be subdivided into three populations as: (a) peloidal/molluscan packstone microfacies, (b) peloidal/molluscan

wackestone microfacies and (c) bindstone. A richness of benthic foraminifera and mollusca but with rare of echinoderms in the middle of the succession indicates a shallow-marine environment with moderate water depth in comparison to the bottom of the succession. The population, characterized by micrite, foraminifera, bivalves, peloids, green algae, and echinoderms is interpreted as deposition occurred in a constantly shallow marine with moderate-energy inner-platform setting that experienced comparatively little temporal variation in environmental factors (Tucker, 1999). The depositional environment therefore represents comparatively stable and unchanging during the deposition of the middle part of the succession.

The upper part of the measured stratigraphic section is shown by the samples GT55–GT68 (Figure 3.23). Allochems and micrite are the abundant sample components. The upper part shows a less dispersed scatter of plots as compared to bottom and middle of the succession. The sample scatter patterns generated can be subdivided into four populations on the basis of the distribution of samples sharing similar sedimentary fabric. These assemblages can be classified as: (a) peloidal/molluscan grainstone microfacies; (b) peloidal/molluscan packstone microfacies; (c) peloidal/molluscan wackestone microfacies; and (d) peloidal rudstone microfacies. The high value of echinoderms and mollusca indicates a shallow-marine depositional environment.

Mollusca is used as modal and spatial parameter to cross check the microfacies overlapping or grouping in order to better understand the depositional condition.

The ternary diagrams suggests that the measured section was deposited at shallow environment with variation in water depth. The upper and bottom portion of the section show shallow environment with high energy environment while the middle part illustrated stable and calm condition comprising shallow benthic foraminifers.

The combined classification scheme for microfacies are described in Table 3.6. Sedimentary log was drawn to interpret depositional environment (Figure 3.24).

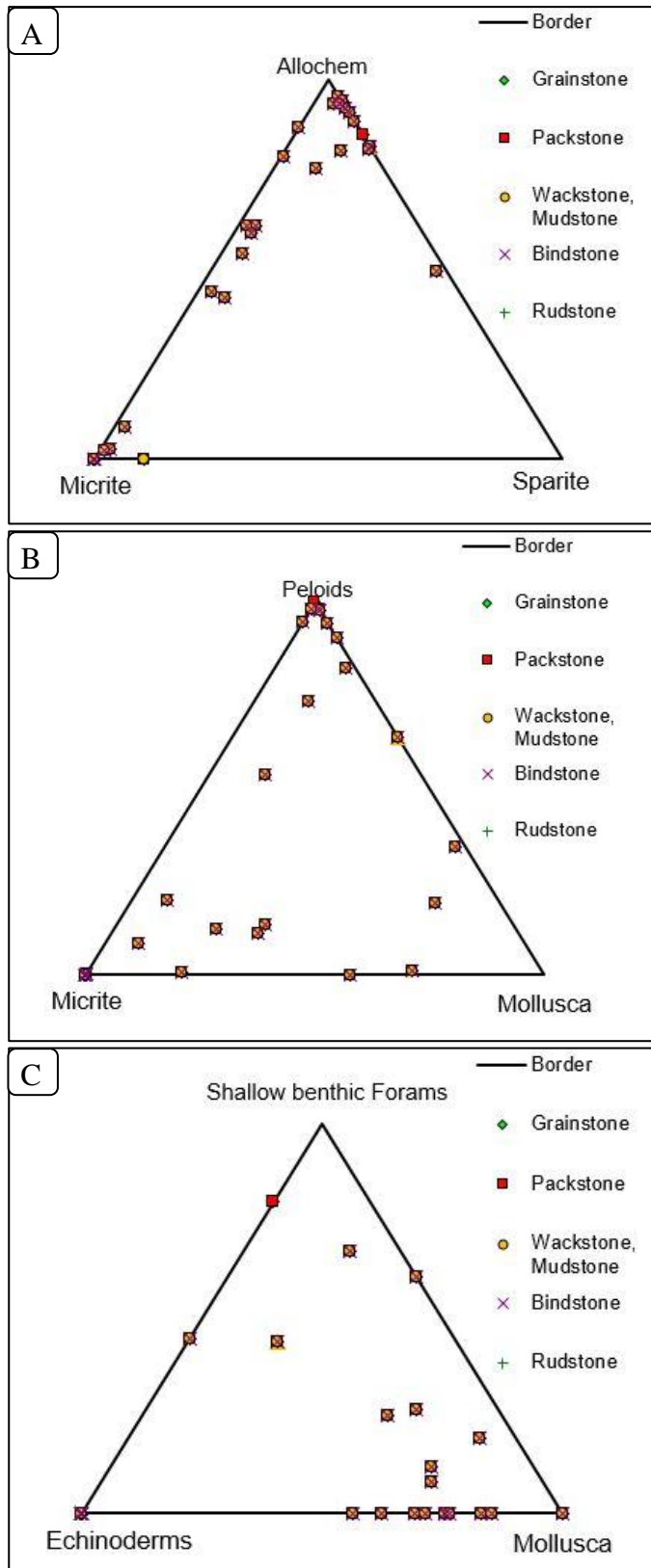


Figure 3.21: Ternary diagrams of compositional modal from the basal part of the Yılanlı Formation used to interpret depositional model of microfacies and high frequency dynamic environmental changes (0-20m represent the samples from GT1-GT42). The ternary diagram, A. represent allochem, micrite and sparite, B. shows peloid, micrite and mollusca, C. displays mollusca, echinoderms and shallow benthic foraminifers.

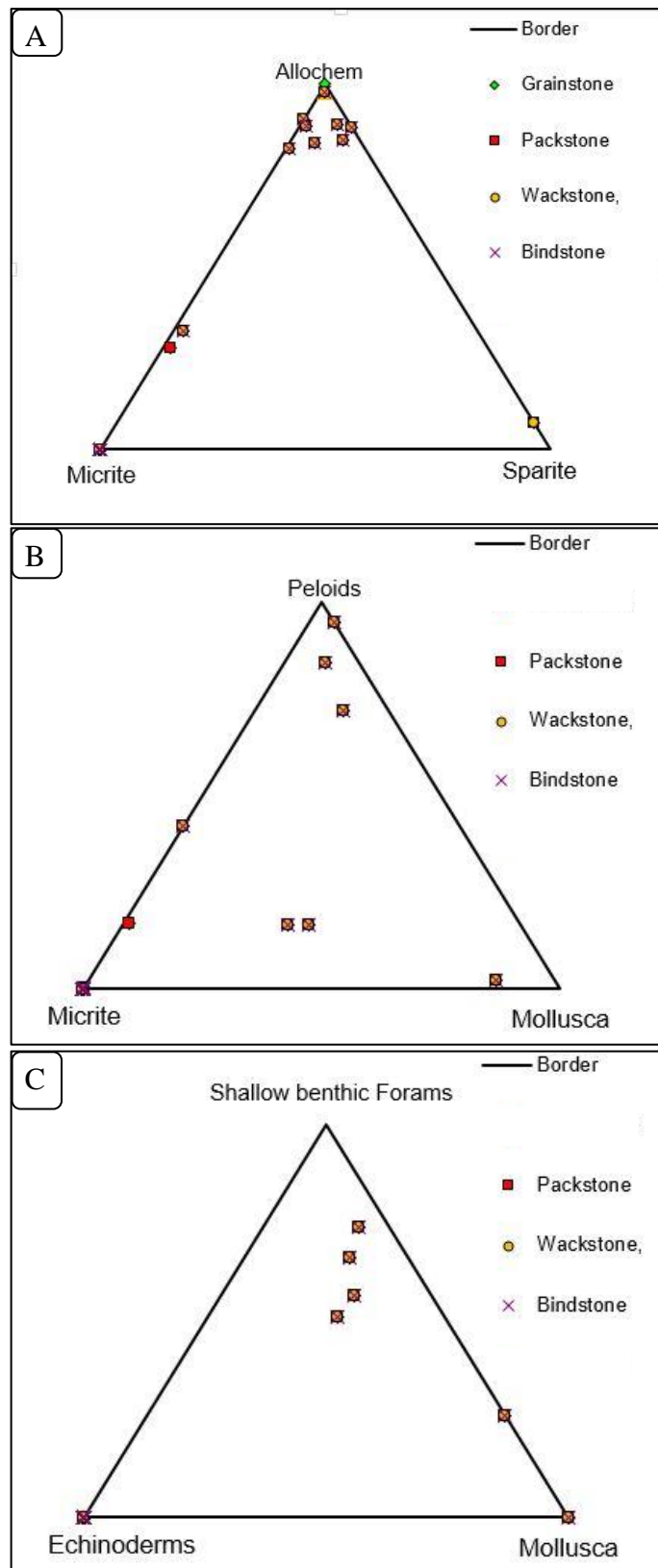


Figure 3.22: Ternary diagrams of compositional modal from the middle part of the Yılanlı Formation used to interpret depositional model of microfacies and high frequency dynamic environmental changes (20-60m represent the samples from GT43-GT54). The ternary diagram, A, represent allochem, micrite and sparite, B, shows peloid, micrite and mollusca, C, displays mollusca, echinoderms and shallow benthic foraminifers.

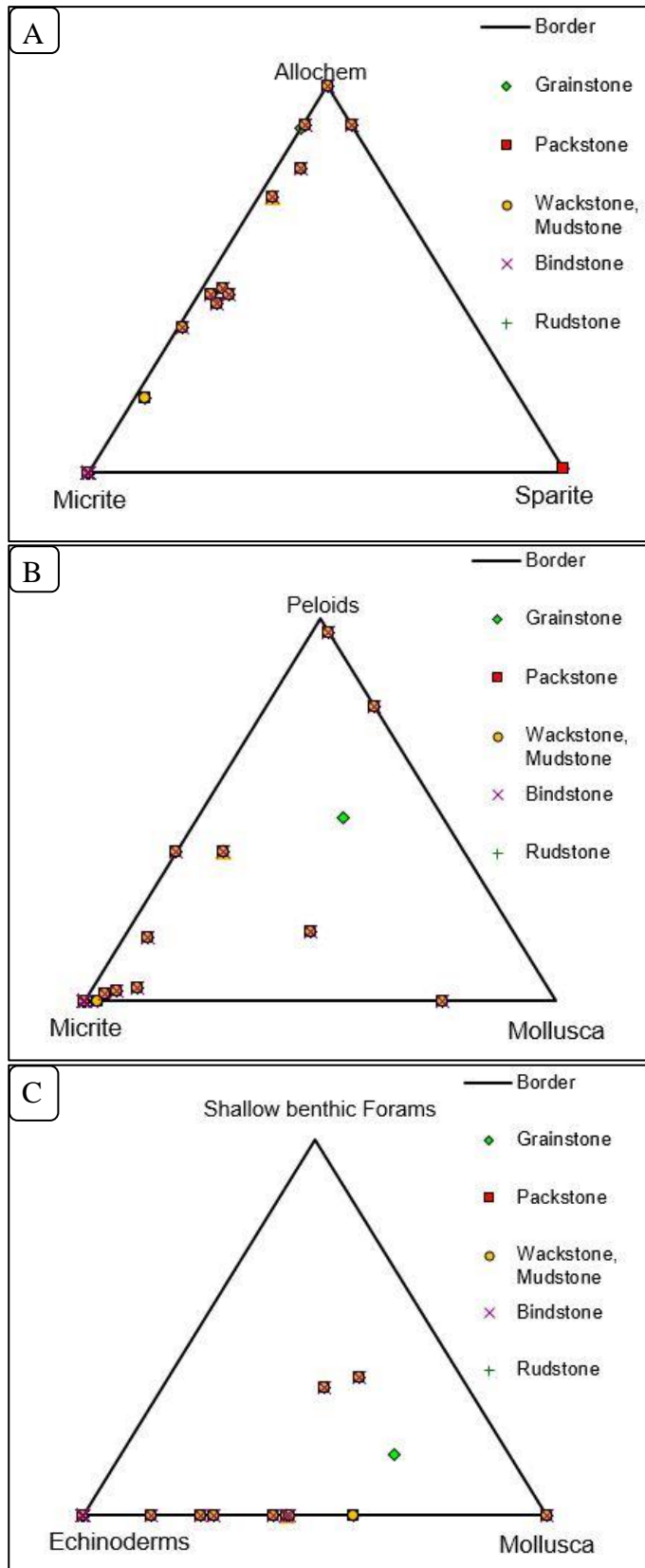


Figure 3.23: Ternary diagrams of compositional modal from the upper part of the Yılanlı Formation used to interpret depositional model of microfacies and high frequency dynamic environmental changes (60-86 m represent the samples from GT55-GT68). The ternary diagram, A. represent allochem, micrite and sparite, B. shows peloid, micrite and mollusca, C. displays mollusca, echinoderms and shallow benthic foraminifers.

Table 3.6: Classifications of the Gököl section based on texture, grain and composition.

| Gököl Section Classification | | | | | |
|-------------------------------------|-----------------|------------------|-------------------|--------------------------------|--------------------------|
| Sample | Picard (1971) | Dunham (1962) | Folk (1959, 1965) | Strohmenger and Wirsing (1991) | This Study |
| GT01 | Clay Shale | - | Clay Shale | - | Clayey Shale |
| GT02 | - | Packstone | Biomicrite | Bio-Intra-pelmicrite | Bioclastic Packstone |
| GT03 | Claystone | - | Claystone | - | Claystone |
| GT04 | - | Packstone | Biomicrite | Bio-intramicro | Bioclastic Packstone |
| GT05 | - | Packstone | Intramicro | Intra-Oo-biomicrite | Intraclastic Packstone |
| GT06 | - | Rudstone | intramicrite | Pel-intramicro | Rudstone |
| GT07 | - | Packstone | intramicrite | Intra-Pel-biomicrite | Intraclastic Packstone |
| GT08 | - | Mudstone | Micrite | Micrite | Burrowed lime Mudstone |
| GT09 | - | Rudstone | Intramicro | Intra-pelmicrite | Rudstone |
| GT10 | - | Packstone | Pelmicrite | Pel-Intra-oomicro | Peloidal Packstone |
| GT11 | - | Wackestone | Biomicrite | Biomicrite | Bioclastic Wackestone |
| GT12 | - | Grainstone | Pelsparite | Pel-intrasparite | Peloidal Grainstone |
| GT13 | Clayey Shale | - | Clay shale | - | Clayey Shale |
| GT14 | - | Rudstone | Intramicro | Intra-biomicrite | Rudstone |
| GT15 | - | Mudstone | Micrite | Micrite | Burrowed Lime Mudstone |
| GT16 | - | Mudstone | Micrite | Micrite | Burrowed Lime Mudstone |
| GT17 | Muddy Shale | - | Muddy Shale | - | Muddy organic rich Shale |
| GT18 | - | Wackestone | Biomicrite | Biomicrite | Bioclastic Wackestone |
| GT19 | - | Packstone | Intramicro | Intramicro | Intraclastic Packstone |
| GT20 | - | Mudstone | micrite | Micrite | Brecciated Mudstone |
| GT21 | - | Packstone | Biomicrite | Biomicrite | Bioclastic Packstone |
| GT22 | - | Grainstone | Pelsparite | Pel-Intra-oomicro | Peloidal Grainstone |
| GT23 | - | Bindstone | Intramicro | Intra-Pel-oomicro | Bindstone |
| GT24 | - | Wackestone | Biomicrite | Biomicrite | Bioclastic Wackestone |
| GT25 | - | Packstone | Pelmicrite | Pel-intramicro | Peloidal Packstone |
| GT26 | - | Rudstone | Biomicrite | Bio-intramicro | Rudstone |
| GT27 | - | Wackestone | Biomicrite | Biomicrite | Bioclastic Wackestone |
| GT28 | - | Wackestone | Biomicrite | Biomicrite | Bioclastic Wackestone |
| GT29 | - | Mudstone | micrite | micrite | Mudstone |
| GT30 | - | Grainstone | Pelsparite | Pel-Intra-Bio-oomicro | Peloidal Grainstone |
| GT31 | - | Packstone | Pelmicrite | Pel-Intra-oomicro | Peloidal Packstone |
| GT32 | - | - | claystone | - | claystone |
| GT33 | - | Packstone | Pelmicrite | Pel-Intra-Bio-oomicro | Peloidal Packstone |
| GT34 | - | Wackestone | Biomicrite | Biomicrite | Bioclastic Wackestone |
| GT35 | Clayey Shale | - | Clayey Shale | - | Clayey Shale |
| GT36 | - | Sparite Dolomite | Dolomite | - | Dolomite |
| GT37 | Shale | - | Shale | - | Shale |
| GT38 | - | Wackestone | Biomicrite | Biomicrite | Bioclastic Wackestone |
| GT39 | claystone | - | claystone | - | claystone |
| GT40 | - | Rudstone | intramicrite | Intra-oomicro | Rudstone |
| GT41 | shale | - | shale | - | Black shale |
| GT42 | - | Bindstone | Intramicro | Intra-pelmicrite | Bindstone |
| GT43 | - | Grainstone | Pelsparite | Pel-Oo-Intra-biosparite | Peloidal Grainstone |
| GT44 | Silty shale | - | Silty shale | - | Silty shale |
| GT45 | - | Wackestone | Pelmicrite | Pel-intramicro | Peloidal Wackestone |
| GT46 | Silty claystone | - | Silty claystone | - | Silty claystone |
| GT47 | - | Packstone | Biomicrite | Bio-intramicro | Bivalve Packstone |
| GT48 | - | Bindstone | Biomicrite | Biomicrite | Bindstone (stromatolite) |
| GT49 | - | Bindstone | Biomicrite | Bio-intramicro | Bindstone (stromatolite) |
| GT50 | - | Wackestone | Biomicrite | Bio-intramicro | Bioclastic Wackestone |
| GT51 | - | Packstone | Biomicrite | Bio-intramicro | Bioclastic Packstone |
| GT52 | - | Packstone | Biomicrite | Bio-Intra-pelmicrite | Bioclastic Packstone |

Table 3.6. Continued

| | | | | | |
|-------------|--------------|------------|--------------|-------------------------|-------------------------|
| GT53 | - | Packstone | Pelmicrite | Pel-intramicro | Peloidal Packstone |
| GT54 | - | Rudstone | Intramicro | Intra-pelmicrite | Rudstone |
| GT55 | - | Packstone | Biomicrite | Bio-Pel-intramicro | Bioclastic Packstone |
| GT56 | Shale | - | Shale | - | Black Shale |
| GT57 | - | Wackestone | intramicrite | Intramicro | Intraclastic Wackestone |
| GT58 | Claystone | - | Claystone | - | Claystone |
| GT59 | - | Wackestone | Intramicro | Intra-Bio-pelmicrite | Intraclastic Wackestone |
| GT60 | - | Wackestone | Biomicrite | Biomicrite | Bioclastic Wackestone |
| GT61 | - | Wackestone | Biomicrite | Bio-intramicro | Bioclastic Wackestone |
| GT62 | - | Grainstone | Pelsparite | Pel-Intra-Oo-biomicrite | Peloidal Grainstone |
| GT63 | - | Wackestone | Biomicrite | Biomicrite | Bioclastic Wackestone |
| GT64 | - | Packstone | Biomicrite | Bio-Intra-pelmicrite | Bioclastic Packstone |
| GT65 | - | Wackestone | Pelmicrite | Pel-intramicro | Peloidal Wackestone |
| GT66 | - | Wackestone | Intramicro | Intra-Bio-pelmicrite | Intraclastic Wackestone |
| GT67 | Clayey Shale | - | Clayey Shale | - | Clayey Shale |
| GT68 | - | Rudstone | Intramicro | Intra-Oo-Pel-biomicrite | Rudstone |

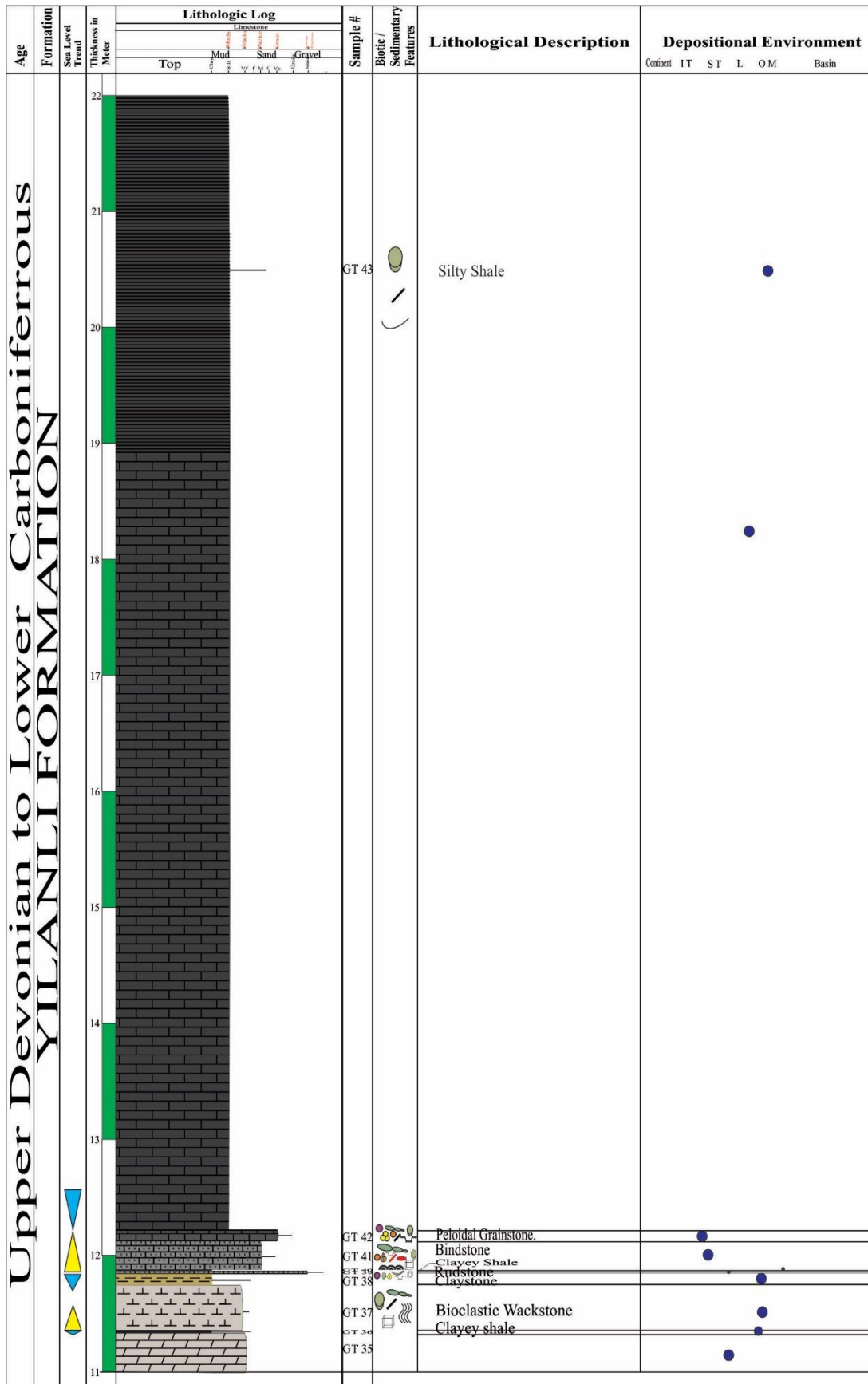


Figure 3.24: Continued (11-22 m).

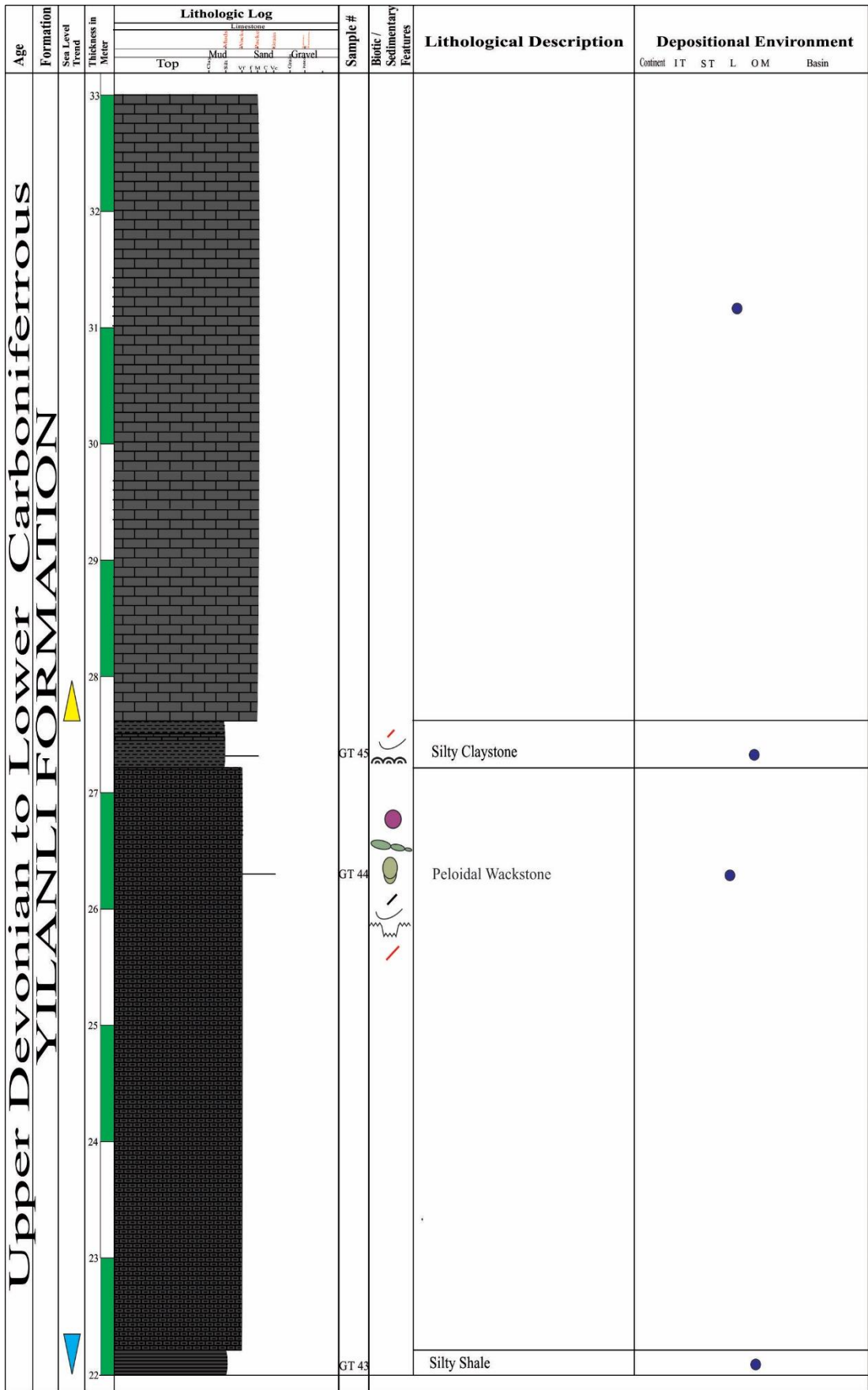


Figure 3.24: Continued (22-33 m).

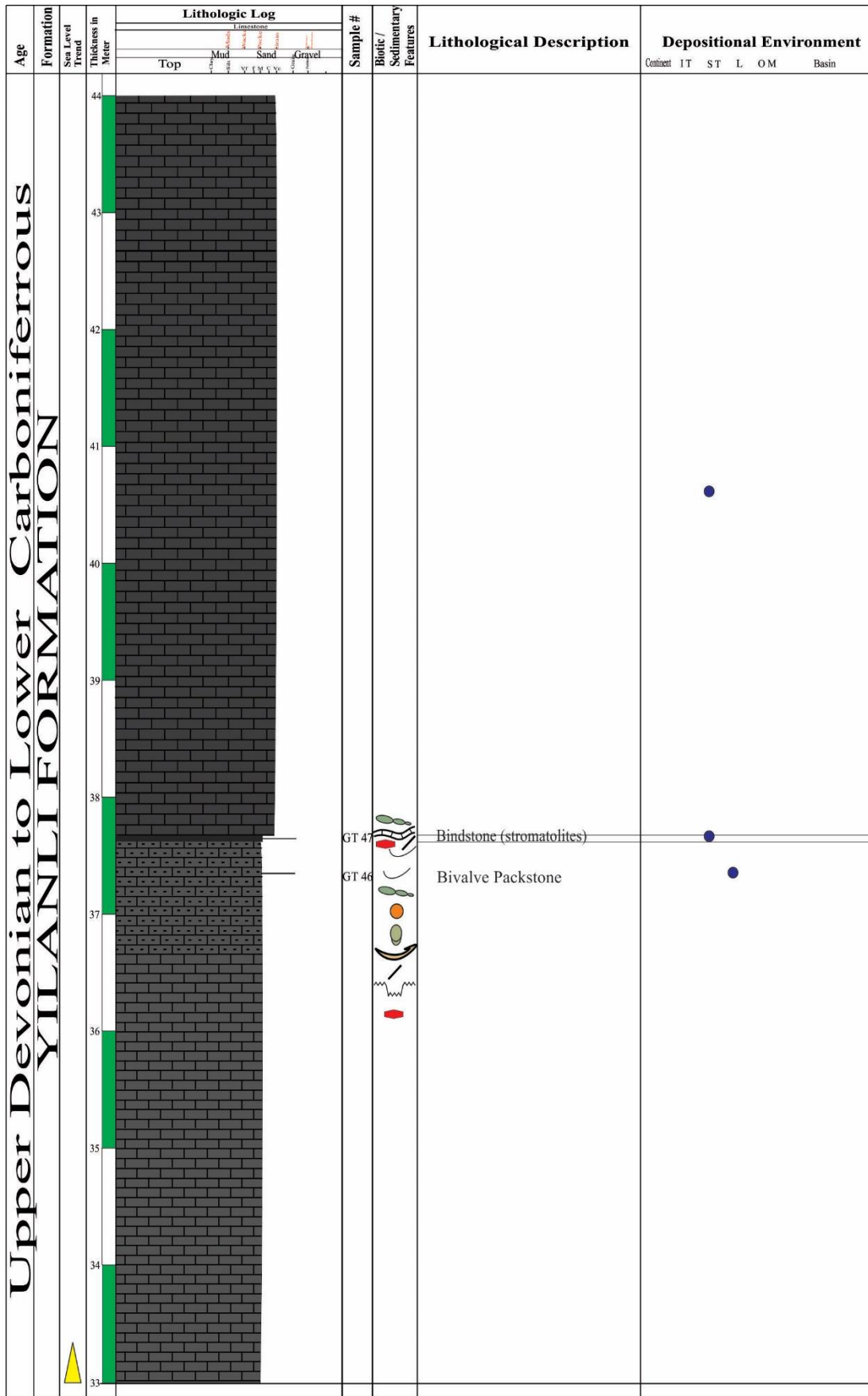


Figure 3.24: Continued (33-44 m).

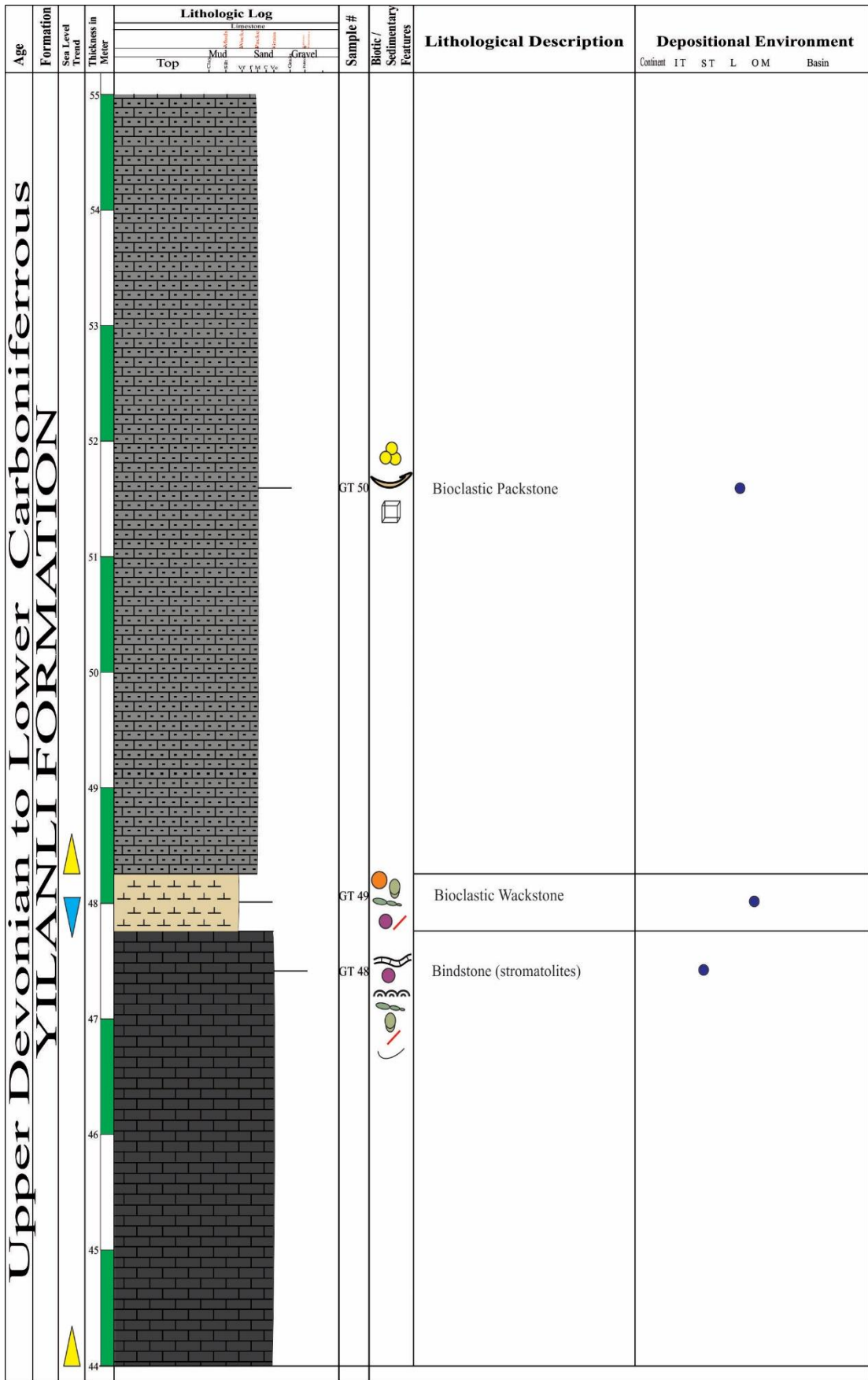


Figure 3.24: Continued (44-55 m).

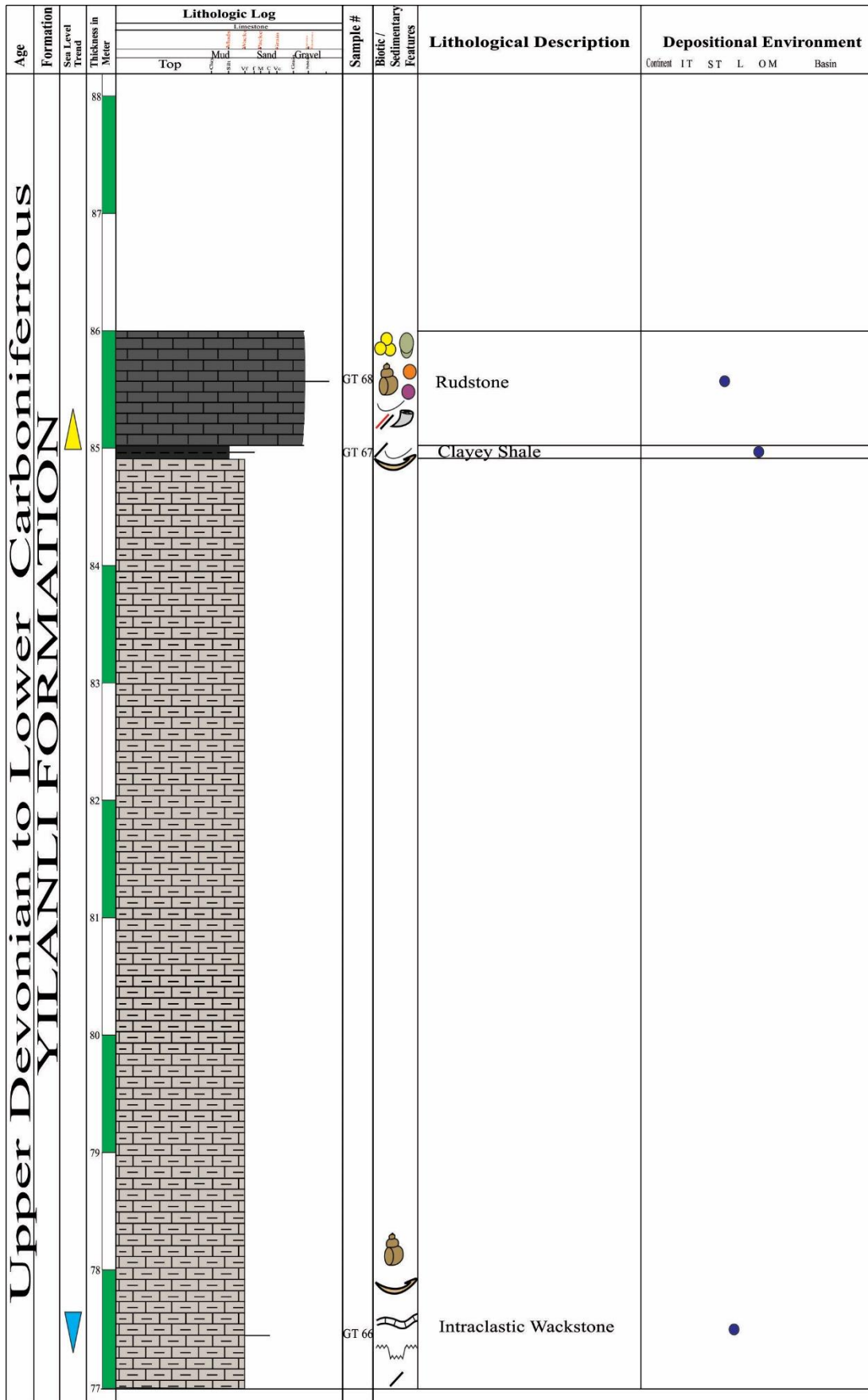


Figure 3.24: Continued (77-86 m).

CHAPTER 4

DEPOSITIONAL ENVIRONMENT

An environment of deposition is defined as a specific part of earth surface influenced by particular physical, chemical and biological processes generate a distinct type of sedimentary rock (Boggs, 2001; Selley, 2000) (Figure 4.1).

The studied section lies in the upper part of the Yılanlı Formation of Upper Devonian - Lower Carboniferous (Denayer, 2014). Based on detailed field work and petrographic analysis, changes in microfacies reflect the environmental condition while vertical repetition represent change in sea level (transgression and regression) can be used to interpret depositional environment. The sub-environments are classified on the basis of variation of textural relationship, faunal assemblage and allochems. The colors of the pelagic sediments give indication to the paleoceanographic condition (Colley et al., 1984; Wilson et al., 1985; Thomson et al., 1987).

The studied section start with a dark grey to black shale overlain by packstone that underneath the laminated claystone that indicate increases of sedimentation rate. This layer is followed by a transgression indicated by deposition of grainstone. After a regular sea fall and a rise has been indicated by grainstone to packstone, mudstone or shale, respectively (Figures 3.2, 3.24). This pattern of deposition is repeated up to middle part of the measured section and shows a shallow to restricted environment. A cyclic depositional pattern is observed on restricted lagoonal to open marine in inner ramp type carbonate platform, strata representing a calm condition followed by regression and transgression (mudstone/ shale , packstone to grainstone / stromatolite) (Figure 3.24).

The cyclic repetitions of dark grey to black shale interbedded with limestone represent anoxic condition and periodic influxes of land-derived, reflecting clastics fluctuating climatic conditions in the area.

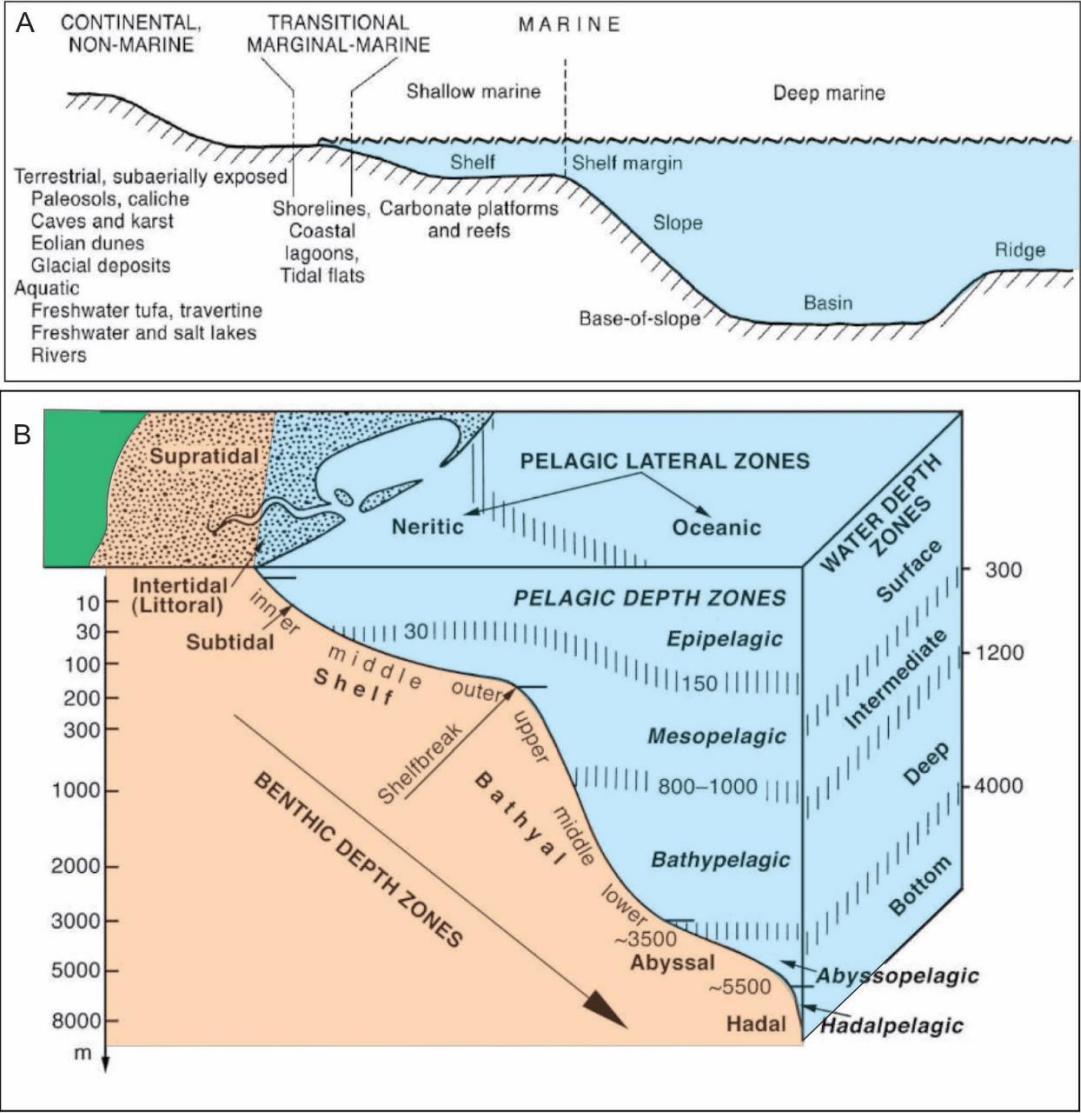


Figure 4.1: A general displays of depositional environment. B Marine depositional environment (Kennett, 1982).

Abundantly peloids are present in measured stratigraphic sections of fecal pellets origin are diagnostic feature of lagoonal environment to shelter shallow environment (MacIntyre, 1985; Chafetz, 1986). This shallow environment is also supported by presence of stromatolite.

The component analysis of the microfacies of the Yılanlı Formation reveal that the lower portion of the succession were deposited in a continuous fluctuation in sea level. Supported by the presence of abundance of echinoderm and mollusca indicate that formation was deposited at different parts of shallow water carbonates of inner ramp type carbonate platform. The interpretation of sub-microfacies in a block diagram illustrates that the Yılanlı Formation represents deposition on a peritidal with near shore subtidal, restricted lagoon to restricted open marine of inner to middle ramp type carbonate platform (Figure 4.2).

Peritidal consists of supratidal, intertidal and subtidal zones formed in marginal-marine and shoreline depositional environments (Flügel, 2004). Folk (1973) describes the term peritidal as a carbonate environments associated with low-energy tidal zones, especially tidal flats. Intertidal zone is define as the region between the normal low-tide and high-tide levels, sub-tidal zone describe as the permanently submerged area seaward of the tidal flats and it may be strongly influenced by wave action or associated with protected low-energy lagoons.

Oolites are important paleoenvironmental indicators for water energy, salinity, and depth. Ooids are micritic in composition and indicate shallow marine depositional setting and are documented in grainstone, and rudstone microfacies (Flügel, 2004).

Fecal pellets are rounded, usually fine grained particles accumulate in intertidal and subtidal, shallow lagoon settings (Flügel, 2004). Stromatolites are laminated benthic microbial deposits (Riding, 1999) and occur in marginal marine and shallow subtidal environments subtidal and basinal environments (Flügel, 2004).

Each microfacies have some distinct characteristics that separate from other and have specific range of deposition (Figure 4.2).

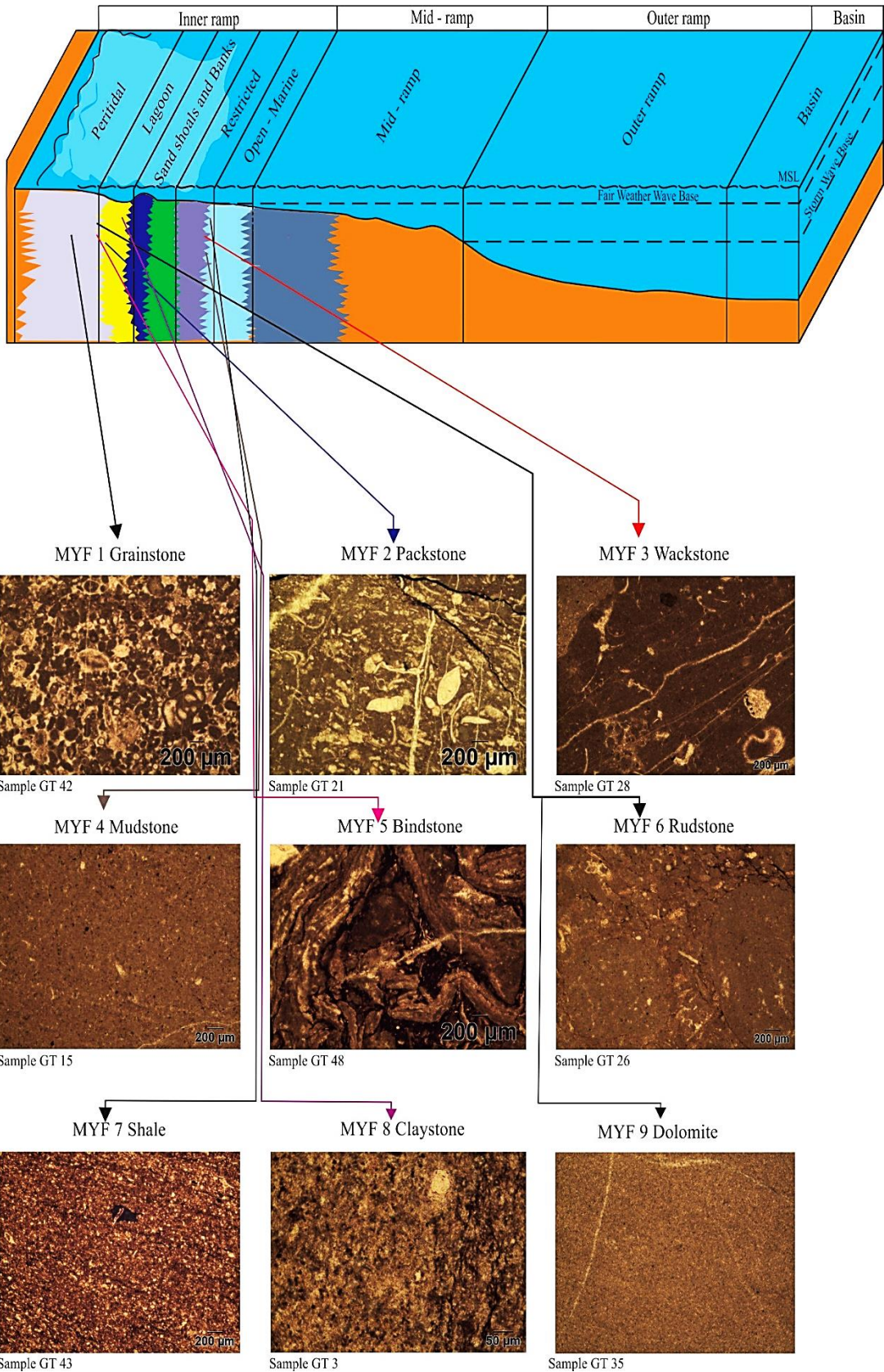


Figure 4.2: Schematic block diagram displaying depositional model of the Yılanlı Formation, Zonguldak, NW Turkey (modified from Flügel, 2004).

CHAPTER 5

DEVONIAN – CARBONIFEROUS SUCCESSIONS

5.1. INTRODUCTION

The Devonian – Carboniferous take eminent position in the geological time period. During Devonian many important events occurred like the closure of Lepetus Ocean, Caledonian orogenesis, Variscan orogenesis, Hangenberg mass extinction (Figure 5.1) and colonization of land (Walliser, 1996). The Hangenberg's event is one of the largest Phanerozoic mass extinction and consider as terminal event of Devonian period (Walliser, 1980a, b, 1984, 1996; Caplan et al., 1998). Devonian – Carboniferous boundary is fixed by occurrence of a new conodont species within an evolutionary lineage, in this case *Siphonodella sulcate*. The coal swamps were well developed during the Carboniferous period all over the world. The occurrence of carbonate and coal during Carboniferous at relatively low latitude area (Scotese et al., 1979, 1990). For this purpose the previous work and microfacies data may be combined in such a way to interpret the wide spread Devonian – Carboniferous strata.

5.2. DEVONIAN – CARBONIFEROUS

In Turkey, Devonian-Carboniferous comprises different rock unit belongs to different paleogeographic origin (Figure 1.5). The Devonian period is represented by various lithological units. These units are part of Pontides, Taurides and Arabian Plate of more than 1000 meters thick sedimentary sequence (Yalçın and Yılmaz, 2010). The study area lies in the north western part of Pontides (Höll, 1966; Erdoğan et al., 1990; Göncüoğlu, 1997; Kaya and Rezsü, 2000).

Devonian limestone of the Zonguldak Terrane illustrates continuous deposition in shallow marine environment (Görür et al., 1997) as compared to the Istanbul Terrane deepening of environment upward from Middle Devonian to Carboniferous (Görür et al., 1997) consists of shale, calciturbidites and deep water limestone (Önal, 1982; Ketin, 1983). Devonian of the Bulgaria and western Romania of Moesian Terrane shows a sequence similar to the Zonguldak Terrane comprising black shale, quartzite and limestone at the base and limestone and dolomite at the top (Garetskiy, 1970; Dachev et al., 1998).

Carboniferous of Zonguldak Terrane is similar to Moesian block present in Bulgaria and Romania consist dark grey shale, siltstone interbedded in form of patches with limestone, marl and coal deposits (Garetskiy, 1970; Dachev et al., 1998; Görür et al., 1997), whereas Istanbul Terrane flysch deposit of Thracian origin, at the base of flysch radiolarites of Visean comprising intercalation of shale, chert and nodular limestone are documented (Abdüsselamoğlu 1963; Kaya, 1973, 1980; Gedik et al., 2005). Balkan Terrane have flysch deposit of Carboniferous (Yanev, 2000) The Targovishte Formation of the Balkan Terrane in NE Bulgaria (Yanev and Cassinis, 1998) is almost equal with the Ereğli Formation of Istanbul Terrane in terms of fossil content and lithostratigraphy.

Nakhchevan (Azerbaijan) and southern Armenia, dominantly consist of coral-brachiopod limestones (often bituminous), quartzite sandstones, and argillites of Devonian–Carboniferous of shelf deposits (Aslanian 1970; Azizbekov 1972; Rustomov, 2005 and Adamia et al., 2011).

The above data suggest that Zonguldak Terrane is similar to Moesian Terrane of Bulgaria and Romania (Table 5.1) and they have shallow water carbonates of same type of facies (Garetskiy, 1970; Dachev et al., 1998; Görür et al., 1997), while Istanbul Terrane is different in terms of facies and close to Balkan Terrane (Figure 1.5, 2.5).

Zonguldak Terrane of Turkey have coal reserves that are main source of coal production in the area (Burger et al., 2000; Gürdal and Yalçın, 2000; Hoşgörmez, 2007).

The Carboniferous flora and fauna in the Zonguldak coal basin resembles with Moesian and other Upper Carboniferous coal basins of Europe.

The paleogeographic maps presented here are taken from Scotese et al. (1990). Balkan, Zonguldak, Moesian and Istanbul all have Perigondwanan origin but behave independently over time during drifting towards Laurasia. Perigondwanan origin of the Istanbul – Zonguldak terranes are discussed by Göncüoğlu et al. (1997). During the Carboniferous anticlockwise rotation of Gondwana and collision with Laurasia widened the Tethyan Sea (Figure 5.2 and 5.3). In early Eocene Zonguldak Terrane attached to Moesian platform (Okay et al., 1994).

Peri-Gondwanan origin of the Zonguldak and Istanbul terranes in Turkey are proved by presence of the Late Pan-African-Cadomian crystalline basement and the fossil provinciality of Early Paleozoic (Göncüoğlu et al., 2006).

Zonguldak Terrane is not a part of Istanbul Terrane during Devonian and Carboniferous that shows it behave independently consist of shallow carbonates of Carboniferous.

Shallow water carbonates platform of upper Devonian and Carboniferous of Zonguldak Terrane may be extended to Moesian Terrane (Bulgaria).

Table 5.1. The Devonian – Carboniferous correlation of Zonguldak region with different parts of the world.

| Age | Balkan Terrane | Moesian Terrane | Istanbul Terrane | Azerbaijan and Southern Armenia | Zonguldak Terrane | This study |
|-------------------------|---|--|--|--|--|---|
| Devonian -Carboniferous | Yanev and Cassinis, 1998, Yanev, 2000 | Garetskiy, 1970, Görür et al., 1997, Dachev et al., 1998 | Abdüselamoğlu 1963; Kaya, 1973, 1980; Görür et al., 1997, Gedik et al., 2005 | Adamia et al., 2011 | Görür et al., 1997 | |
| | Flysch deposits / deep water deposits | Shallow water deposits | Flysch deposits / deep water deposits | Shelf type deposits. | Shallow water deposits | Shallow water deposits of inner ramp type |
| | shale, calciturbidites siliciclastic, and limestone | black shale, quartzite, dolomite and limestone | shale, calciturbidites and deep water limestone | Coral-brachiopod limestones, bituminous, quartzite sandstones, and argillites. | black shale, quartzite, dolomite and limestone | Mainly limestone, black shale, dolomite, mudstone and claystone |

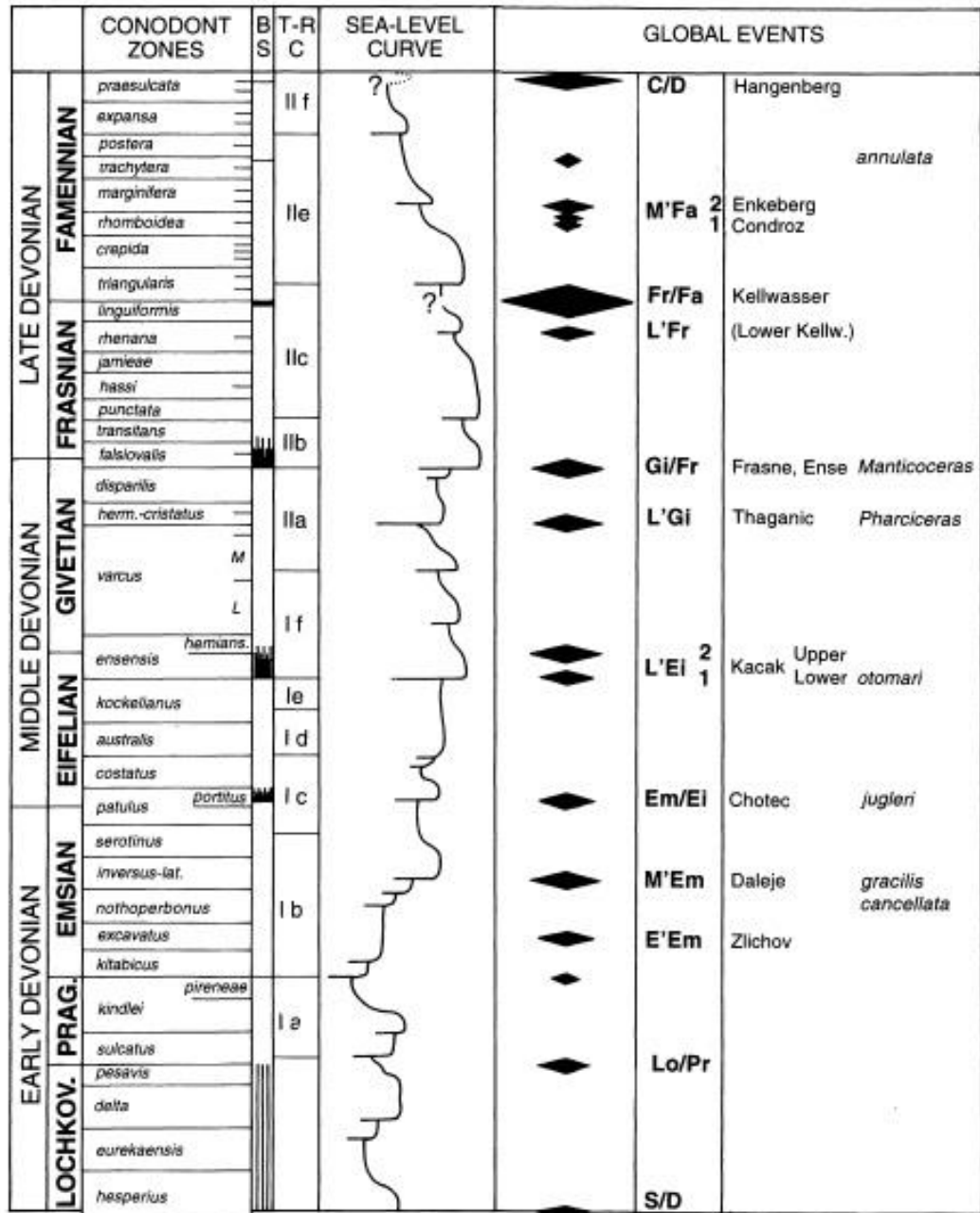


Figure 5.1: A major Devonian event and sea level change, black rhombs represent global event (Johnson et al., 1985).

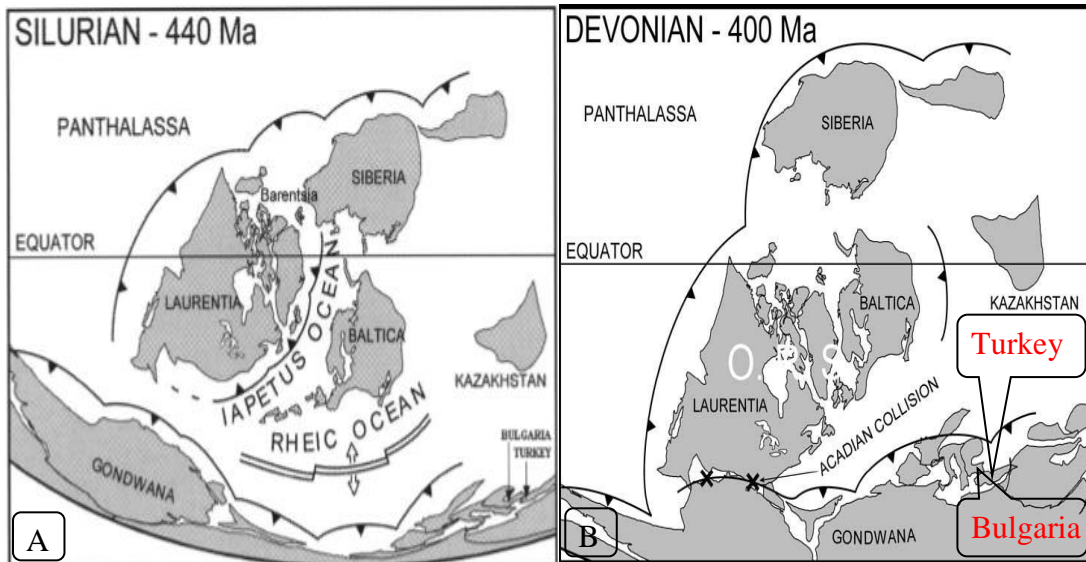


Figure 5.2: Paleogeographic reconstruction of Gondwana, Baltica and Peri-Gondwanan European Terrane; A. Silurian; B. Devonian (Scotese et al., 1990).

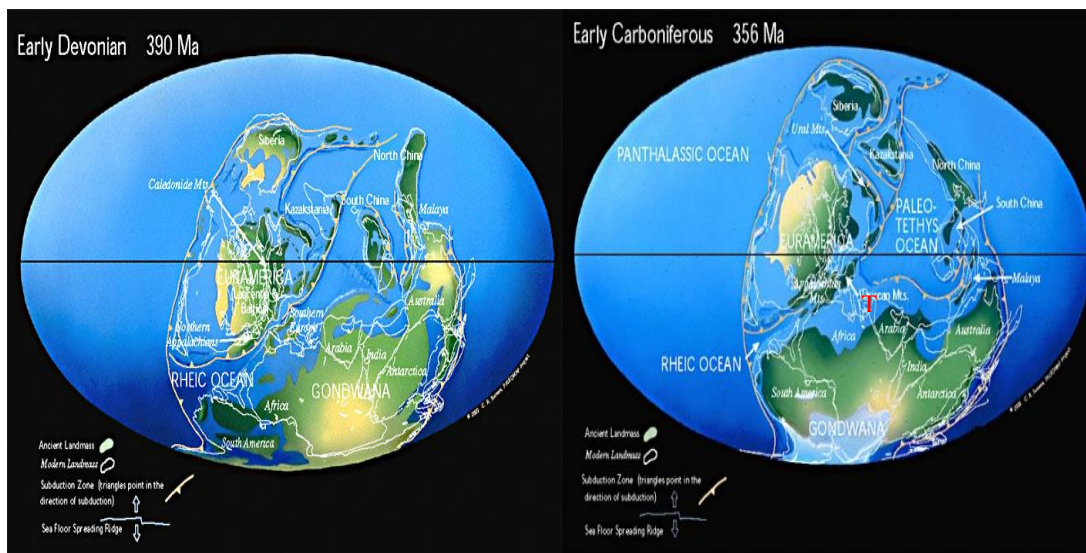


Figure 5.3: Paleogeographic reconstruction map. A. Early Devonian; B. Early Carboniferous T represent location of Turkey (Scotese et al., 1990).

CHAPTER 6

DISCUSSION AND RECOMMENDATIONS

The Upper Devonian – Lower Carboniferous succession of the Yılanlı Formation of the Zonguldak were measured for detailed studies. The total thickness of the measured section is eight thousand six hundred centimeter (8600 cm). The Yılanlı Formation comprises thick beds of limestone with thin beds of black shale and claystone. A detailed sedimentologic and microfacies analysis and point counting studies have been carried out in order to identify the lithofacies and establish ternary diagram to model the microfacies in context component variation during deposition and dynamic environmental conditions. A total of nine microfacies and fifteen sub-microfacies were identified.

To understand the depositional environment and change in sea level, component analysis was carried out. Ternary diagrams were drawn by using different parameters (texture, modal abundance, spatial) for bottom, middle and upper part. These ternary diagrams illustrates that in the lower measured section there was abrupt changes in sea level indicated by sub-tidal to lagoonal or open marine. The middle of section represents static and stable condition of sea level and facies are in cluster. The upper part of the Yılanlı Formation represents shallow environment supported by the presence of mollusca and echinoderms.

In this study the measured section of the Yılanlı Formation is assigned as Upper Devonian –Lower Carboniferous (Bozkaya et al., 2016). If the TOC and geochemical analysis will be carried out in the study area that may be attractive to the oil industry. The general TOC value for Yılanlı Formation in the Zonguldak region ranges from 0.47 – 7.94. The kerogen II and kerogen III type were reported from Yılanlı Formation of the Zonguldak region. In one sample from Yılanlı Formation have a TOC value 6.5

(Harput et al., 1999). Bozkaya et al. (2016) assigned the Yılanlı Formation of Gökgöl tunnel section as Late Devonian-Early Carboniferous.

The author described the TOC value for source rock to generate hydrocarbon potential. The TOC value 2-5 is considered as good source rock, therefore shale of the Yılanlı Formation have potential to produce hydrocarbons (McCarthy et al., 2011).

Table 6.1. Source rock chart for hydrocarbon potential (McCarthy et al., 2011).

| Source Rock Quality | TOC % | |
|---------------------|-------|--|
| None | < 0.5 | |
| Poor | 0.5-1 | |
| Fair | 1-2 | |
| Good | 2-5 | |
| Very good | > 5 | |

Yılanlı Formation of Zonguldak Terrane has different facies as compared to Istanbul Terrane. Zonguldak Terrane of Perigondwanan origin is similar to Moesian platform and has good reserves of coal that is economically feasible for exploration.

Paleogeographic origin of the Zonguldak Terrane is similar to Moesian Terrane of Eastern Europe (Bulgaria and Romania) and not similar to Istanbul Terrane.

CHAPTER 7

CONCLUSION

1. The Yılanlı Formation of Upper Devonian-Lower Carboniferous of Zonguldak Terrane in the study area is dominantly consist of limestone with subordinate shale and claystone. 8600 cm (86m) were measured near Gökgöl tunnel, Zonguldak Terrane of NW Turkey. The Yılanlı Formation is composed of light to dark grey, beige, cream, khaki and black, thin to very thick, planar bedded limestone having stromatolite and corals at places. Other lithologies are the black shale, dolomite and claystone.
2. Nine microfacies and fifteen sub-microfacies are identified in the studied area. The microfacies include: 1. MYF I grainstone comprises sub-microfacies. S-MYF 1 peloidal grainstone. 2. MYF II Packstone consist four sub-microfacies. S-MYF 1 bioclastic packstone, S-MYF 2 intraclastic packstone, S-MYF 3 peloidal packstone, S-MYF 4 bivalve packstone. 3. MYF III wackstone include three sub-microfacies. S-MYF 1 peloidal wackstone, S-MYF 2 bioclastic wackstone and S-MYF 2 intraclastic wackstone. 4. MYF IV mudstone consist two sub-microfacies. S-MYF 1 burrowed lime mudstone and S-MYF 2 brecciated mudstone. Bivalve lenticular laminae indicates storm condition in mudstone. 5. MYF V bindstone having stromatolite. 6. MYF VI rudstone. 7. MYF-VII shale microfacies comprises three sub-microfacies. 1. S-MYF clayey shale. 2. S-MYF silty shale and 3. S-MYF black shale. 8. MYF-VIII claystone microfacies comprises two sub-microfacies. 1. S-MYF claystone and 2. S-MYF silty claystone. 9. MYF IX dolomite microfacies.
3. MYF I grainstone microfacies is interpreted as intertidal to subtidal shallow marine environment of inner ramp. MYF II packstone microfacies shows shallow marine to lagoonal environment. MYF III wackstone microfacies was

deposited shallow lagoonal to open marine of inner ramp carbonate environment. MYF IV mudstone microfacies may be deposited shoals to protected lagoonal. MYF V bindstone microfacies represent intertidal, restricted to open marine environment of deposition. MYF VI rudstone microfacies shows subtidal to lagoonal environment. MYF VII shale microfacies is deposited at open marine to lagoon with low energy. MYF VIII claystone microfacies may be deposited at restricted lagoonal to subtidal below fair wave weather base. MYF IX dolomite microfacies is considered as secondary dolomite and deposited at shallow marine environment.

4. The Yılanlı Formation is characterized by variety of faunal constituents. These include mollusca (ostracods, bivalves), foraminifera, gastropods, echinoderms, sponges, corals and algae. The mollusca and forams are used to interpret the depositional environment on the basis of component analysis and shows shallow to lagoonal depositional environment.
5. Component analysis are used to produce a microfacies carbonate model. This model is based on three parameters that are used in triangular plots or ternary diagram. The measured section is divided into three parts: basinal, middle and upper. The basinal and upper part almost represents same scatters pattern and illustrate shallow water deposition and continuous and abrupt fluctuation in sea level whereas the middle part displays as shallow environment with increased water depth as compared to bottom and upper part.
6. The interpretation of intraclasts measurement through microscope shows shallow marine depositional conditions.

REFERENCES

Abdüselamoğlu, M.S. (1963). Nouvelles observations stratigraphiques et paleontologiques sur les terrains Paléozoïques affleurment à l'Est du Bosphore. MTA Bulletin 60:1–7.

Adamia Shota, Guram Zakariadze, Tamar Chkhotua, Nino Sadradze, Nino Tsereteli, Aleksandre Chabukiani and Aleksandre Gventsadze. (2011). Geology of the Caucasus: a review.

Akman, A. Ü., 1992. Karadeniz çevresi havzalarının açılış mekanizmaları ve yaşı, KB Türkiye. 9. Petrol Kongresi bildiri özetleri kitabı, Hilton, Ankara Turkish.

Aksay, A. and Timur, E. 2002. 1/100.000 scaled geological maps of Turkey, Sheet Zonguldak-F29. General Directorate of Mineral Research and Exploration No. 30, Ankara; 20 pp.

Akyol, Z; Arpat, E; Erdögan, B; Göger, E. S; Aröglu, F Ş; Entürk, I; Tütüncü, K; and Uysal, Ş. 1974. Geologic Map of Turkey Quadrangle Series, Zonguldak E29a, E29b, E29c, E29d, Kastamonu. E30a, E30d. Mineral Research and Exploration Institute of Turkey, Ankara.

Allen, Philip A., Maria A. Mange-Rajetzky 1992. “Devonian-Carboniferous sedimentary evolution of the Clair area, offshore north-western UK: impact of changing provenance” Marine and Petroleum Geology, Volume 9, Issue 1, February 1992, Pages 29-52.

Arni, P. 1938. Information about the stratigraphy of the northern Anatolia coal basin and travelling with Prof. Jongman through Ereğli Zonguldak Amasra. Mineral Research and Exploration Institute of Turkey (MTA) Report No. 674, (Turkish).

Arni, P., 1940a. A short report on Amasra coal basin. Mineral Research and Exploration Institute of Turkey (MTA) Report No. 1315, (Turkish).

Arni, P., 1940b. First report on the result of well drilling No. 2 in Kilimli coal basin. Mineral Research and Exploration Institute of Turkey (MTA) Report No. 1141, (in Turkish).

Arni, P., 1940c. Report on the geology of Amasra coal basin and its value. Mineral Research and Exploration Institute of Turkey (MTA) Report No. 1266, (in Turkish).

Arni, P. 1940d. Survey in western part of the Zonguldak and Amasra coal basin and exploration of iron mine in Bartın Strait. Mineral Research and Exploration Institute of Turkey (MTA) Report No. 1113, (in Turkish).

Arni, P., 1941. Supply report on estimation and geology of the Amasra- Tarlağzı coal field. Mineral Research and Exploration Institute of Turkey (MTA) Report No. 1274, (in Turkish).

Arslan, İ., 1978. Report on “siferton” research in E.K.İ. Coal mines of Amasra carboniferous field. Mineral Research and Exploration Institute of Turkey (MTA) Report No. 6069, (in Turkish).

Aslanian, A. (ed) 1970. Geology of the USSR. Armenian SSR. Moscow, ‘Nedra’ XLIII, 1–464 (in Russian).

Aydın M, Serdar HS, Şahintürk O, Yazman M, Cokuğraş R, Demir O, Özcelik Y (1987). Camdağ (Sakarya) - Sunnicedağ (Bolu) yoresinin jeolojisi. Bull Geol Soc Turkey 30/1: 1–4 (in Turkish).

Azizbekov, SH. (ed) 1972. Geology of the USSR. Azerbaijanian SSR. Moscow, ‘Nedra’ XLVII, 1–520 (in Russian).

Baccelle, L. and Bosellini. A. (1965): Diagrammi per la stima visiva della composizione percentuale nelle rocce sedimentarie. – Annali della Università di Ferrara, Sezione IX, Science Geologiche e Paleontologiche, 1, 59-62.

Blackey, R. 2009 Regional Paleogeographic Maps: <https://www2.nau.edu/rcb7/publications.html>.

Bozkaya, Ö. Yalçın H, and Göncüoğlu M. C. 2012, Mineralogical evidences of a mid-Paleozoic tectono-thermal event in the Zonguldak terrane, northwest Turkey: implications for the dynamics of some Gondwana-derived terranes during the closure of the Rheic Ocean. *Can. J. Earth Sci.* 49: 559–575 (2012).

Bozkaya, Ö. -Türkmenoğlu A G, Göncüoğlu M. C, Ünlüce Ö, Yılmaz İ. Ö, Schroeder P. A. 2016. Illitization of Late Devonian-Early Carboniferous K-bentonites from Western Pontides, NW Turkey: Implications for their origin and age. *Applied Clay science*, 2016: <http://dx.doi.org/10.1016/j.clay.2016.08.020>.

Boztuğ, D. and Yılmaz, O. 1995. Metamorphism and geological evolution of the Daday-evrekani massif, Kastamonu region, Western Pontides, Northern Turkey. *Geol. Bull. Turkey*, 38, 33-58.

Bulut, M.; Özdemir, M.; Altıparmak, S.; Bozkutr, H. E. 1982. Geology of Bartın-Amasra coal basin. Mineral Research and Exploration Institute of Turkey. (MTA) Report No. 7201, (Turkish).

Bulut, M.; Özdemir, M.; Altıparmak S. 1992. Geological report on Bartın-Amasra coal basin. Mineral Research and Exploration Institute of Turkey (MTA) Report No. 9659, (in Turkish).

Burger K., Friedrich K. B , Bieg G. 2000. Pyroclastic kaolin coal-tonsteins of the Upper Carboniferous of Zonguldak and Amasra, Turkey *International Journal of Coal Geology* 45 (2000) 39–53.

Caplan M. L. 1, R. Mark Bustin, 1999. Devonian–Carboniferous Hangenberg mass extinction event, widespread organic-rich mudrock and anoxia: causes and consequences Received 8 August 1997; revised version received 4 September 1998; accepted 26 October 1998.

Chafetz, H. S. (1986). Marine peloids: A product of bacterially induced precipitation of calcite. *J. Sediment. Petrol* 56, 812-817.

Chen, F., Siebel, W., Satır, M., Terzioglu, M. N. 2002. Geochronology of the Karadere basement (NW Turkey) and implications for the geological evolution of the Istanbul zone. *International Journal Earth Sciences*, 91; 469—481.

Colley, S., Wilson, T.R.S. and Higgs, N.C., 1984. Post-depositional migration of elements during diagenesis in brown clay and turbidity sequences in the North East Atlantic. *Geochimica et Cosmochimica Acta*, Vol. 48, pp. 1223-1235.

Dachev C., Stanev V. & Bokov P. (1988) Structure of the Bulgarian – Black sea area. – *Boll. Geofis. Teor. Applicata*, 30, 79-107pp.

Dean, W. T., Martin, F., Monod, O. 1993. Report on Field Programme with Turkish Petroleum Company in Northern and Southern Turkey (1990 -1992). Turkish Petroleum Corporation (TPAO) unpublished Report.

Dean, W. T., Martin, F., Monod, O., Demir, O., Rickards, R. B., Bultynck, P. and Bozdoğan, N. 1997. Lower Paleozoic stratigraphy, Karadere-Zirze area, central Pontides, northern Turkey. In: Göncüoğlu M. C. and Derman A. S. (Eds.): Early Paleozoic evolution in NW Gondwana. IGCP Project No. 351, II. International Meeting, November 5-11, 1995, Ankara, Turkey. *Spec. Publ. Turkish Assoc. Petrol. Geol.*, Ankara, 3, 32-38.

Dean, W. T., Monod, O., Rickards, R. B., Demir, O., and Bultynck, P. 2000. Lower Paleozoic Stratigraphy and Paleontology, Karadere-Zirze area. Pontus Mountains, northern Turkey. *Geol. Mag.*, 137, 555-582.

Denayer, J. 2014. Viséan Lithostrotonidae (Rugosa) from Zonguldak and Bartın (NW Turkey). *Bulletin of Geosciences* 89(4), 737–771 (19 figures, 1 table). Czech Geological Survey, Prague. ISSN 1214-1119.

Derman, S. 1990. Batı Karadeniz Bölgesinin Geç Jura-Erken Kretase evrimi. 8. Petrol Kongresi Proceedings, 328-339.

Derman, A., S. Alis ,An, C. & Özçelik, Y. 1995.Himmetpas ,A Formation: New Palynological ge Data And Significance. In Proceedings of The Internationalsymposium On The Geology Of The Black Sea Region (EdsA. Erler, T. Ercan, E. Bingöl, And S. Örçen), Pp. 99–104.General Directorate Of Mineral Research And Exploration And Chamber Of Geological Engineers, Ankara, Turkey.

Derman AS (1997). Sedimentary characteristics of Early Paleozoic rocks in the western Black Sea region, Turkey. In: Göncüoğlu MC, Derman AS, editors. Early Paleozoic Evolution in NW Gondwana. Ankara, Turkey: Turkish Association of Petroleum Geologists Special Publication 3, pp. 24–31.

Deveciler E. 1986. Geological report of Aladlı-Bartın-Cide (Western Black Sea). Mineral Research and Exploration Institute of Turkey (MTA) Report No. 7938, (in Turkish).

Dil N (1976). Assemblages caractéristiques de foraminifères du Devonien supérieur et du Dinantien de Turquie (Bassin Carbonifère de Zonguldak). *Annales de la Société Géologique de Belgique* 99: 373–400 (in French).

Dunham, J.B. and Olson, E.R., 1980. Shallow subsurface dolomitization of sub-tidally deposited carbonate sediments in the Hanson Creek Formation (Ordovician-Silurian) of Central Nevada: in Zenger, D.H., Dunham, J.B., and Ethington, R.L., eds., Concepts and models of dolomitization: Tulsa, Ok, SEPM Special Pub., Vol28: 139-161.

Dunham, R. J. (1962). Classification of carbonate rocks according to depositional texture. In: Ham, W. E. (ed.), Classification of carbonate rocks. *American Association of Petroleum Geologists Memoir*, 108-121.

Eğemen, R., and Pekmezciler, S. 1945. Geological report on formation of Amasra coal. Mineral Research and Exploration Institute of Turkey (MTA) Report No. 1636, (Turkish).

Embry, A. F., & Klovan, J. E. (1971). A Late Devonian reef tract on Northeastern Banks Island, NWT. *Canadian Petroleum Geology Bulletin*, v. 19, 730-781.

Erdoğan, D. 1963. Report on the natural gas observed in Budurga village, Ulus, Zonguldak. Mineral Research and Exploration Institute of Turkey (MTA) Report No. 3221, (in Turkish).

Erdoğan B., Güngör T. & Özer S. 1990: Stratigraphy of the Karaburun Peninsula. Bull. Min. Res. Exp. 111, 1—20 (in Turkish).

Flügel, E., Haditsch, J.G. (1975): Vorkommen hochreiner und reiner Kalke im Steirischen Salzkammergut. – *Archiv für Lagerstättenforschung*, 15, 65-84.

Flügel, E., 1982, *Microfacies Analysis of limestones*: pp.633, Springer-Verlag, Berlin.

Flügel, E. 2004. *Microfacies of carbonate rocks: analysis, interpretation and application*. Springer-Verlag. 976 pp.

Folk, R. L. (1959). Practical petrographic classification of limestones: *American Association of Petroleum Geologists Bulletin*, v. 43, 1-38.

Folk, R.L. (1962). Spectral subdivision of limestone types, in Ham, W.E.,ed., *Classification of Carbonate Rocks-A Symposium: American Association of Petroleum Geologists Memoir*, 1, 62-84.

Folk, R.L. and Land, L.S., 1975, Mg/Ca ratio and salinity: Two controls over crystallization of dolomite: Amer. Assoc. of Petrol. Geol. Bull., 59, 60-68.

Fratschner, W. T. 1952. The first report on the geological studies of Amasra-Bartın-Kumluca and Kurucaşile-Ulus regions performed between 19 May-24 November. Mineral Research and Exploration Institute of Turkey (MTA) Report No. 1960, (in Turkish).

Friedman, G.M. (1965): Terminology of recrystallization textures and fabrics in sedimentary rocks. – J. Sed. Petrol., 35, 643-655.

Garetskiy, R.G., (1970) . – On the basement of the Moesic Plate - Geo, 4, 272-277.

Gedik, A. & Korkmaz, S. (1984). Sinop havzasının jeolojisi ve petrol olanakları. Geological Engineering (in Turkish with English abstract), 19, 53-79.

Gedik, I. and önalın, M. 2001. New observations on the Paleozoic stratigraphy of Çamdağ (Sakarya Province). *Yerbilimleri*, **14**, 61–76.

Geological Society of America Rock-Color Chart Committee, 2009, “The Geological Rock color chart (GSA, 2009): <http://www.geosociety.org/index.htm>.

Göncüođlu, M. C., 1997. Distribution of Lower Paleozoic units in the Alpine Terranes of Turkey. Paleogeographic constrains. In: Göncüođlu, M. C. and Derman, A. S. (Eds.): Lower Paleozoic evolution in northwest Gondwana. Turkish Assoc. Petrol. Geol., Spec. Publ., Ankara 3, 13—24.

Göncüođlu, M.C. and Kozur, H.W. 1998, Facial development and thermal alteration of Silurian rocks in Turkey. *Temas Geologico – Mineros, ITGE*, 23, 87–90.

Göncüođlu, M.C. and Kozur, H.W. 1999. Remarks on the Pre-Variscan Development in Turkey. In: Linnemann U., Heuse T., Fatka O., Kraft P., Brocke,R. and Erdtmann,

B.T. (eds), Pre -Variscan Terrane Analyses of“Gondwanean Europa”. Schriften des Staatlichen Museums für Mineralogie und Geologie Dresden, 9, 137–138.

Göncüoğlu, M. C., Boncheva, I., Gedik, I., Lakova, I., Sachanski, V., Saydam, G., Okuyucu, C., Özgül, N. and Yanev, S. 2005b: Perigondwana versus Laurussian Origin of the NW Anatolian Paleozoic Terranes: A correlation of Mid-Paleozoic Events in Istanbul and Zonguldak. International Workshop Depositional Environments of the Gondwanan and Laurasian Devonian. Abstracts and field trip guidebooks. 15—16.

Göncüoğlu, M. C. S. Yanev , I. Gedik , I. Lakova , I. Boncheva L, V. Sachanskp, C. Okuyucu, N. Ozgul , E. Timur , Y. Maliakov & G. Saydam.2006. Stratigraphy, correlations and palaeogeography of Palaeozoic terranes of Bulgaria and NW Turkey: a review of recent data. Tectonic Development of the Eastern Mediterranean Region. Geological Society, London, Special Publications, 260, 5147.

Göncüoğlu, M. C., 2010. Introduction to the Geology of Turkey: Geodynamic Evolution of the Pre Alpine and Alpine Terranes. General Directorate and Mineral Research and Exploration, MTA, 66 p.

Göncüoğlu, M.C. Valeri Sachanski, Mehmet, Iskra Lakova, Iliana Boncheva & Gülnur Saydam Demiray, 2011. Silurian Graptolite, Conodont and Cryptospore Biostratigraphy of the Gülüç Section in Ereğli, Zonguldak Terrane, NW Anatolia, Turkey.

Göncüoğlu, M. C., Valeri Sachanski, Juan Carlos Gutierrez-Marco and Cengiz Okuyucu 2014. Ordovician graptolites from the basal part of the Paleozoic transgressive sequence in the Karadere area, Zonguldak Terrane, NW Turkey. Estonian Journal of Earth Sciences, 2014, 63, 4, 227–232 doi: 10.3176/earth.2014.23.

Görür, N., Monod, O., Okay, A. I., Sengör, A. M. C., Tüysüz, O., Yigitbas, E., Sakinc, M. and Akkök, R., 1997. Paleogeographic and tectonic position of the Carboniferous rocks of the western Pontides (Turkey) in the frame of the Variscan belt. Bull. Soc. Géol. France 168, 197-205.

Gregg, J.M. and Sibley D.F., 1984. Epigenetic dolomitization and the origin of Xenotopic dolomite texture. *Journ. Sedim. Petrol.*, Vol54: 908-931.

Gürdal, G., Yalçın, M.N., 1995. An investigation of factors controlling gas adsorption in coals of the Zonguldak Basin, NW Turkey. *Organic Geochemistry: Development and Applications to Energy, Climate, Environment and Human History, Selected Papers from the 17th International Meeting on Organic Geochemistry, Donostia – San Sebastian, The Basque Country, Spain, September*, 1104–1107.

Gürdal G., 1998. Zonguldak havzası kömürlerinde gaz depolanmasını kontrol eden parametreler (The controlling parameters of gas storage in coals of the Zonguldak basin). Unpublished PhD, thesis, Istanbul Technical University, Istanbul, 237 pp.

Gürdal, G., Yalçın, M.N., 2000. Gas adsorption capacity of Carboniferous coals in the Zonguldak Basin (NW Turkey) and its controlling factors. *Fuel* 79, 1913–1924.

Harput, B. O. , Demirel I. H. ,Karayigit A. I., Aydın. M. Şahintürk Ö . and Bustin R. M. 1999 Preliminary Hydrocarbon Source Rock Assessment of the Paleozoic and Mesozoic Formations of the Western Black Sea Region of Turkey. 21:10, 945-956, DOI: 10.1080/00908319950014317.

Hennebert, M., and Lees, A., 1985, Optimized similarity matrices applied to the study of carbonate rocks: *Geological Journal*, v. 20, p. 123–131.

Höll R. 1966: Genese und Altersstellung von Vorkommen der SbW-Hg Formation in der Türkei und auf Chios-Griechenland. *Bayer. Acad. Wiss. Math., Naturwiss. Kl., Abh.* 127, 118.

Hoşgörmez Hakan 2007, Origin and secondary alteration of coalbed and adjacent rock gases in the Zonguldak Basin, western Black Sea Turkey. *Geochemical Journal*, Vol. 41, pp. 201 to 211, 2007.

Johnson, J.G. Klapper, G. and Sandberg, C.A. 1985. Devonian Eustatic fluctuations in Euramerica. Geol. Soc. Am. Bull. 96, 567-587, Boulder.

Karayigit, A.I ., Gayer, R.A., Demirel, I .H., 1998. Coal and rank and petrography of Upper Carboniferous coal seams in the Amasra coalfield, Turkey. Int. J. Coal Geol. 36, 277–294.

Kaya, O., 1973, The Devonian and Lower Carboniferous stratigraphy of the İstinye, Bostancı and Büyükada subareas: In Kaya, O., ed., Paleozoic of İstanbul: Ege Üniv. Fen Fak., Kitaplar Ser., 40,1 -36.

Kaya. O. and Rudolf Birenheide 1988, contribution to the stratigraphy of the middle Devonian in the surroundings of Adapazarı, northwest Turkey.

Kaya O. and Rezsü U. 2000: Mesozoic and Paleozoic stratigraphic-structural entities of the Karaburun Peninsula, Western Turkey. Int. Earth Sci. Colloquium on the Aegean Region (IESCA) 2000, Izmir—Turkey, 15.

Ketin, I and O ve Gümüs, 1963 Sinop –Ayancik guneyinde ucuncu bolgeye dahil sahaların jeolojisi hakkında rapor, II. Kisim Jura ve kretase formations etudu, Turkish Petroleum Company Report 288. Unpublished.

Ketin I., 1983, A General view of Geology of Turkey: Istanbul Technical University Library. Numb. : 1250, 591p (In Turkish).

Kerey I.E. (1984). Facies and tectonic setting of the Upper Carboniferous rocks of NW Turkey. In: Robertson AHF, Dixon J, editors. The Geological Evolution of the Eastern Mediterranean. Oxford, UK: Blackwell Scientific, pp. 123–128.

Kipman, E., 1974, Sakarya Çamdağ deniz çökeltisi demir cevherinin jeolojisi: İstanbul Üniv. Fen Fak. Monogr, 25, 1 - 72. (Turkish).

Kostka, A., 1993. The age and microfacies of the Maruszyna Succession (Upper Cretaceous-Paleogene), Pieniny Klippen Belt, Carpathians, Poland, *Studia Geologica Polonica*, Vol. 102, pp. 7-134.

Langbein, R., Peter, H., Schwahn, H.J. (1982): *Karbonat- und Sulfatgesteine. Kalkstein-Dolomit-Magnesit-Gips-Anhydrit. – Nutzbare Gesteine und Industrieminerale*, Monographienreihe, 5, 335 pp.

Lucius, M. 1926. Report on my investigation trip, made along the coasts from Zonguldak to İnebolu. Mineral Research and Exploration Institute of Turkey (MTA) Report No. 14, (in Turkish).

Lucius, M. 1931. Geological research on Karadeniz coal field. Mineral Research and Exploration Institute of Turkey (MTA) Report No. 1, (in Turkish).

MacIntyre, I. G. (1985). Submarine cements- the peloidal question. *Spec. Publ.--Soc. Econ. Paleontol. Mineral* 36, 109-116.

Mann, U., Hertle, M., Horsfield, B., Radke, M., Schenk, H.J., Yalçın, M.N., 1995. Petrographical, organic–chemical and Petrophysical characterization of Upper Carboniferous coals from well K20/G, Zonguldak Basin, NW Turkey. In: Yalçın, M.N., Gürdal, G. (Eds.), *Zonguldak Basin Research Wells-I: Kozlu K20/G*. Special Publication of TUBITAK, Marmara Research Centre, Gebze, Turkey, pp. 133–165.

McCarthy Kelvin, Katherine Rojas, Martin Niemann, Daniel Palmowski, Kenneth Peters and Artur Stankiewicz. 2011. *Basic Petroleum Geochemistry for source rock evaluation*.

Menning M., A.S. Alekseev, B.I. Chuvashov, V.I. Davydov , F.-X. Devuyst, H.C. Forke , T.A. Grunt, L. Hance, P.H. Heckel, N.G. Izokh , Y.-G. Jin, P.J. Jones, G.V. Kotlyar, H.W. Kozur, T.I. Nemyrovska, J.W. Schneider, X.-D. Wang, K. Weddige, D. Weyer, D.M. Work. 2006 “Global time scale and regional stratigraphic reference scales of Central and West Europe, East Europe, Tethys, South China, and North

America as used in the Devonian–Carboniferous–Permian Correlation Chart 2003 (DCP 2003) Elsevier. *Palaeogeography, Palaeoclimatology, Palaeoecology* 240 (2006) 318–372.

Moore, C.H., 2001, Carbonate reservoirs porosity evolution and diagenesis in a sequence stratigraphic framework: Elsevier, Amsterdam. 444 p.

Mount, J. (1985): Mixed siliciclastic and carbonate sediments: a proposed first-order textural and compositional classification. – *Sedimentology*, 32, 435-442.

Nejdi, Ü. Karakullukçu T. 1994a. Mining geology report of the “siferton” field number Ö.İ.R.:2510 around Gömü, Bartın, Zonguldak. Mineral Research and Exploration Institute of Turkey (MTA) Report No. 9750, (Turkish).

Nejdi, Ü. Karakullukçu T. 1994b. Mining geology report of the “siferton” field number Ö.İ.R.:2516 around Kazpınar, Bartın, Zonguldak. Mineral Research and Exploration Institute of Turkey (MTA) Report No. 9757, (in Turkish).

Nekir, G., Hökelekli, E., Bulut, M., Üçer, A. 1996. Geological and geophysical report (magnetic study of CSAMT) on coal explorations in Bartın- Kurucaşile and Gegen-Arit regions. Mineral Research and Exploration Institute of Turkey (MTA) Report No. 9980, (Turkish).

Oates, J.A.H. (1998): Lime and limestone. Chemistry and technology. Production and uses. – 455 pp., Weinheim (Wiley-VCH).

Okay, A.I. 1989. Tectonic units and sutures in the Pontides, northern Turkey. In: *Tectonic Evolution of the Tethyan Region* (Ed. A.M.C. Şengör), NATO Advanced ASI Series, Kluwer Academic Publications, Dordrecht, 109- 116.

Okuyucu C., Djenchuraeva A.V., Neyevin A.V., Saydam G.D.,Çakôrsoy Ö.B., Vorabiev.T,Çörekçioçlu E. & Ekmekçi E.2005: The biostratigraphic correlation of Paleozoic succession in Krygzhistan and Turkey. *MTA Report* 10746, 1—94.

Özgül N. 2011. Stratigraphy and Some Structural Features of the İstanbul Paleozoic, Turkish Journal of Earth Sciences (Turkish J. Earth Sci.), Vol. 21, 2012, p. 817–866. doi:10.3906/yer-1111-6. First published online 29 December 2011.

Passega, R. (1964): Grain size representation by CM patterns as a geological tool. – J. Sed. Petrol., 34, 830-847.

Pettijohn, F. J., 1957. Sedimentary Rocks [2nd ed.]: New York, John Willey & Sons. 718.

Pettijohn, F. J., Potter, P. E. and Siever, R., 1972. Sand and Sandstones. Springer-Verlag, New York.

Pettijohn, F. J., 1975. Sedimentary Rocks, 3rd Edition, Harper and Row, New York.

Picard, M. 1971. Classification of fine grained sedimentary rock: Journal of Sedimentary Petrology, Vol. 41, p. 179-195.

Potter, P.E., J.B. Maynard, and P.J. Depetris, 2005. Mud and mudstones introduction and overview: New York, Springer Berlin Heidelberg, p. 297.

Pince A. 1982. Report on the shallow seismic study of Karadeniz Amasra Karapınar village. Mineral Research and Exploration Institute of Turkey (MTA) Report No. 7250, (in Turkish).

Pohl. 1903. Notes on the field trip, in April 1903 of Ereğli company coal mines. Mineral Research and Exploration Institute of Turkey (MTA) Report No. 10, (in Turkish).

Randazzo, A.F., Zachos, N.G. (1983): Classification and description of dolomitic fabrics of rocks from Floran aquifer, U.S.A. – Sedimentary Geology, 37,151-162.

Rustamov, M. 2005. South Caspian Basin-Geodynamic Events and Processes. Baki, Institute of Geology NASA, 1–345 (in Russian).

Sachanski, V., Tenchov, Y. 1993. Lithostratigraphic subdivision of the Silurian deposits in the Svoje anticline. — Rev. Bulg. geol. Soc., 54, 1; 71—81.

Sachanski, V. 1994. Age assessment of the Cerecel and Sirman Formation in Sofia Stara Planina Mountain (Ordovician, Ashgill). — Rev. Bulg. geol. Soc., 55, 2; 83—90.

Saner, S., Siyako, S., Aksoy, Z., Bürkan, k.A. and demir, o. 1980. Geology and petroleum possibilities of Zonguldak region. TPAO, report No: 1021, 79 pp. [unpublished].

Saner, S.; Taner, İ.; Aksoy, Z.; Siyako, M. & Burkan, K. (1980). Safranbolu havzasının jeolojik yapısı ve Tersiyer paleocoğrafyası. *Türkiye 5. Petrol Kong.* 111-122.

Scotese A. M., Ziegler, C. R., McKerrow, W. S., Johnson, M. E., & Bambach, R. K. 1990. Paleozoic Paleogeography,. Journal: Annual Review of Earth and Planetary Sciences, Vol. 7, p, 473.

Selley R.C. 2001. Applied Sedimentology, 2nd Edition. Elsevier. 524pp.

Sibley, D.F., 1982. The origin of common dolomite fabrics. Journ. Sedim. Petrol., Vol 52: 1987-1100.

Sibley, D.F. and Gregg, J.M., 1987. Classification of dolomite rock textures. Journ. Sedim. Petrol., Vol 57: 967-975.

Sibley, D.F., 2003. Dolomite textures. In: Middleton, G.M., Church, M.J., Coniglio, M., Hardie, I.A. and Longstaffe, F.S. (eds.). Encyclopedia of sediments and sedimentary rocks. Kluwer, Dordrecht, 231-234.

Stanissopoulos, S. 1898. Report on the Kilimli mine numbered 226 of the Ereğli coal basin. Mineral Research and Exploration Institute of Turkey (MTA) Report No. 8, (Turkish).

Strohmenger, C., Wirsing, G. (1991): A proposed extension of Folk's textural classification of carbonate rocks. – Carbonates and Evaporites, 6, 23-28.

Şengör, A. M. C and Yılmaz, Y 1981 'Tethyan Evolution of Turkey: A Plate Tectonic Approach' Tectonophysics, 75 (1981) 181-241.

Taşman, C. E. 1981. Probability of petroleum in Bartın. Mineral Research and Exploration Institute of Turkey (MTA) Report No. 699, (Turkish).

Taylor, A.M. and Goldring, R., 1993. Description and analysis of bioturbation and ichno fabric. Journal of the Geological Society of London, v. 150, p. 141-148.

Thomson, J., Colley, S., Higgs, N.C., Hydes, D.J., Wilson, T.R.S., Sorensen, J., 1987. Geochemical oxidation trends in NE Atlantic distal turbidites and their effects in the sedimentary record. In: Weaver, P.P.E., Thomson, J. (Eds.), Geology and Geochemistry of Abyssal Plains. Geological Society, London, Special Publication, Vol. 31, pp. 167-177.

Tissot B. P and D. H. Welte. 1984. Petroleum Formation and occurrence. Springer-Verlag Berlin Heidelberg, New York, Tokyo 1984.

Tokay, M. 1954. Report on the geology of Filyos river mouth-Amasra Bartın-Kozcağız-Çaycuma region. Mineral Research and Exploration Institute of Turkey (MTA) Report No. 2099, (in Turkish).

Tucker M. E. and Spence G. H., 1999. Modeling carbonate microfacies in the context of high-frequency dynamic relative sea-level and environmental changes. Journal of Sedimentary Research, vol. 69, no. 4, July, 1999, p. 947–961.

Türkmenoğlu Asuman Günal-, Ömer Bozkaya, M. Cemal Göncüoğlu, Özge Ünlüce, İsmail Ömer Yılmaz, Cengiz Okuyucu, 2015. Clay mineralogy, chemistry, and diagenesis of Late Devonian K-bentonite occurrences in northwestern Turkey: <http://journals.tubitak.gov.tr/earth/issues/yer-15-24-3/yer-24-3-1-1501-14.pdf>.

Tüysüz, O., 1993, Karadeniz'den Orta Anadolu'ya bir Jeotravers: Kuzey Neo-Tetisin Tektonik evrimi. TPJD Bülteni, 5/1, 1-33.

Tüysüz, O. 1999. Geology of the Cretaceous sedimentary basins of the Western Pontides. Geological Journal. Geol. J. 34: 75-93 (1999).

Tüysüz, Okan. and Sunal Gürsel.,2002. Palaeostress analysis of Tertiary post-collisional structures in the Western Pontides, northern Turkey. Geol. Mag. 139 (3), 2002, pp. 343–359.

Ünlüce, Özge M. Sc., Department of Geological Engineering, Supervisor: Prof. Dr. Asuman Günal Türkmenoğlu, January 2013, 80 pages Thesis.

Walliser, O.H., 1984a. Pleading for a natural D=C boundary. Cour. Forsch. Senckenb. 67, 241–246.

Walliser, O.H., 1996a. Patterns and causes of global events. In: Walliser, O.H. (Ed.), Global Events and Event Stratigraphy in the Phanerozoic. Springer, Berlin, pp. 7–19.

Walliser, O.H., 1996b. Global events in the Devonian and Carboniferous. In: Walliser, O.H. (Ed.), Global Events and Event Stratigraphy in the Phanerozoic. Springer, Berlin, pp. 225– 250.

Wedding, H., 1968, Amasra – Cide -Ülüs Bölgesindeki Karbon gaz etüdüleri, 1. Mevren ve Arıtdere / Karbon gaz studien im Raume Amasra – Cide - Ülüs. 1. Mevren und Arıtdere, 1 c, 2h .27cm: Unpublished. MTA Report 4004.

Wedding, H., 1969, Amasra – Cide Ülüs Bölgesinde Karbon gaz etüdleri , ümit verici sahanin bati Kenari / Karbon gaz studien im Raume Amasra – Cide - Ülüs Der Westrand des Hoffnungen gebeites 36.48 s. 1 harita , 1 Kesit, 27cm: Unpub. MTA Report 4280.

Wilson, J.L. (1975): Carbonate facies in geologic history. – 471 pp., Berlin (Springer).

Yalçın, M.N., 1991. Geology and coal occurrences of Zonguldak basin as a potential source for coal bed methane. Am. Assoc. Pet. Geol. Bull. 75, 697 (Abstract).

Yalçın, M.N Schenk, H.J., Schaefer, R.G., 1994. Modelling of gas generation in coals of the Zonguldak Basin (NW Turkey). Int. J. Coal Geol. 25, 195–212.

Yalçın, M.N., 1997. Role of basin modelling in coalbed methane resource assessment. Proceedings of the 1997 International Coalbed Methane Symposium. The University of Alabama, Tuscaloosa, AL, USA, pp. 357–364.

Yalçın, M.N, Gülbin G. 2001. Pore volume and surface area of the Carboniferous coals from the Zonguldak basin (NW Turkey) and their variations with rank and maceral composition. International Journal of Coal Geology 48 (2001) 133–144.

Yalçın, M.N., and Inan, S. 2001. Timing of the Generation and Expulsion of Oil from the Carboniferous Humic Coals of the Zonguldak Basin, NW Turkey. Proceedings of the 2nd International Symposium on the Petroleum Geology and Hydrocarbon Potential of the Black Sea Area. 22-24 September 1996, Şile- Istanbul-Turkey. Turkish Association of Petroleum Geologists Special Publication 4, p.133-147.

Yalçın, M.N and Yilmaz I, 2010. Devonian in Turkey – a review *Geologica Carpathica*, June 2010, 61, 3, 235—253.

Yanev, S. and Cassinis, G. 1998. Some remarks on the Late Paleozoic evolution of Bulgaria. *Permophiles*, 31, 25-31.

Yanev, S. 2000. Palaeozoic terranes of the Balkan Peninsula in the framework of Pangea assembly. *Palaeogeography, Palaeoclimatology, Palaeoecology*, 161, 151-177.

Yavuz, Y., Özdemir, M., Kır, N., and Alkılıç Ç. 2000. Coal presence of Bartın-Amasra (Bostanlar) coal field. Mineral Research and Exploration Institute of Turkey (MTA) Report No. 10414, (in Turkish).

Yeğin F. 1912. Report on the coal mine in the Ereğli basin-İlisu. Mineral Research and Exploration Institute of Turkey (MTA) Report No. 3, (Turkish).

Yiğitbaş E., Elmas A. and Yılmaz Y., 1999. Pre-Cenozoic tectono-stratigraphic components of the Western Pontides and their geological evolution. *Geological Journal. Geol. J.* 34: 55-77 (1999).

Yılmaz, İ. Ö. 2002. Applications of cyclostratigraphy and sequence stratigraphy in determination of the hierarchy in peritidal and pelagic successions (NW, SW and WNW of Turkey) by using sedimentology and sedimentary geochemistry (stable isotopes). Thesis (PhD), METU, Ankara.

Yılmaz Y., Tüysüz O., Yiğitbaş E., Genc S.C. and Şengör A.M.C. 1997. Geology and tectonic evolution of the Pontides. In: A.G. Robinson (ed). *Regional and petroleum geology of the Black Sea and surrounding region. Am. Assoc. Petrol. Geol. Memoir*, 68, 183-226.

Yılmaz, Y. and Şengör, A. M. C. 1985. Palaeo-Tethyan ophiolites in northern Turkey: Petrology and tectonic setting. *Ofioliti*, 10, 485-504. Ziglstra, G. 1950. Geology of İncüvez territory. Mineral Research and Exploration Institute of Turkey (MTA) Report No. 1937, (in Turkish).

Ziglstra, G. 1950. Geology of İncüvez territory. Mineral Research and Exploration Institute of Turkey (MTA) Report No. 1937, (in Turkish).

APPENDIX

PLATE 1

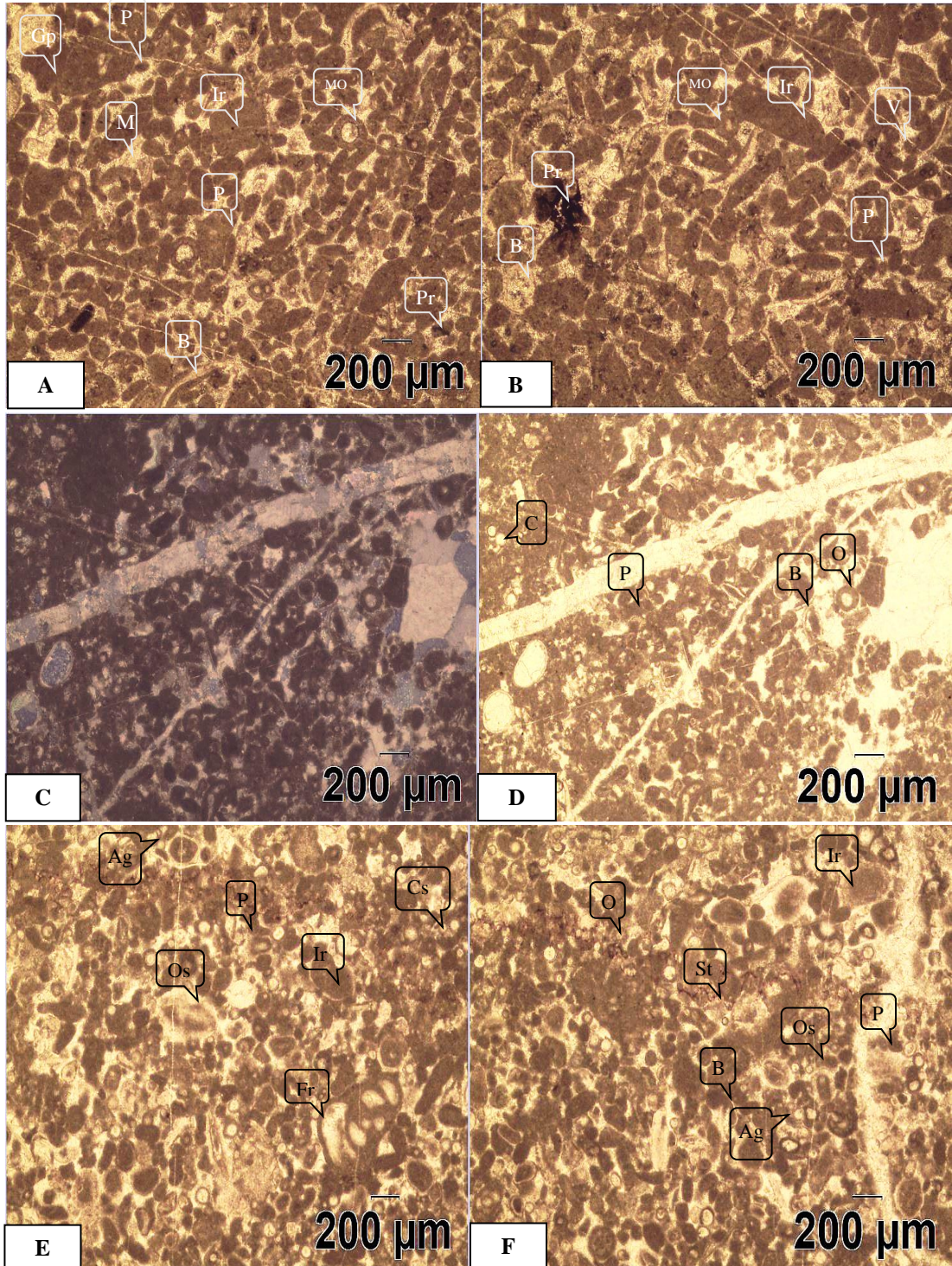


Plate 1: Figure A and B: Photomicrograph of peloidal grainstone sub-microfacies showing micritized ooids (MO), intraclast (Ir), peloid (P), bioclasts (B), grapestone (GP), microcrystalline vein (V) and sparry calcite cement (M) (PPL, GT/S 22).

Figure C and D: Photomicrograph of peloidal grainstone sub-microfacies displaying micritized laminated ooids (O), intraclast (Ir), peloid (P), bioclasts (B) and calcisphere (Cs) (XPPL & PPL, GT/S 30).

Figure E and F: Photomicrograph of peloidal grainstone sub-microfacies displaying peloid (P), aggregate grain (Ag), micritized laminated ooids (O), foraminifera (Fr), intraclast (Ir), bioclasts (B), ostracods (Os), calcisphere (Cs) and stylolite (St) (PPL, GT/S 42).

PLATE 2

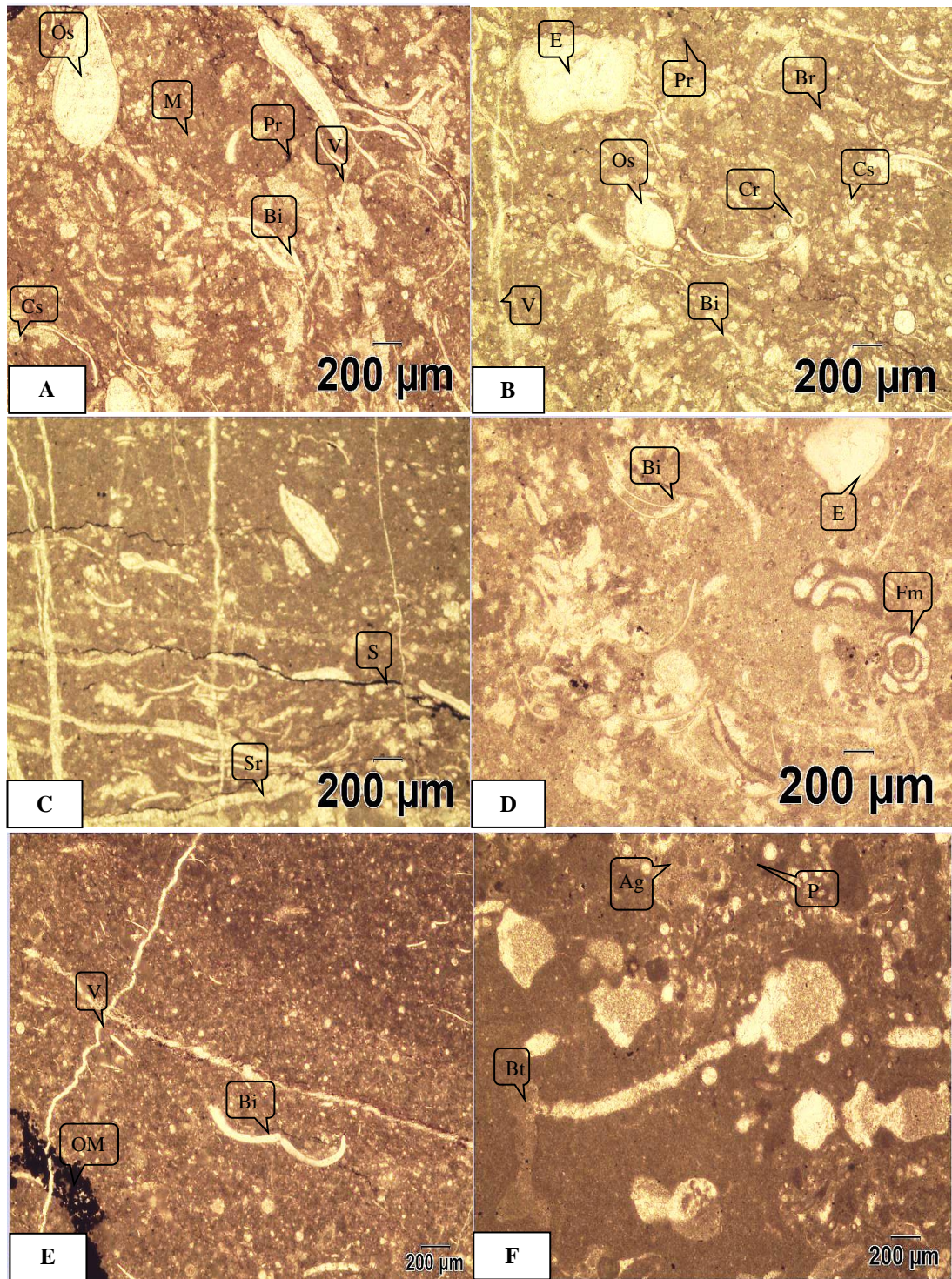


Plate 2: Figure A: Photomicrograph, of bioclastic packstone sub-microfacies showing partially sparite ostracods (Os), pyrite (Pr), bivalves (Bi), calcisphere (Cs), vein (V) and micrite matrix (M) (PPL, GT /S 4).

Figure B and C: Photomicrograph of bioclastic packstone sub-microfacies showing ostracods (Os), echinoderm (E), burrows (Br), charophyta (Cr), Pyrite (Pr), calcisphere (Cs) bivalves (Bi), calcite vein (V) and stylolite (S) (PPL, GT /S 21).

Figure D: Photomicrograph represent bioclastic packstone sub-microfacies showing foraminifers (Fm), echinoderm (E) and bivalves (Bi) (PPL, GT/S 50).

Figure E: Photomicrograph of bioclastic packstone sub-microfacies illustrating organic matter (OM), bivalves (Bi) and calcite vein (V). (PPL, GT/S 50).

Figure F: Photomicrograph of bioclastic packstone sub-microfacies showing aggregate grain (Ag), peloids (P) and bioturbation (Bt) (PPL, GT/S 64).

PLATE 3

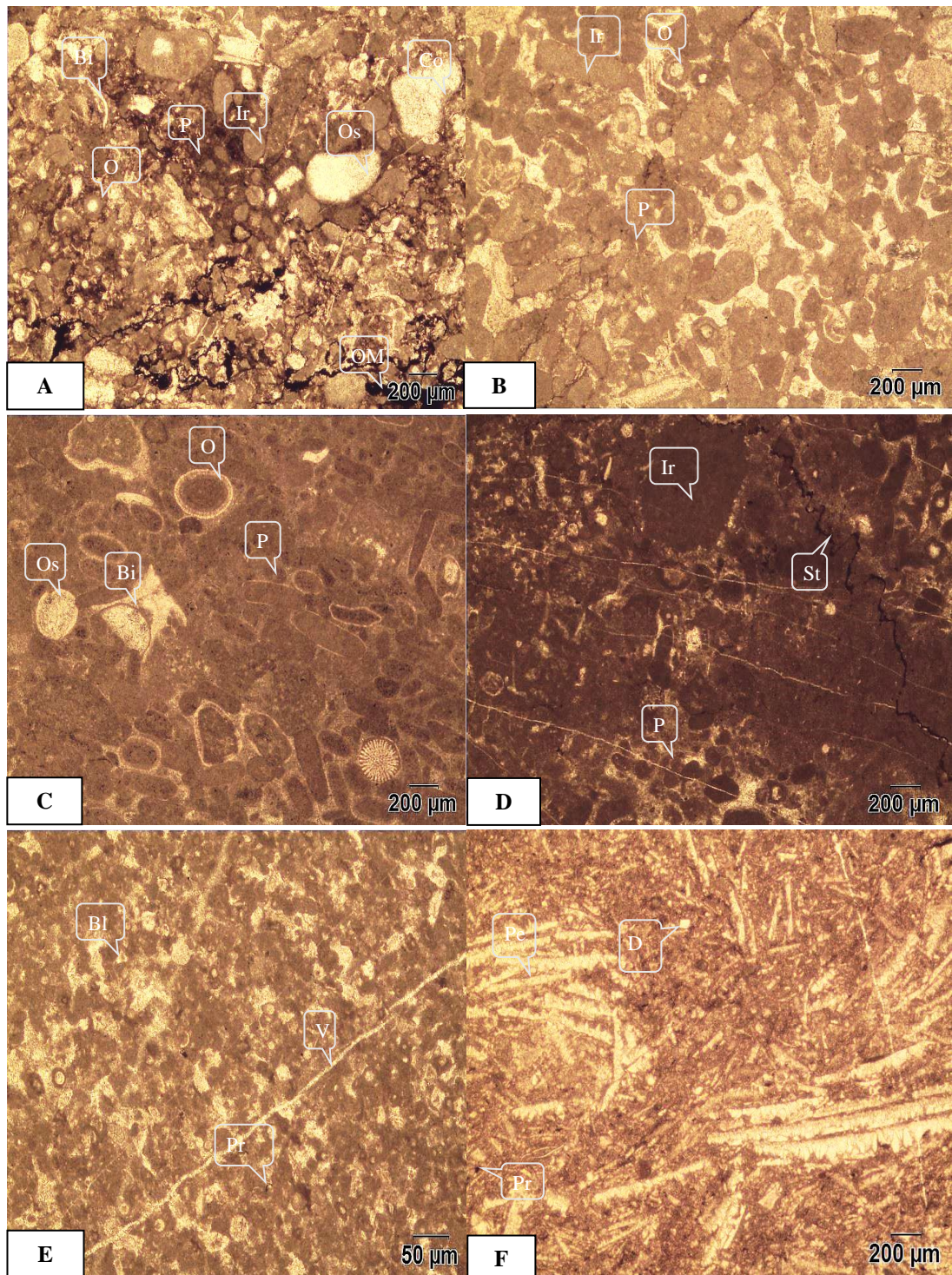


Plate 3: Figure A: Photomicrograph of intraclastic packstone showing intraclast (Ir), corals (Co), ostracods (Os), ooids (O), bivalves (Bi), peloids (P), and organic matter (OM) (PPL, GT /S 7).

Figure B: Photomicrograph of intraclastic packstone showing peloids (P), ooids (O) and intraclast (Ir) (PPL, GT /S 5).

Figure C: Photomicrograph of peloidal packstone sub-microfacies showing Peloids (P), Ooids (O), ostracods (Os) and bivalves (Bi) (PPL, GT/S 10).

Figure D: Photomicrograph of peloidal packstone showing peloids (P) bivalves (Bi), intraclast (Ir) and stylolite (St) (PPL, GT/S 25).

Figure E: Photomicrograph of peloidal packstone sub-microfacies showing bioclasts (Bi) pyrite (Pr) and calcite vein (V) (PPL, GT/S 32).

Figure F: Photomicrograph of bivalve packstone sub-microfacies showing bivalves (pelecypods, Pe), dolomite crystal (D) and pyrite (Pr) (PPL, GT/S 46).

PLATE 4

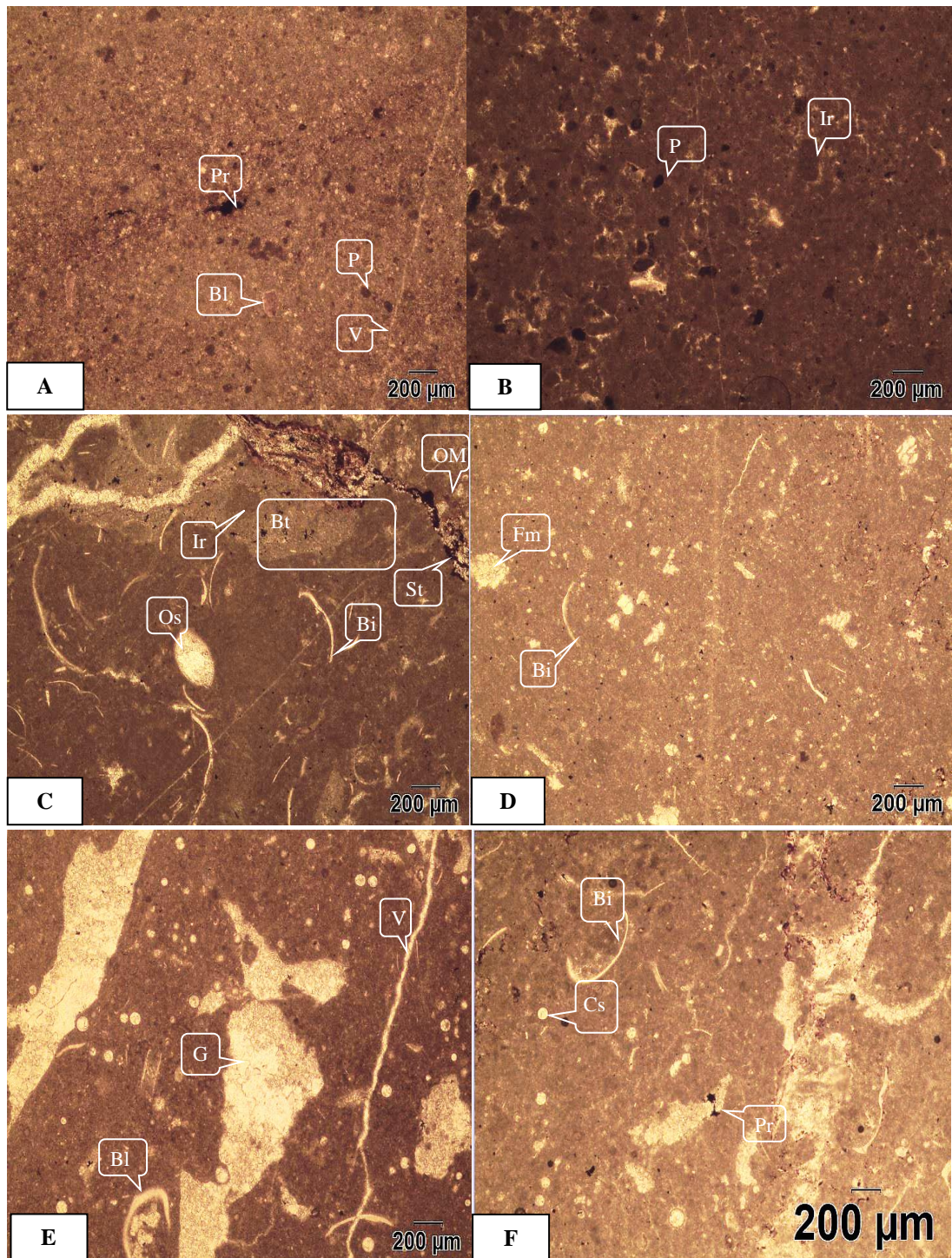


Plate 4: Figure A: Photomicrograph of peloidal wackestone showing bioclast (BI), peloids (P), pyrite (Pr) and calcite vein (V) (PPL, GT /S 44).

Figure B: Photomicrograph of peloidal wackestone showing peloids (P) and intraclast (Ir) (PPL, GT /S 65).

Figure C: Photomicrograph of bioclastic wackestone showing bivalve (Bi), ostracods (Os), organic matter (OM), stylolite (St), intraclast (Ir) and bioturbation (Bt) (PPL, GT/S 28).

Figure D: Photomicrograph of bioclastic wackestone sub-microfacies showing forams (Fm) and bivalves (Bi), (PPL, GT/S 60).

Figure E: Photomicrograph of bioclastic wackestone sub-microfacies showing gastropods (G), bivalve (Bi) and calcite vein (V) (PPL, GT/S 61).

Figure F: Photomicrograph of bioclastic wackestone showing Bivalve (Bi) calcisphere (Cs) and pyrite (Pr) (PPL, GT/S 63).

PLATE 5

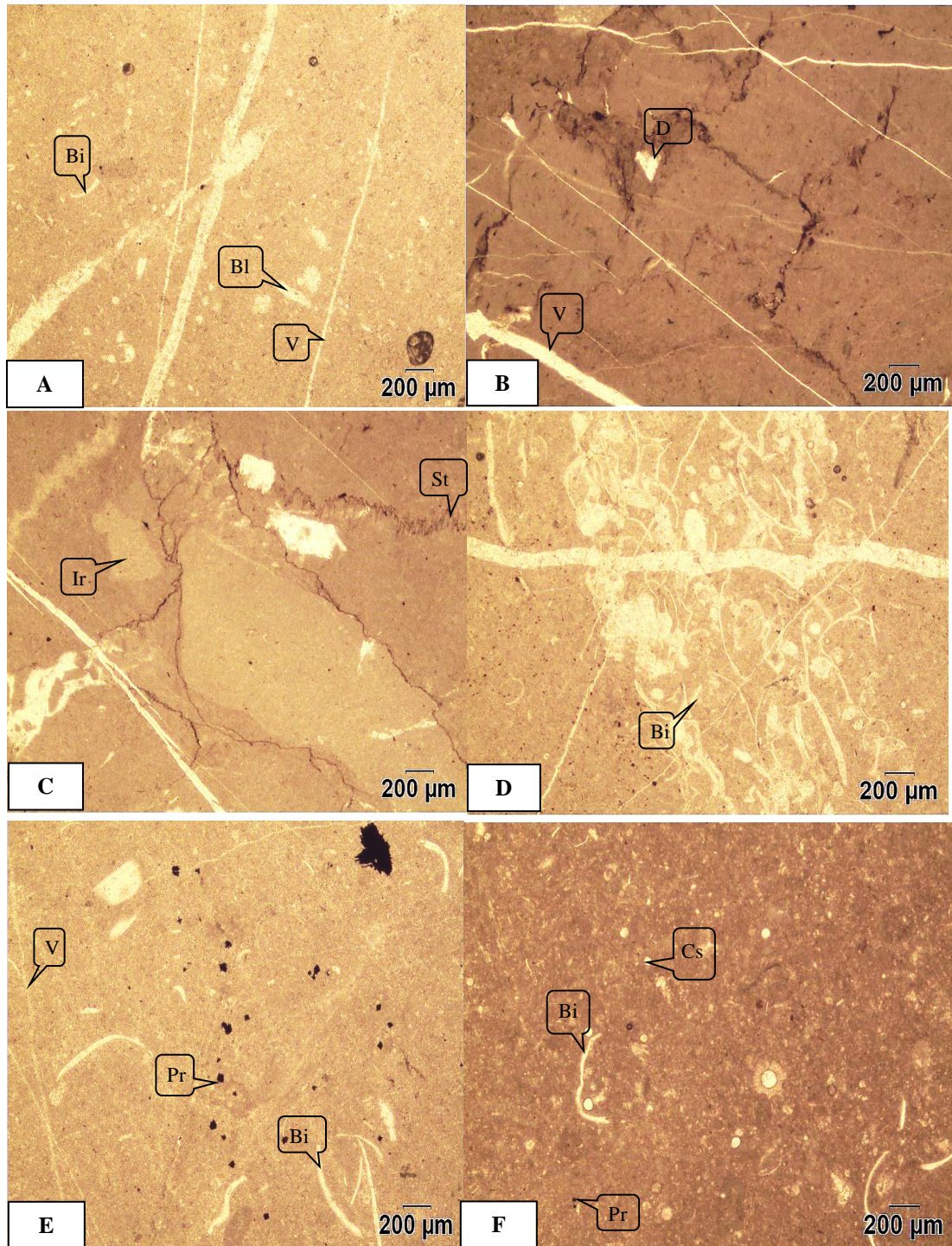


Plate 5: Figure A: Photomicrograph of wackstone showing intraclast (Ir), bivalve (Bi), peloids (P), intraclast (Ir) and calcite vein (V) (PPL, GT/S 11).

Figure B and C: Photomicrograph of brecciated lime mudstone displaying stylolaminated, rhombohedral crystal of dolomite (D), intraclast (Ir) and stylolite (St) (PPL, GT /S 20).

Figure D: Photomicrograph of wackstone displaying tempestite and bivalves (Bi), (PPL, GT/S 24).

Figure E: Photomicrograph of wackstone represents bivalve (Bi) pyrite (Pr) and calcite vein (V) (PPL, GT/S 61).

Figure F: Photomicrograph of wackstone represents bivalve (Bi) calcisphere (Cs) and pyrite (Pr) (PPL, GT/S 57).

PLATE 6

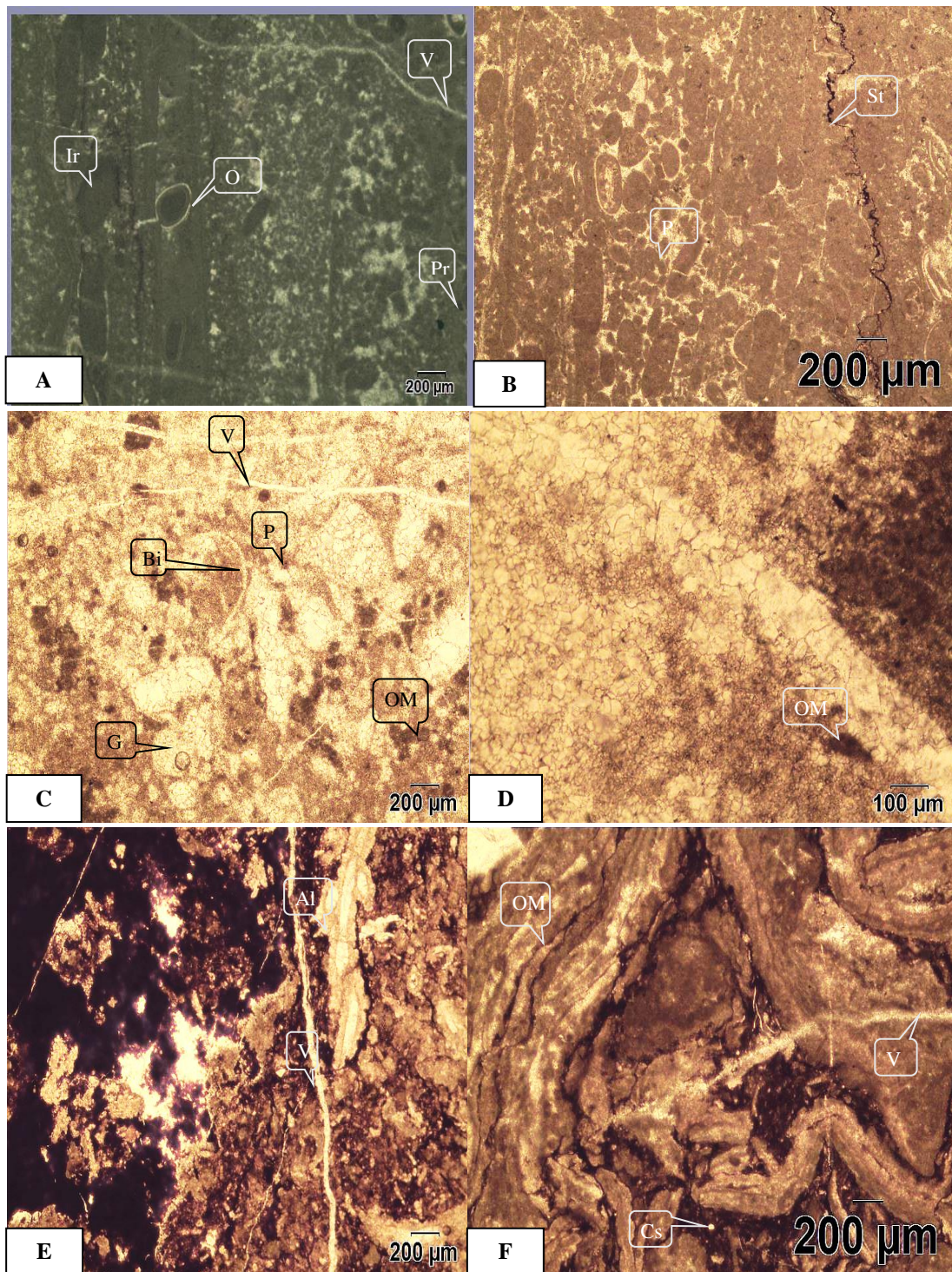


Plate 6: Figure A and B: Photomicrograph of bindstone displaying fine layer between peloidal layer .consist of intraclast (Ir), ooids (O), peloids (P), stylolite (St) and calcite vein (V) (PPL, GT /S 23).

Figure C and D: Photomicrograph of bindstone microfacies showing dolomitization of fossil fragment and lime mud matrix, peloids (P), gastropods (G), bivalves (Bi), organic matter (OM) and calcite vein (V) (PPL, GT/S 41).

Figure E: Photomicrograph, of stromatolite bindstone microfacies showing algae (Al), organic matter (OM) and calcite vein (V) (PPL, GT/S 47).

Figure F: Photomicrograph of displaying skeletal stromatolite bindstone having agglutinated fabric. calcisphere (Cs), organic matter (OM) and vein (V) (PPL, GT/S 48).

Plate 7

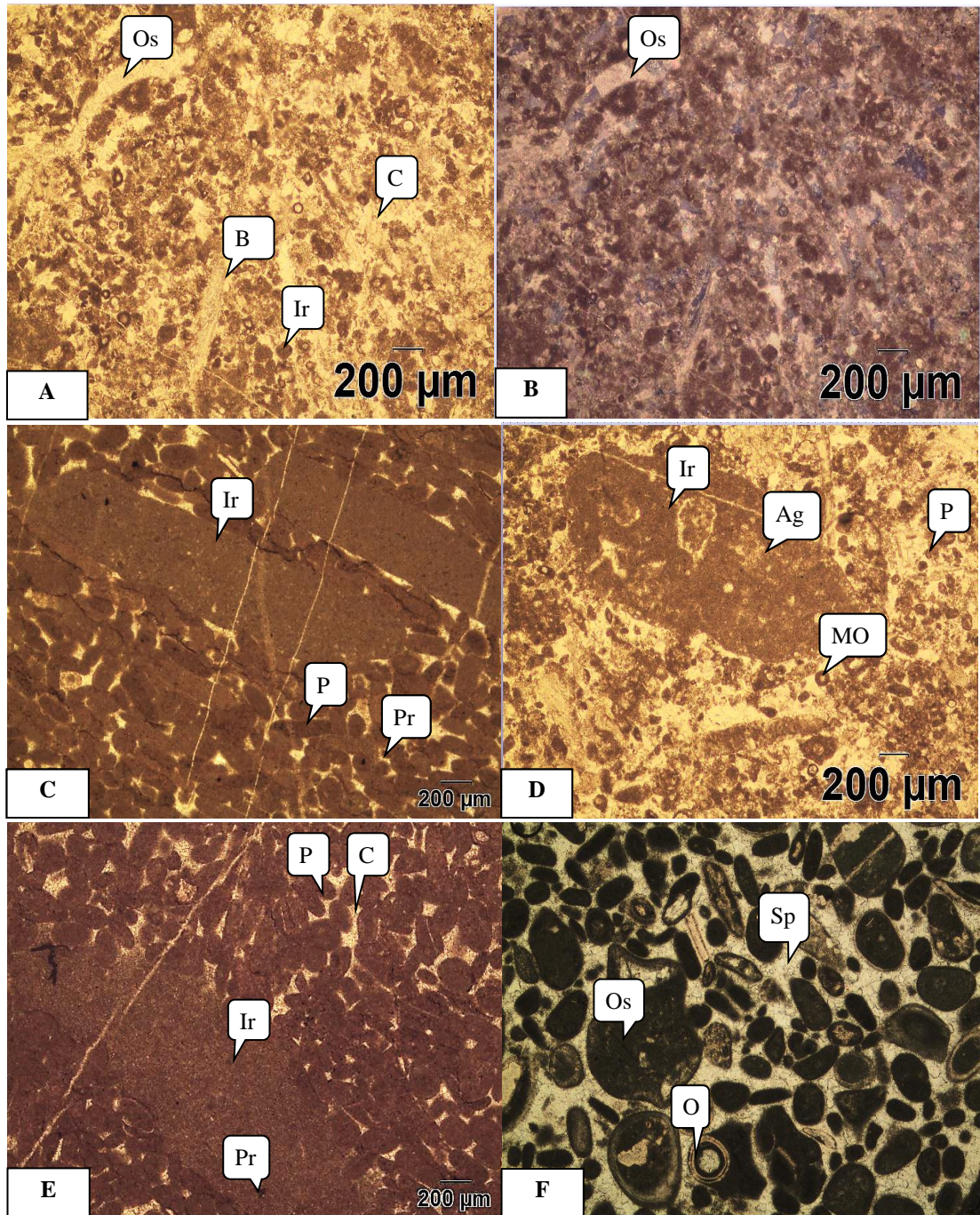


Plate 7: Figure A and B: Photomicrograph illustrating rudstone microfacies showing dark grey intraclast (Ir), bioclast (B) and calcite cement (C), ostracods (Os) (A, PPL, and B XPPL GT/S 54).

Figure C: Photomicrograph displays rudstone microfacies showing micritic intraclast (Ir), peloid (P) and pyrite (Pr) (PPL GT/S 9).

Figure D: Photomicrograph displaying rudstone microfacies showing intraclast (Ir), peloid (P) and micritic ooids (MO) and aggregate grain (Ag) (PPL GT/S 54).

Figure E: Photomicrograph of rudstone microfacies showing A. peloids (P), intraclast (Ir), pyrite (Pr) and calcite cement (C). (PPL, GT/S 6)

Figure F: Photomicrograph of rudstone showing laminated ooid (O), ostracods (Os), embedded in sparite cement (Sp) (PPL, GT/S 68).

PLATE 8

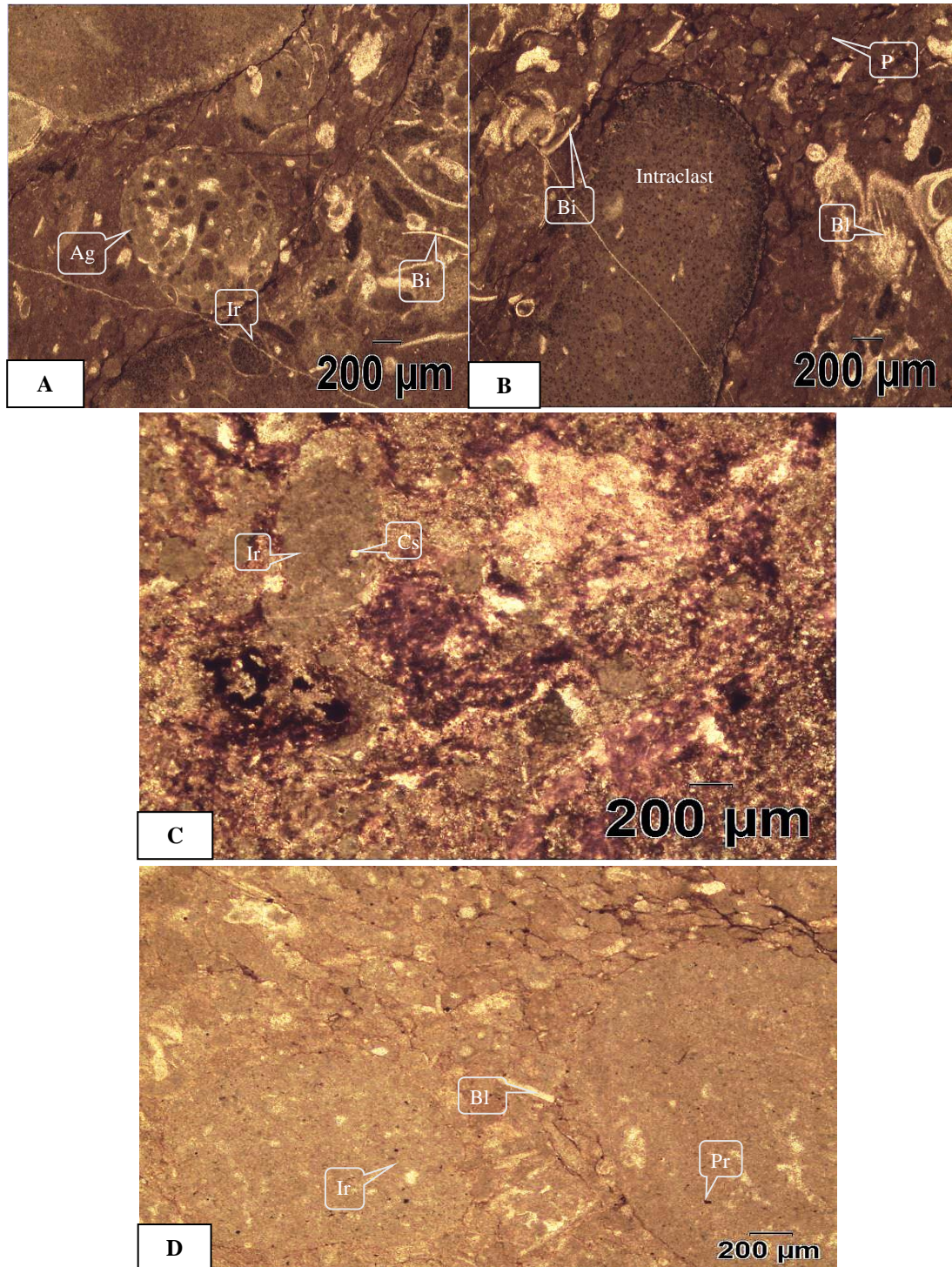


Plate 8: Figure A and B: Photomicrograph shows rudstone displaying intraclast (Ir), bivalves (Bi), peloids (P), aggregate grain (Ag) and bioclast (Bi) (PPL, GT /S 14).

Figure C: Photomicrograph of rudstone microfacies showing calcisphere (Cs) Intraclast (Ir) (PPL, GT/S 26).

Figure D: Photomicrograph of peloidal packstone showing bioclast (Bl), intraclast (Ir) and pyrite (Pr) (PPL, GT/S 25).

PLATE 9

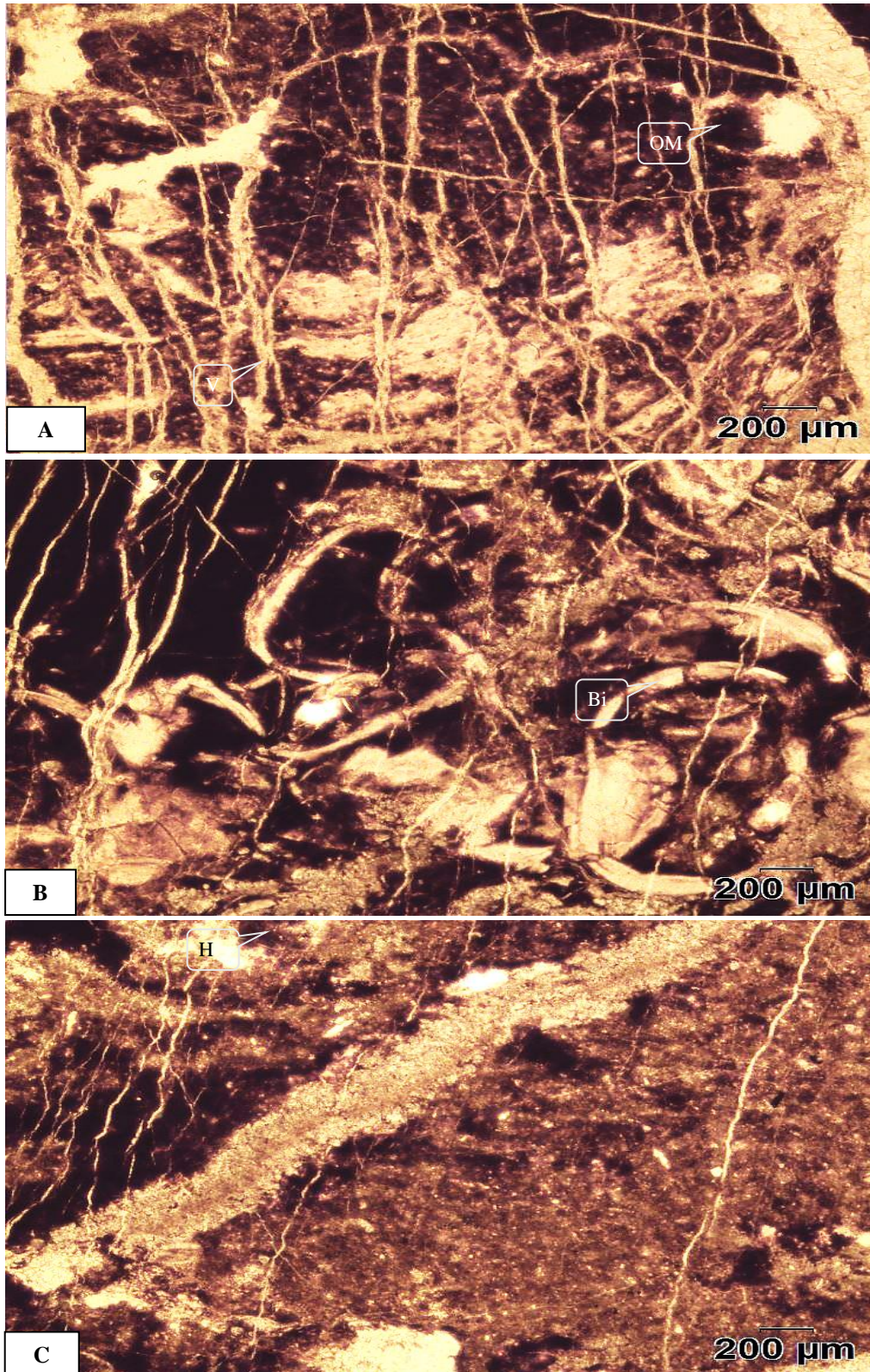
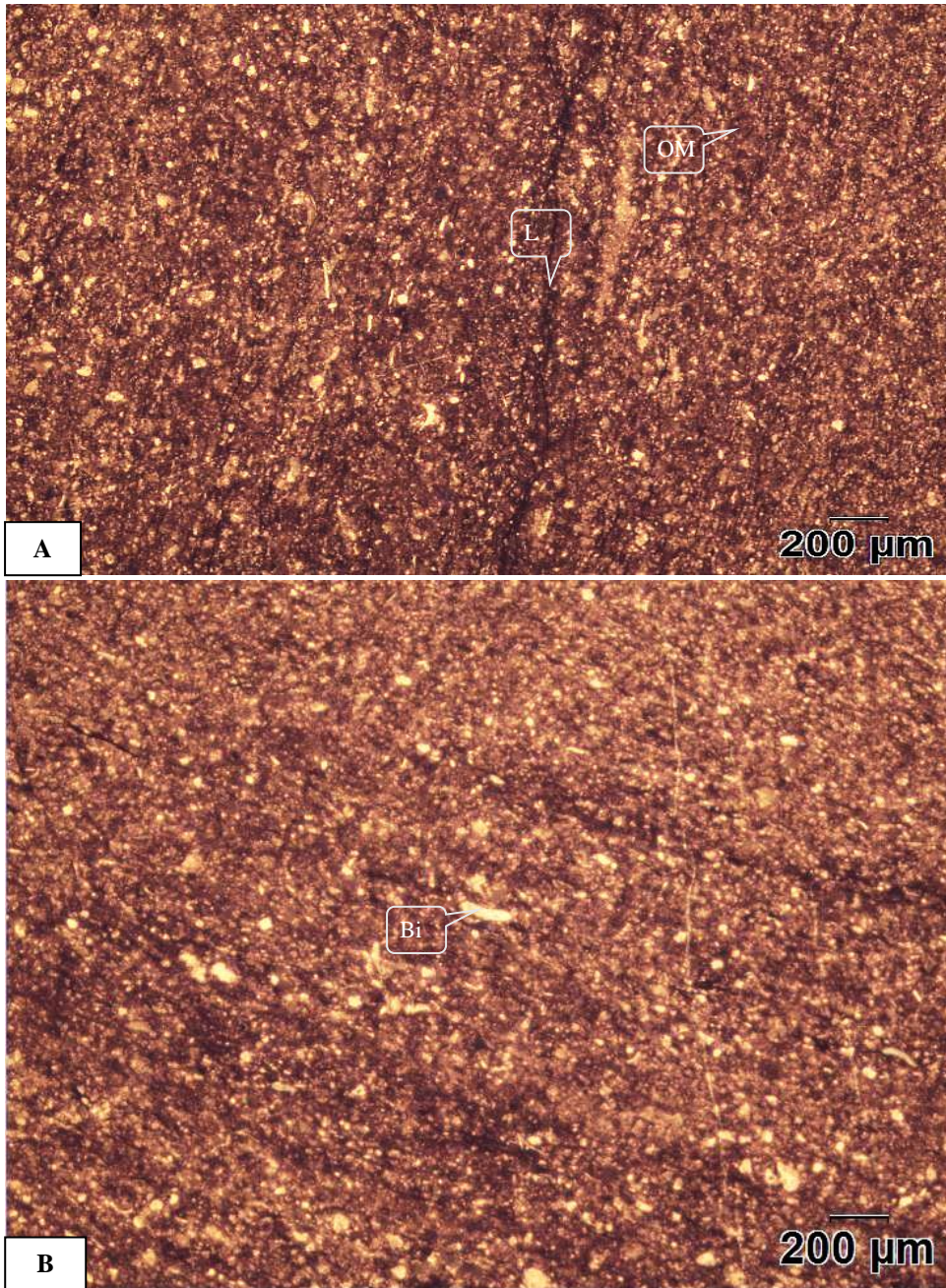


Plate 9: Figure A, B and C: Photomicrograph of grey to black color clayey shale showing unidentified fossil fragment (Fl), bivalve (Bi), hematite (H) calcite vein (V) and organic matter (OM) (GT/S 13).

PLATE 10



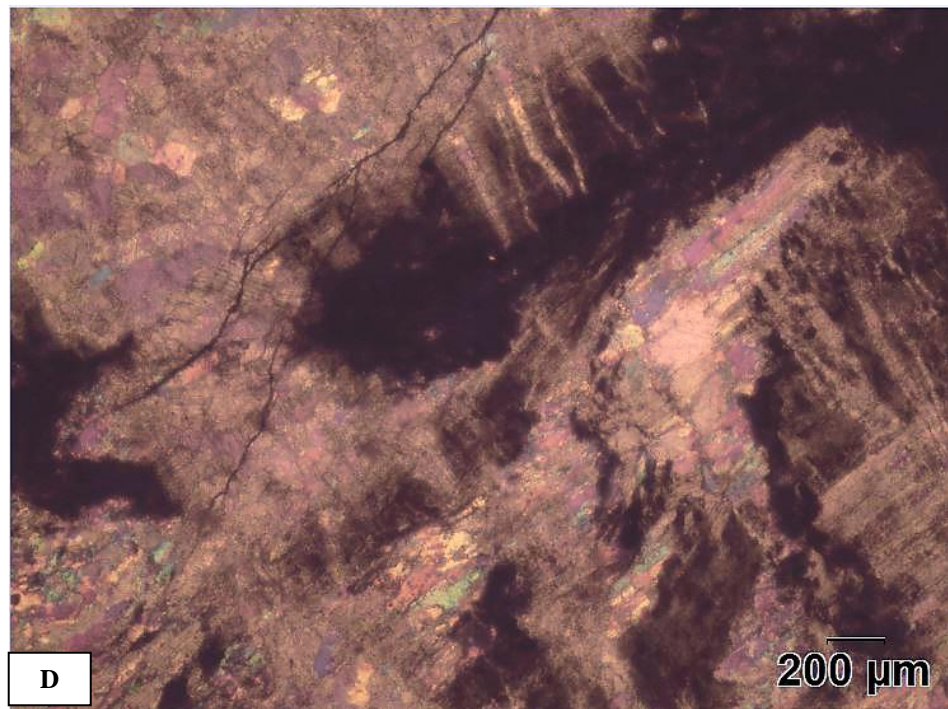
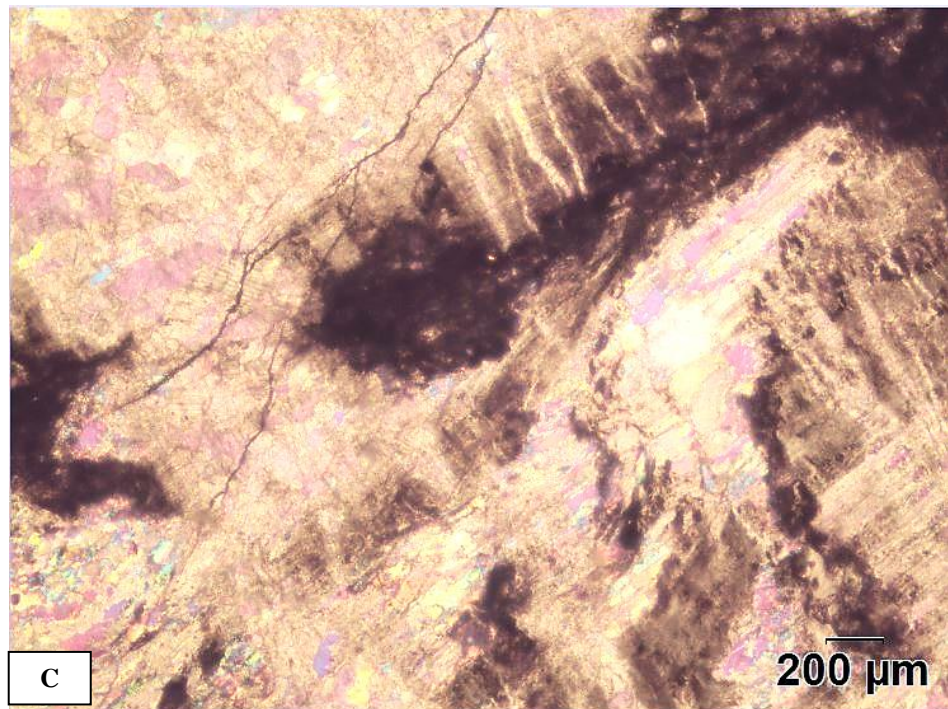
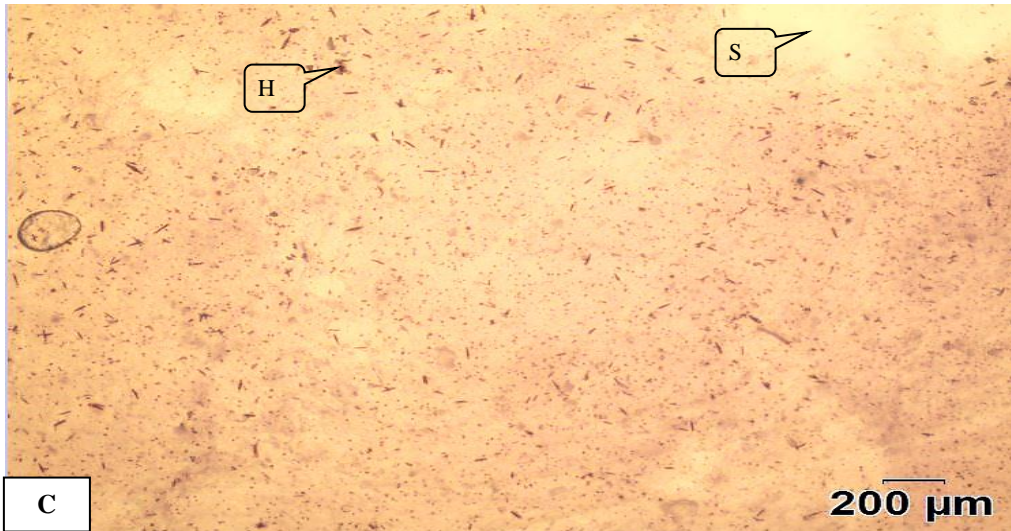
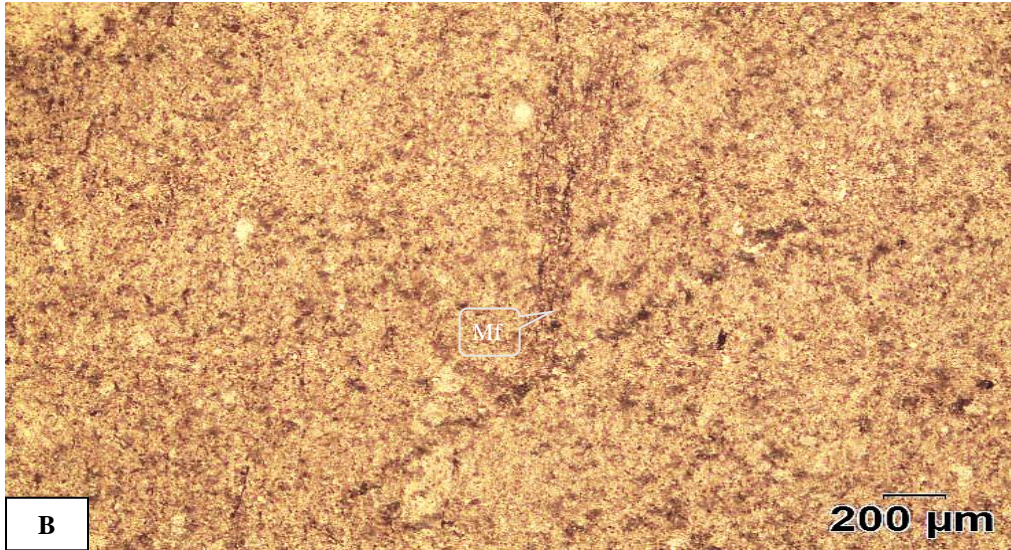
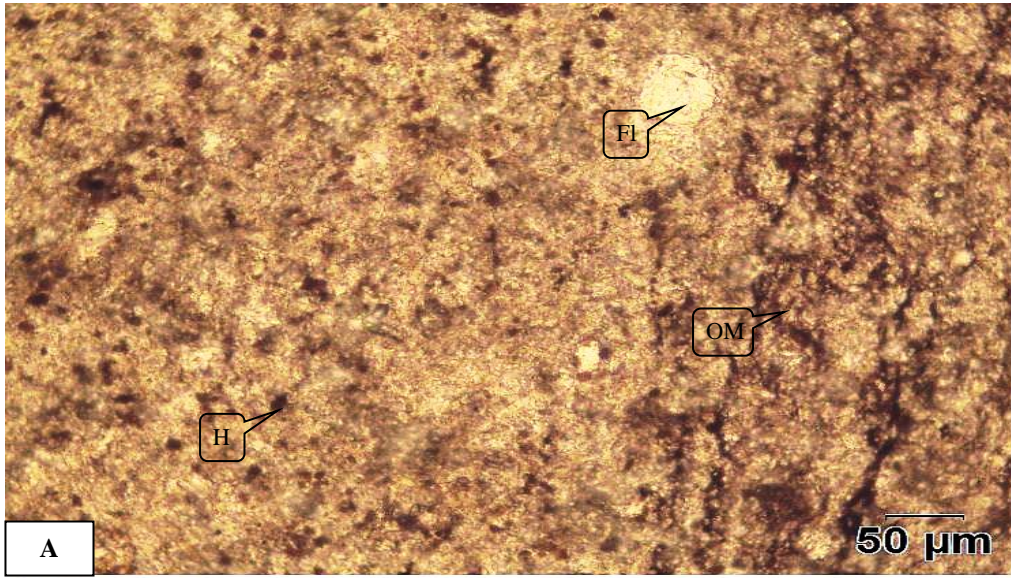


Plate 10: Figure A and B: Photomicrograph, represent dark grey to black color silty shale showing parallel lamination (L), bivalve (Bi) and organic matter (OM) (GT/S 43).

Figure D and E: Photomicrograph of dark grey to black color black shale showing intraclast, calcite vein, fracture and organic matter (OM) (Figure A, XPPL; B. PPL, GT/S 56).

PLATE 11



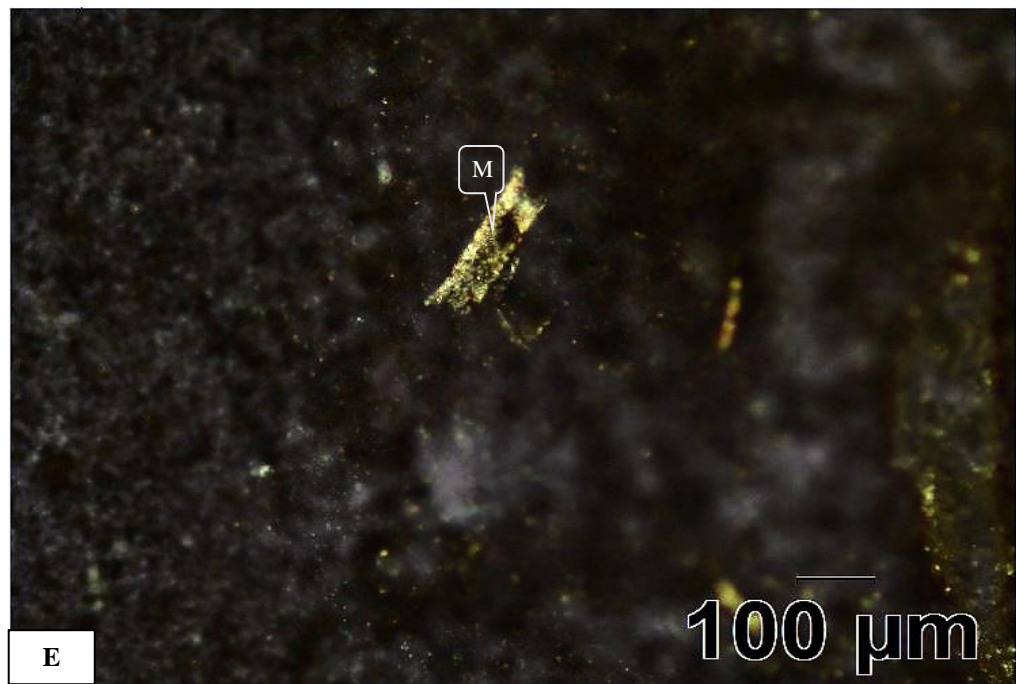
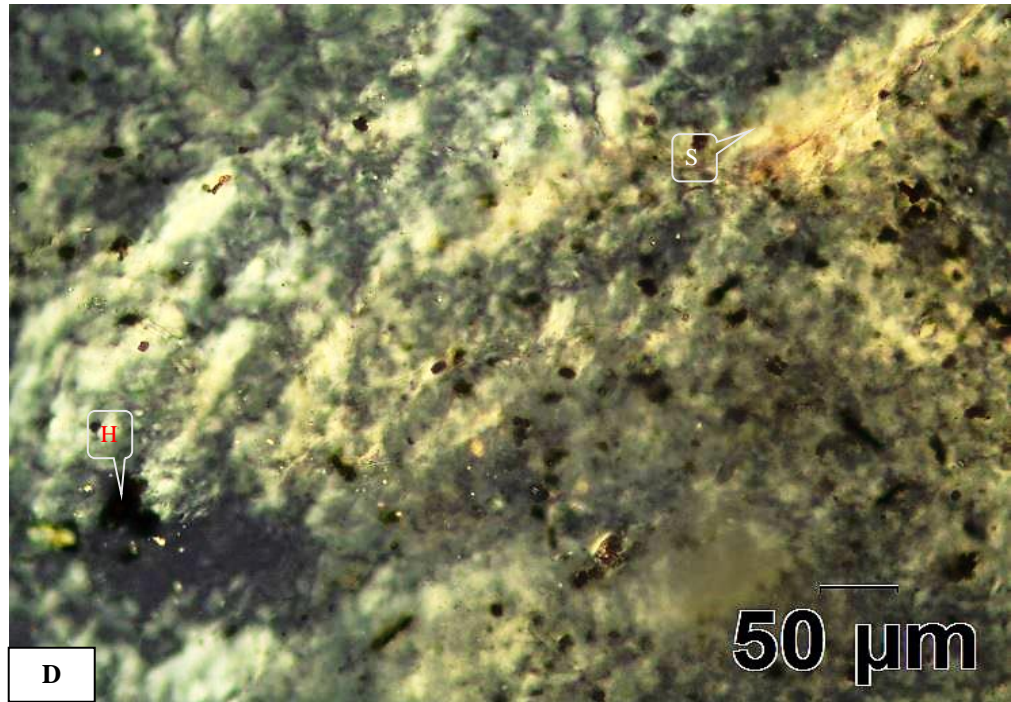


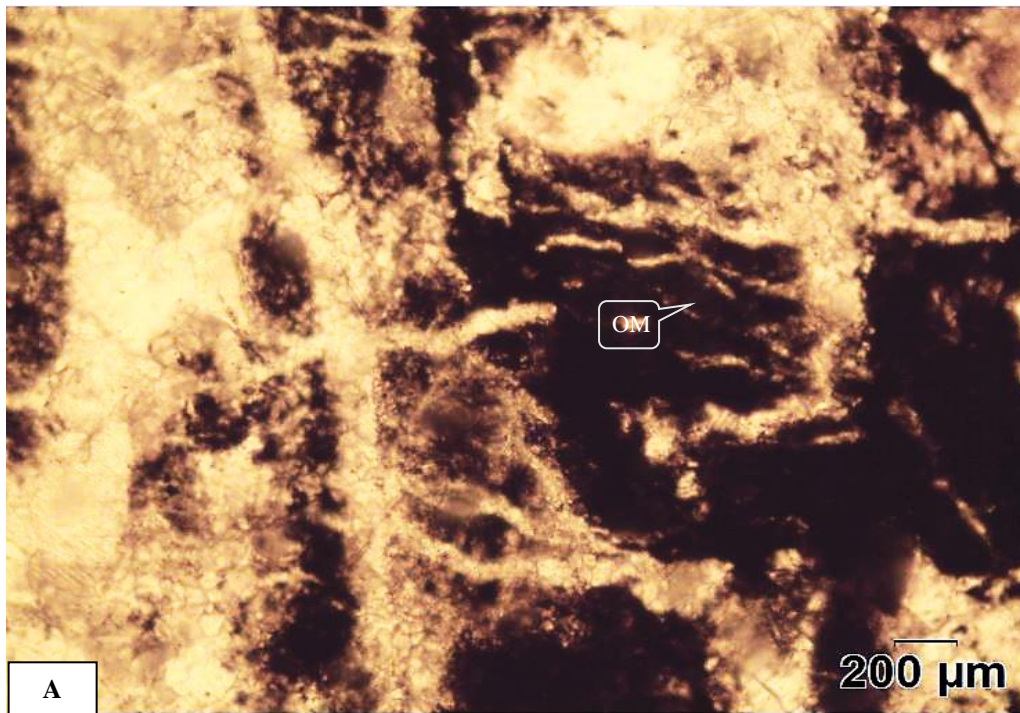
Plate 11: Figure A and B: Photomicrograph of grey to black color claystone including unidentified fossil fragment (Fl), hematite (H) micro fracture (Mf) and organic matter (OM) (Figure 1. 20X, PPL, Figure 2. 4X, GT/S 3).

Figure C: Photomicrograph representing hematite (H) and silicification (4X, PPL, GT/S 58).

Figure D: Thin section photograph of grey to black color claystone showing hematite (H) and silicification (S) (XPPL, GT/S 58).

Figure E: Photomicrograph of grey to black color claystone showing relict of Muscovite (M)
(XPPL, 10 X, GT/S 3).

PLATE 12



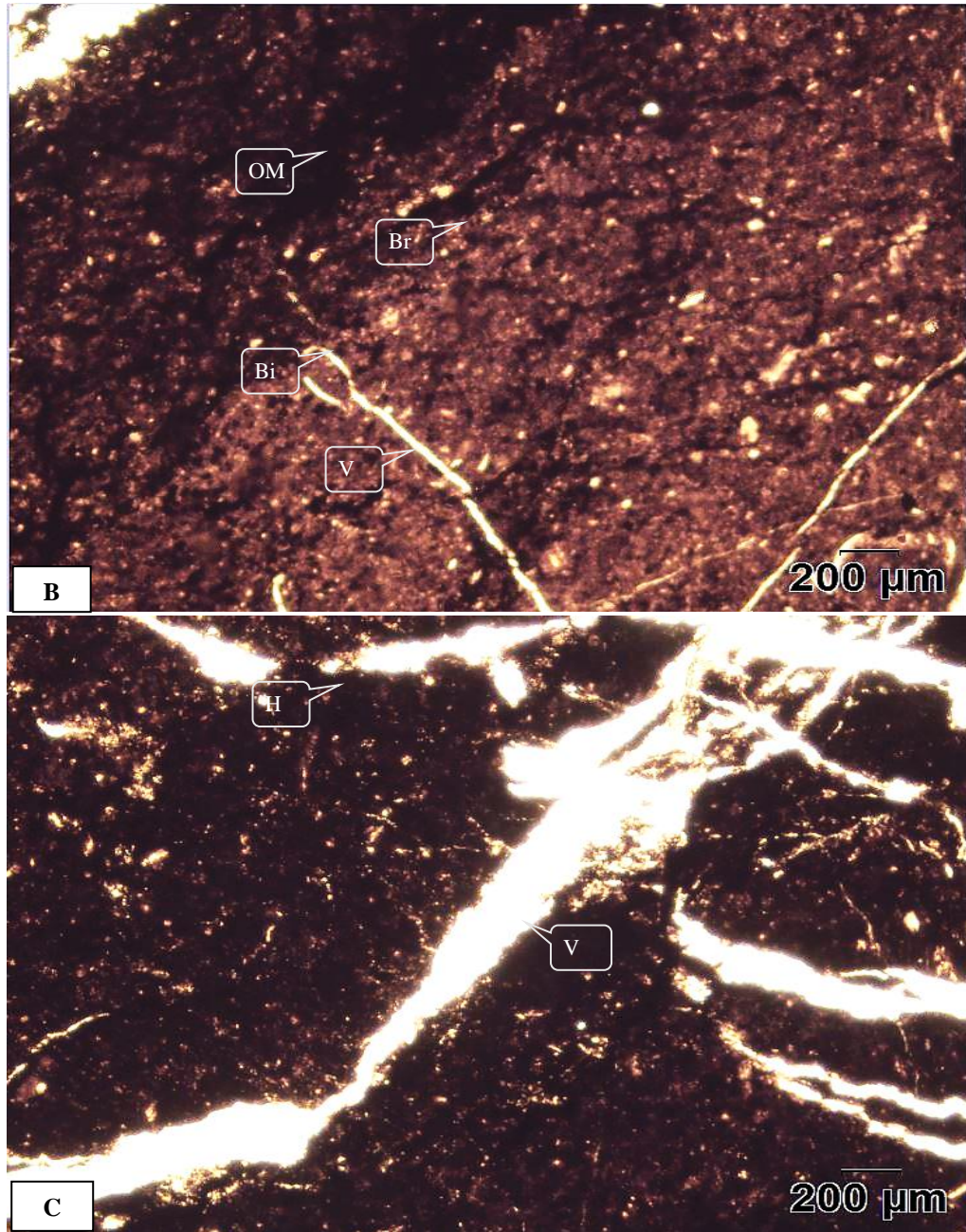
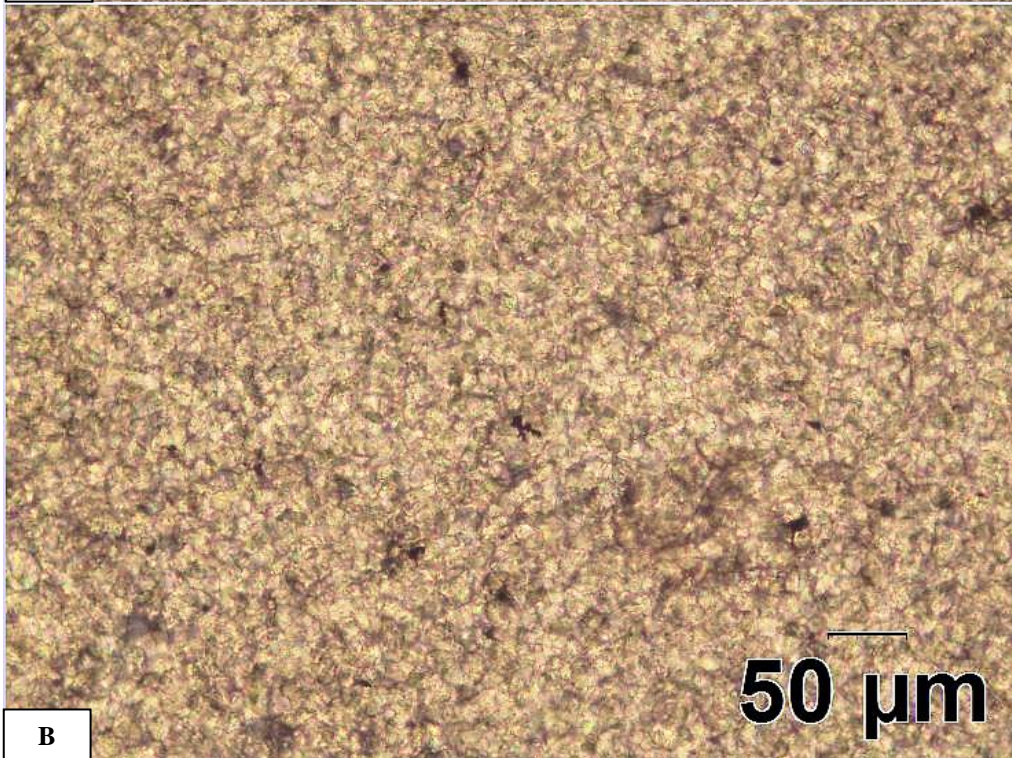
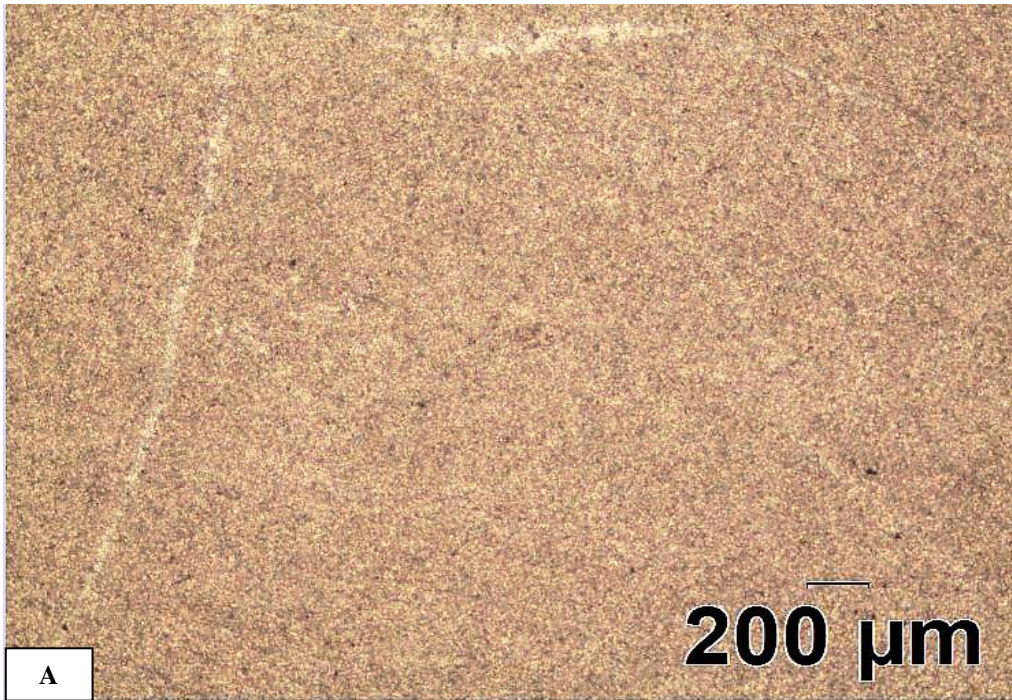


Plate 12: Figure A, B and C: Photomicrograph represents black color silty claystone displaying bivalves (Bi), burrows (Br), calcite vein (V) and organic matter (OM). (PPL, 4X, GT/S 45).

PLATE 13



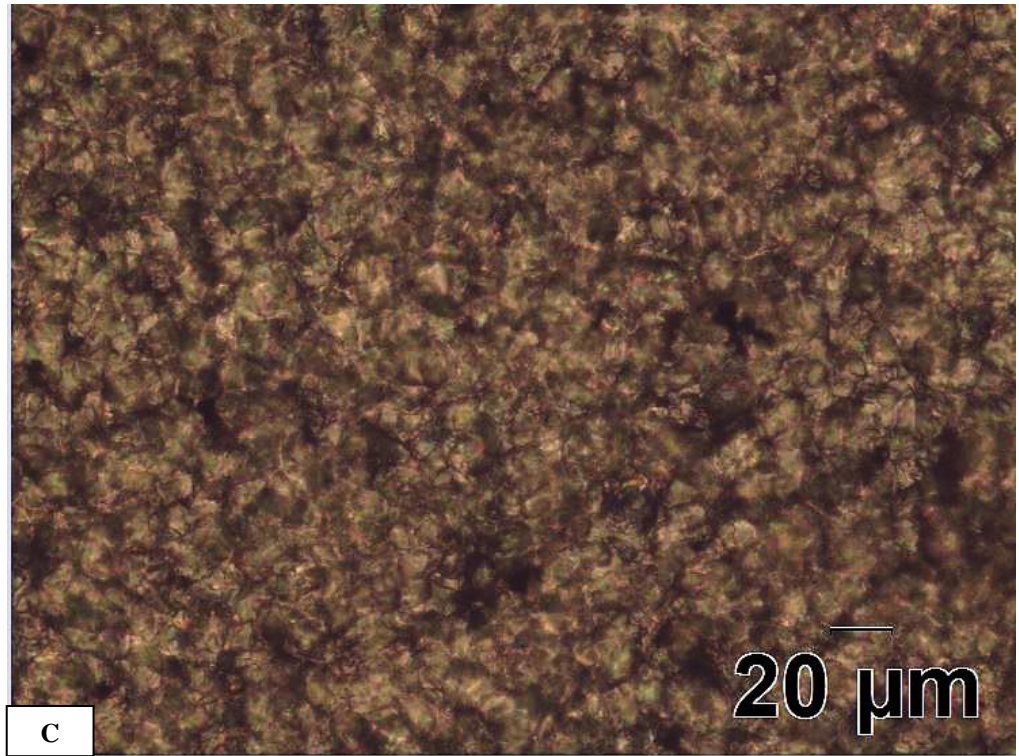


Plate 13: Figure A and B: Microphotograph of microcrystalline dolomite fabrics consist of pyrite cubic crystal and calcite vein (A: PPL, 4X, B: PPL, 20 X, GT/S 35).

Figure C: Photomicrograph of dolostone including xenotopic dolomite texture and disseminated pyrite cubic crystals (PPL, 40 X GT/S 35).